2012

Lipid raft formation and peptide-lipid interactions in myelin model membranes

Ashtina R. Appadu
Wilfrid Laurier University, appa4220@mylaurier.ca

Lipid raft formation and peptide-lipid interactions in myelin model membranes

By

Ashtina Appadu

B.Sc. Biochemistry/Biotechnology, Wilfrid Laurier University, 2009

THESIS

Submitted to the Department of Chemistry

In partial fulfillment of the requirements for

Master of Science in Chemistry

Wilfrid Laurier University

2012

Abstract

Multiple sclerosis (MS), a demyelinating disease affecting 75,000 Canadians and almost 400,000 Americans, is one of the most prevalent diseases in young adults. Unfortunately, there exist no known cures to date and the pathways involved in the progression of the disease remain relatively obscure. The demyelination process triggered by the onset of MS, affects the lipid composition of the myelin membrane and causes a loss in viable myelin which can in turn greatly impact the proper functioning of the central nervous system (CNS). The cholesterol content of myelin fluctuates during MS and consequently this could affect the fluidity as well as the lipid microdomain profile in the membranes. Using model membranes such as a fluid POPC (1-palmitoyl-2-oleoyl-sn-glycero-3-phosphocholine) system and the "canonical' raft system (POPC/sphingomyelin/cholesterol 1:1:1) to represent the two extremes of the fluidity scale, as well as myelin-mimicking membranes (healthy and diseased) which have intermediate lipid fluidities, the lipid domains in each of the systems were probed using fluorescence resonance energy transfer (FRET). FRET analysis indicated that the myelin membrane models contained lipid domains than were overall smaller that those found in the raft system. The addition of melittin, a positively-charged (+6) peptide, to these lipid systems triggered lipid rearrangement to yield larger lipid domains in the myelin systems, whereas in the raft system a change from large domains to smaller ones in the presence of the peptide was observed. Melittin interacted differently with each of the lipid systems where the lipid composition determined the overall conformation of the peptide which, according to circular dichroism (CD) spectroscopy, was shown to be mostly α-helical in membrane environments. It is believed that melittin can exist in a number of different states; a monomer at low concentrations, and as the concentration increases self-association results in either dimers consisting of two parallel α-helices or even a tetramer which would be a dimer of dimers (four α-helices). Tryptophan fluorescence indicated that melittin had a strong affinity for the myelin mimicking models which were negatively-charged and the peptide appeared to be buried relatively deep into the hydrocarbon core of the bilayer, whereas melittin was located nearer the interfacial region in the raft system which was not

charged. Furthermore, melittin appeared to interact more strongly with the healthy myelin model compared to the diseased model which contained a higher level of cholesterol. This would indicate that melittin's interaction is strongly dictated by electrostatic interactions as well as the presence of cholesterol which would affect the fluidity and physical properties of the lipid bilayer, thus making it harder for the peptide to penetrate deeply. Since the lipid composition is affected during demyelination and the cholesterol content has been shown to increase, this could suggest that similarly to melittin, other basic proteins found in the CNS could also suffer reduced lipid interactions which would affect their overall structure and consequently their function. The proteolipid protein (PLP) is amongst one of the most abundant proteins found in the myelin membrane. This extremely hydrophobic integral membrane protein consisting of four transmembrane α-helices is known to induced encephalomyelitis in experimental animals and is consequently of great interest in MS research. Among the different loops that connect the helices, the C-terminus located on the cytoplasmic side of the membrane, is of particular interest since it has been hypothesized that it could be involved in guiding and properly positioning PLP in myelin, as well as potentially interacting with other myelin proteins. A PLP C-terminus peptide (residues 258-277 in the human sequence) was synthesized and its interaction and secondary structure were studied using CD spectroscopy. CD measurements indicated that this loop region adopted different conformations in the different lipid systems, but all in all, it appeared to be mostly randomly coiled and it had a limited amount of interaction with the lipid vesicles. The structure of the peptide also seemed unaffected by the change in lipid composition of the healthy and diseased myelin model systems. This would suggest that the lack of structure of the peptide could allow it to interact with other cytosolic myelin proteins. These studies on the lipid domains in myelin membrane models as well as their interactions with melittin and the PLP C-terminus peptide suggest that within the myelin sheath protein structure and protein-lipid interactions are affected during MS.

Acknowledgements

I would like to express my gratitude and thanks to my wonderful supervisor Dr Lillian DeBruin, for being an amazing mentor and giving me the opportunity to work on this project. Without her guidance and continuous support, this project would have been impossible to complete. I would also like to thank Dr Masoud Jelokhani for his advice and help in understanding and analyzing my data and for allowing me to use the equipment in his lab. I would also like thank my good friend Patrick Hoang for all the help he has provided me in the lab as well as my lab mates Baindu Kosia, Matthew Nichols, Vatsal Patel and Miljan Kuljanin for their company and help during the long hours spent in the lab. Finally I would also like to thank my family, specially my mother, who have always supported me in my studies and encouraged me do better.

Declaration of work performed

All data presented and described in this thesis are the results of my own work. Furthermore, I hereby declare that I am the sole author of this thesis that includes all final revisions, as accepted by my examiners.

TABLE OF CONTENTS

LIST OF FIGURES

LIST OF TABLES

LIST OF ABBREVIATIONS

AFM	…..	Atomic Force Microscopy
CHAPS	…..	3-[(3-Cholamidopropyl)dimethylammonio]-1-propanesulfonate
CD	…..	Circular Dichroism
CNP	…..	3’-Cyclic Nucleotide 3’-Phosphodiesterase (CNP)
CNS	…..	Central Nervous System
DMPG	…..	1, 2-Dimyristoyl-*sn*-Glycero-3-Phosphoglycerol
DMPC	…..	1, 2-Dimyristoyl-*sn*-Glycero-3-Phosphocholine
DRM	…..	Detergent Resistant Membrane
EPR	…..	Electron Paramagnetic Resonance
ER	…..	Endoplasmic Reticulum
FRET	…..	Fluorescence Resonance Energy Transfer
GUV	…..	Giant Unilamellar Vesicles
HEPES	…..	2-[4-(2-hydroxyethyl) piperazin-1-yl]ethanesulfonic acid
ITC	…..	Isothermal Titration Calorimetry
L_d	…..	Liquid Disordered
L_o	…..	Liquid Ordered
LUV	…..	Large Unilamellar Vesicle
MAG	…..	Myelin Associated Glycoprotein
MBP	…..	Myelin Basic Protein
MLV	…..	Multi Lamellar Vesicle
MOG	…..	Myelin Oligodendrocyte Glycoprotein
MS	…..	Multiple Sclerosis

NaCl	…..	Sodium Chloride
NaF	…..	Sodium Fluoride
NBD-DPPE	…..	1,2-Dipalmitoyl-*sn*-glycero-3-phosphoethanolamine-N-7-nitro-2-1, 3-benzoxadiazol-4-yl
NMR	…..	Nuclear Magnetic Resonance
PLP	…..	Proteolipid Protein
PNS	…..	Peripheral Nervous System
POPC	…..	1-Palmitoyl-2-Oleoyl-sn-Glycero-3-Phosphocholine
POPE	…..	1-Palmitoyl-2-Oleoyl-sn-Glycero-3-Ethanolamine
POPI	…..	1-Palmitoyl-2-Oleoyl-sn-Glycero-3-Inositol
POPS	…..	1-Palmitoyl-2-Oleoyl-sn-Glycero-3-Serine
Rhod-DOPE	…..	1, 2-Dioleoyl-*sn*-glycero-3-phosphoethanolamine-N-lissamine rhodamine B sulfonyl
R_o	…..	Forster Distance
REES	…..	Red Edge Excitation Shift
SLB	…..	Supported Lipid Bilayers
SM	…..	Sphingomyelin
SPT	…..	Single Particle Tracking
SUV	…..	Small Unilamellar Vesicle
t-BLM	…..	Tethered Bilayer Lipid Membranes
TFE	…..	Trifluoroethanol
Tris	…..	2-Amino-2-hydroxymethyl-propane-1,3-diol

CHAPTER 1

THE MYELIN MEMBRANE AND LIPID RAFTS

1.1 A brief introduction to the myelin membrane

1.1.1 Structure, function and morphology

The myelin sheath is a multilamellar, dielectric membrane that wraps itself many times around the nerve axons in the central nervous system (CNS) and the peripheral nervous system (PNS), in order to provide them with protection and insulation. Myelin, an extended and modified plasma membrane, is produced by the oligodendrocytes in the CNS and by the Schwann cells in the PNS. The production of myelin is a very strictly regulated process, the amount of which is dictated by the diameter of the axon, where the thicker axons have greater amounts of myelin than thinner axons (Friede and Bischhausen, 1982; Baumann and Pham-Dihn, 2001). The membrane is very dynamic and functionally active, playing a major role in the rapid and efficient action potential conduction in the nervous system through saltatory conduction (Taylor *et al*., 2004; Deber and Reynolds, 1991). One feature of myelin that enables this type of conduction is its segmental wrapping of the nerve cells' axons. The membrane does not continuously surround the axons in one solid structure but instead is made of segments that line up one after the other. The region between two adjacent segments is known as the node of ranvier and at this location a small portion of the axons is exposed to the extracellular space. Axonal sodium channels are located at the nodes of ranvier and as such, when the node is excited during signal transmission, the local circuit generated cannot flow through the high resistance sheath but instead flows out through and depolarized the membrane at the next node, thereby jumping from node to node and increasing the speed of signal transmission (Friede and Bischhausen, 1982; Taylor *et al*., 2004; Deber and Reynolds, 1991). For the longest time, myelin was thought to be only a

passive agent to the conduction of nerve impulses through increased internodal membrane resistance and decreased membrane capacitance. Recent studies have however shown that the myelin sheath is actually involved in a number of different roles such as the development and proper function of the nervous system. Not only does the membrane regulate the nerve axon's diameter and the formation of microtubular networks, but it is also an important participant in the clustering of ion channels at the nodes of ranvier (Taylor *et al*., 2004).

1.1.2 Lipid and protein composition of the myelin membrane

Myelin is a complex community of proteins and lipids but one feature that sets it apart from other mammalian cell membranes, is its unusually high lipid content compared to other plasma membranes. The synthesis of most of these lipids originates from the endoplasmic reticulum (ER) and it is estimated that lipids make up almost 80% of the membrane while proteins make up the other 20% (Jahn *et al*., 2009, Podbielska and Hogan, 2009). Glycosphingolipids, long chain fatty acids containing around 22-26 carbon atoms that are usually saturated, are particularly rich in myelin, with their major component being galactosylceramide (Baumann and Pham-Dinh, 2001). Another unusual characteristic of myelin is the presence of a high proportion of ethanolamine phosphoglycerides in the plasmalogen form, which accounts for one-third of the phospholipids and the presence of cholesterol which makes up more than 25% of the total lipid content (Podbielska and Hogan, 2009). The molar ratio of the myelin lipids is estimated to be approximately 2: 2: 1: 1 for cholesterol / phospholipids/ galactolipids / plasmalogen (Jahn *et al*., 2009, Baumann and Pham-Dihn, 2001). This high amount of cholesterol and glycosphingolipids might lead to an

increase in membrane lipid order, which could be important for myelin to perform its insulating function (Simons and Ehehalt, 2002). When it comes to the protein composition in myelin, previous studies using gel electrophoresis techniques have shown that a small number of proteins are extraordinarily abundant in CNS myelin. The myelin proteolipid protein (PLP) and its smaller splice isoform DM20 make up almost 30-45% of the total protein composition. The myelin basic protein (MBP) and its isoforms are the second most abundant protein at 35%, followed by the 2', 3'-cyclic nucleotide 3'-phosphodiesterase (CNP) at around 4–15%, and finally the remaining proteins such as the myelin oligodendrocyte glycoprotein (MOG) and the myelin associated glycoprotein (MAG) amongst other, make up around 5–25% of the total protein content (Jahn *et al*., 2009; Deber and Reynolds, 1991). It is still unclear as to why the proteins are enriched to their unusual relative abundance and while many of their functions are still unknown, they are known to be active in the compaction and maintenance of the membrane. A simple view of the myelin membrane's structure would be to have lipid bilayer containing integral proteins such as PLP as well as other extrinsic proteins attached to either the cytoplasmic or extracellular side of the membrane as shown in Figure 1.1.

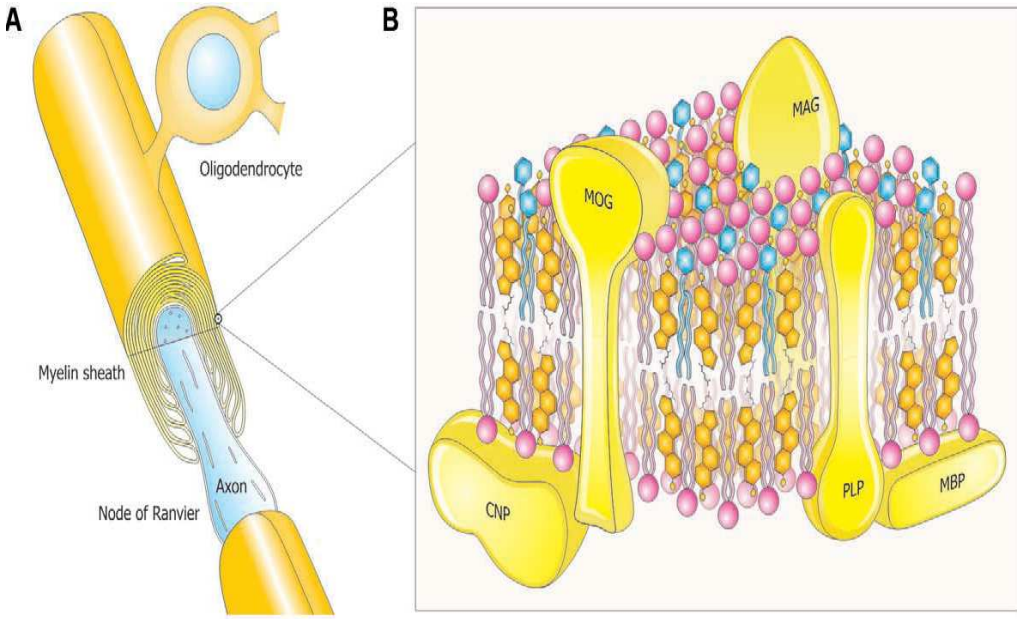

Figure 1.1: A composite diagram summarizing features of CNS myelin

(A) Architecture of CNS myelin. An oligodendrocyte and myelin sheath in CNS; a simplified version with fewer myelin sheaths per oligodendrocyte. The cutaway view shows a multi-layer membrane (only a few drawn for clarity) formed by oligodendrocytes. (B) Molecular composition of CNS myelin (three-dimensional view). The myelin is a multi-layer membrane formed by oligodendrocytes, containing a high lipid (80%) to protein (20%) ratio and asymmetric distribution of lipids (PLP, proteolipid protein; MBP, myelin basic protein; MOG, myelin oligodendrocyte glycoprotein; MAG, myelin-associated glycoprotein; CNP, 2'3'-cyclic-nucleotide 3'-phospodiesterase). Reprinted with permission from SAGE Publications (Podbielska, M. and Hogan, E.L. (2009). Molecular and immunogenic features of myelin lipids: incitants or modulators of multiple sclerosis? *Mult. Scler*. 15: 1011–1029), Copyright (2009).

1.2 Demyelinating diseases – multiple sclerosis (MS)

Demyelinating disorders appear in many forms, the most common of which is multiple sclerosis (MS). MS affects almost 75,000 Canadians, 400,000 Americans and almost 2.1 million people worldwide and has been found to be more prevalent in females than males (Alonso and Hernan, 2008). It is an unpredictable condition which once triggered,

causes inflammations in the CNS (Reipert, 2004). There is no known cure up to date, with treatments available only slowing the progression of the disease, and the factors that trigger the disease remain relatively unknown. However, MS is known to be an autoimmune reaction and it has been hypothesized that the disease spreads due to myelin-specific autoreactive T-cells, which when activated will cross the blood-brain barrier due to an overexpression of chemokines (Pender and Greer, 2007; Sospedra and Martin, 2005). It would be reasonable to assume that these T cells could drive the inflammatory process in the CNS; however, the stimulus behind the activation of these cells remains unclear. Once the autoimmune response is triggerred, the body targets the myelin sheath as being a foreign body and consequently attacks and degrades it, leaving behind patches of damage called plaques or lesions, predominantly located in the CNS (Pender and Greer, 2007; Balashov *et al.*, 1999). Areas affected by these inflammatory plaques often experience a decrease in viable myelin, a process usually termed demyelination in literature.

Since myelin contributes to the quick and efficient transmission of action potentials in the brain, demyelination would cause nerve impulses to be slowed or even potentially stopped as shown in Figure 2 (Sospedra and Martin, 2005; Pender and Greer,2007). If sufficient oligodendrocytes are present at sites of lesion, remyelination could take place but at this point the myelin sheath will only be partially restored. Eventually as the disease progresses, it becomes harder and harder for remyelination to take place, and consequently the oligodendrocytes and even the axons will be affected thus leading to many health complications (Fancy *et al.,* 2011). MS patients can experience partial or complete loss of any functions controlled by the CNS and symptoms can range anything from muscle weakness,

speech impairment, vision loss amongst others, to paralysis and ultimately death (Reipert, 2004).

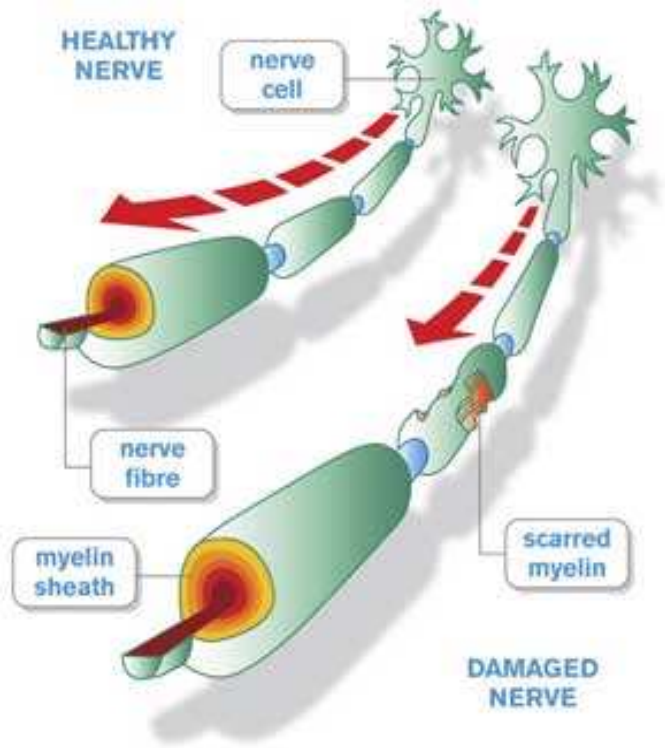

Figure 1.2: Nerve signal transmission across healthy and diseased myelin sheaths
Signals are transferred quickly and efficiently in healthy myelin membrane. MS causes the development of plaques and lesions on the membrane leaving it scarred and damaged which results in the loss of efficient signal transmission. Figure modified from http://www.headache-adviser.com/what-does-vitamin-b12-do.html.

1.3 *Lipid Rafts*

1.3.1 Lipid phases in the cell membrane

Although the myelin sheath is made up predominantly of lipids which differentiate it from the other plasma membranes, it can still be represented as a dynamic bilayer where its proteins and lipids have a certain amount of lateral and rotational freedom. By definition, the cell membrane acts as a barrier which controls the movement of molecules in and out of the

cell and is made up of a wide variety of biological molecules, primarily proteins and lipids (Verb *et al.,* 2003). These molecules are involved in a number of cellular processes such as cell adhesion, ion channel conductance and cell signaling. Lipids in the membrane are arranged and held together by hydrophobic interactions and other intermolecular forces like the van der Waal's forces and hydrogen bonding, in such a way that they still have a limited amount of lateral and rotational movement which gives the membrane its fluid property described by the Singer Nicolson membrane model (Verb *et al.,* 2003). Due to the fact that the membrane is fluid in nature and its molecules are not rigidly held in place, this gives rise to the coexistence of two different phases, namely the liquid ordered phase (L_o) and the liquid disordered phase (L_d) (London, 2002; Dupree and Pomicter, 2010). The L_o phase is usually thicker than the rest of the bilayer and has an ordered arrangement which can be attributed to the presence of long chained saturated lipids such as sphingolipids. The L_d on the other hand contains unsaturated lipids and due to the presence of double bonds that introduce kinks in the acyl chains, this prevents the lipids from tightly packing together, hence giving rise to a more disordered arrangement (Dupree and Pomicter, 2010; Lingwood and Simons, 2010). This coexistence of the liquid ordered and disordered lipid phase behavior is the basis for the lipid raft theory.

1.3.2 Membrane rafts: properties and function

Rafts are considered to be regions that are thicker and more ordered than the rest of the membrane and one interesting analogy would be to think of these small ordered domains (L_o) as being small vessels floating in a sea of phospholipids that are more fluid and disordered (L_d). These microdomains have been defined as being linear regions of the

membrane that are "small (10–200 nm), heterogeneous, highly dynamic, sterol and sphingolipid-enriched domains that compartmentalize cellular processes" according to the Keystone Symposium on Lipid Rafts and Cell Function (Pike 2006). Membrane rafts are believed to be transient and unstable nanoscale clusters of different sizes which can be stabilized by the binding of ligand molecules. They are known to be involved in several important biological functions and since they have been found to exist in both neuronal and glial cells, they are proposed to be critical for the normal functioning of the brain (DeBruin *et al.,* 2007; Simons and Ehehalt, 2002; Lingwood and Simons, 2010). Recent work has shown that the disruption of raft functions has been implicated in diseases like MS, Parkinson's and the Alzheimer's disease (Simons and Ehehalt, 2002; Cherukuri, *et al.,* 2001).

The naturally fluid membrane can form a number of different types of microdomains such as the lipid rafts, caveolae, and cellular junctions like the tight junctions found in the radial component of CNS myelin, all of which are usually commonly called rafts (DeBruin and Harauz, 2005). Rafts arise mainly due to cholesterol molecules which have a planar structure and can hence intercalate between the straighter, stiffer hydrocarbon chains of saturated lipids and disfavours interactions with the more bulky unsaturated lipid species (Korade and Kenworthy, 2008; Simons and Ehehalt, 2002). Interaction with cholesterol also forces neighbouring hydrocarbon chains into more extended conformations, increasing membrane thickness and promoting segregation further through hydrophobic mismatch (Lingwood and Simons, 2010; Korade and Kenworthy, 2008; Samsonov *et al.,* 2001). The microdomains are usually assumed to be in the L_o phase and depending on the functions they have to carry out, they contain specific sets of proteins such as the glycosylphosphatidylinositol (GPI)-anchored

proteins and the acylated Src family (DeBruin and Harauz, 2007; London, 2002). As mentioned before, rafts are involved in numerous cellular functions and are mainly implicated in secretion, endocytosis, cell surface proteolysis, and signalling, including initiating mitogen-activated protein kinase (MAPK) cascades (Dupree and Pomicter 2010; Mukherjee and Maxfield, 2000). Studies suggest that upon cell activation, through ligand binding, small, highly dynamic membrane rafts coalesce to form larger more stable platforms through protein-protein and lipid-protein interactions (Lingwood and Simons, 2010). This dynamic process is depicted in Figure 1.3.

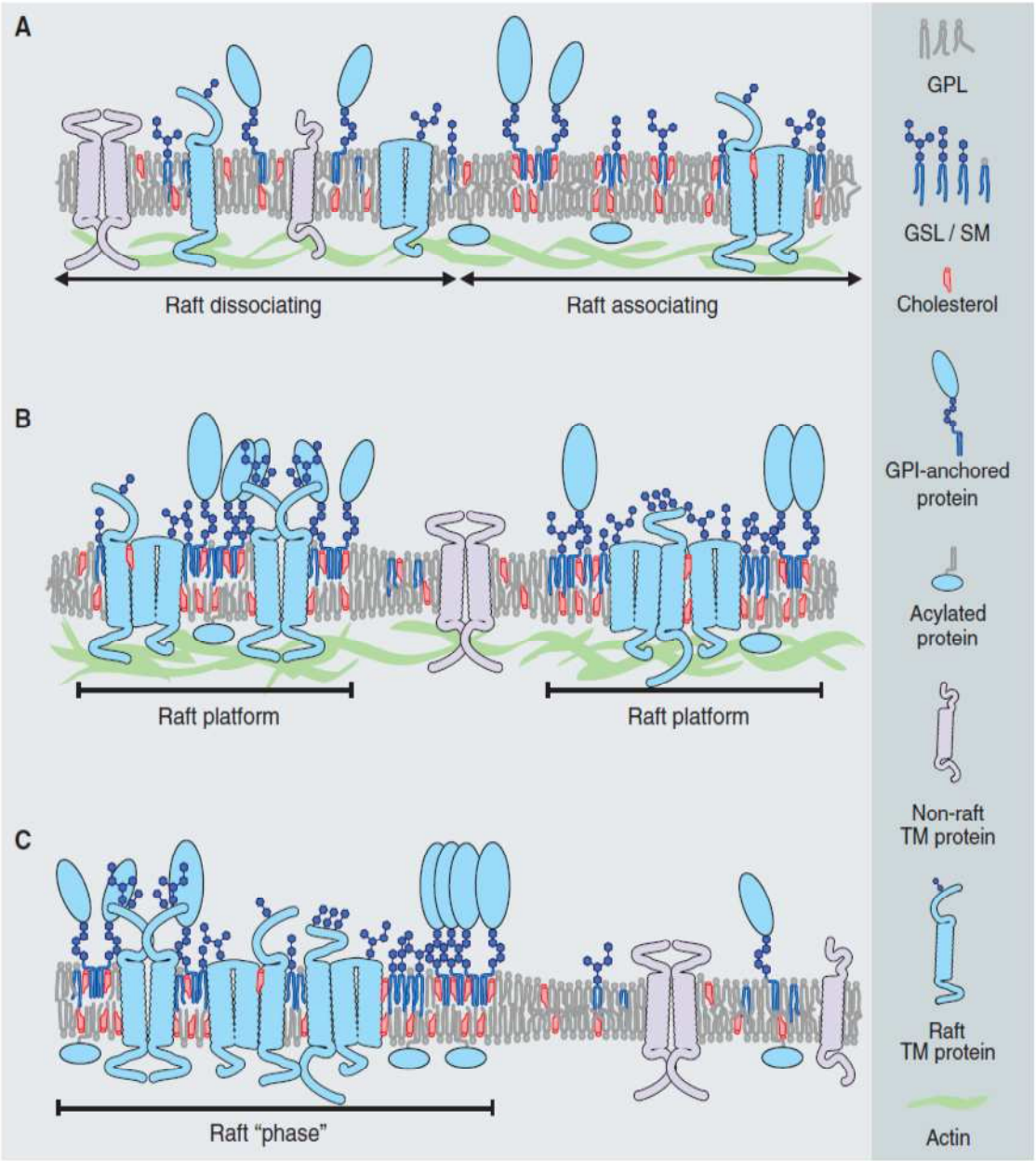

Figure 1.3: Lipid rafts association in cell membrane

(A) Sphingolipid/sterol associations floating through cell membrane. Some proteins such as GPI-anchored proteins and other transmembrane (TM) proteins can readily associate with these nanoclusters. (B) Formation of raft platforms is activated by lipid and protein mediated activation events such as ligand binding, synapse formation or protein oligomeriaztion which trigger the coalescence of ordered domains with specific sets of biomolecules. (C) Raft platforms come together bringing specific proteins together to trigger a chain of processes in the cell. Reprinted with permission from AAAS Publications (Lingwood, D. and Simons, K. (2010) Lipid rafts as a membrane-organizing principle. Science 327:46-50), Copyright (2010)

1.3.3 Biosynthesis of raft clusters

For the longest time, the formation of rafts has been a mystery and the discovery of their development pathways came fairly recently. The two main components of rafts, cholesterol and sphingolipids, are initially synthesized in the endoplasmic reticulum (ER), but while cholesterol undergoes complete synthesis, only the hydrophobic backbone of sphingolipids, ceramide, is produced at this location (Van Meer, 1989; Mukherjee and Maxfield, 2000). Completion of sphingolipids synthesis takes place in the Golgi complex where the polar head groups are affixed onto the ceramide backbone. Once cholesterol and the sphingolipids are moved to the Golgi complex, the rafts are then assembled before being moved forward to the plasma membrane. It should be noted that cholesterol is toxic and its cellular levels are tightly controlled. If this process is disturbed in any way and the concentration of cholesterol is allowed to fluctuate, it can lead to many diseases involving lipid metabolism, MS being one of them (Van Meer, 1989; Mukherjee and Maxfield, 2000; Korade and Kenworthy, 2008).

Cholesterol is a major player when it comes to the CNS and not only is it involved in the formation of rafts but it is also implicated in the production of steroid hormones as well as the development of the myelin membrane. The presence of ionic receptors and neurotransmitters in ordered domains suggest that rafts could play an important role in neurotransmission (Tillman and Cascio, 2003). Since cholesterol affects the properties of rafts, this would imply that the biomolecule could in fact control the ion conductance and excitability of membranes. If cholesterol levels happen to be deficient, this would result in oligodendrocytes delaying the myelination process (Korade and Kenworthy, 2008; Van Meer,

1989). Any disturbances in lipid homeostasis could cause alterations to CNS structure and function while causing defects in the production of myelin. In order to maintain the proper development and maintenance of the myelin membrane, it is important that lipid biosynthesis be controlled and it would seem that rafts may play a critical role in this balance (DeBruin and Harauz, 2005; Tillman and Cascio, 2003.)

1.3.4 Techniques used to study microdomains

Over the years, many techniques have been developed to study microdomains in living cells. These include atomic force microscopy (AFM), fluorescence resonance energy transfer (FRET), electron paramagnetic resonance (EPR), nuclear magnetic resonance (NMR) spectroscopy, and single particle tracking (SPT). However, because rafts are so small and transient, this makes them very hard to study and for this reason, model membranes that mimick rafts are often used in studies to mimick rafts since they are more stable and easier to analyse. Cell membranes on the other hand are extremely complex lipid systems and since lipids are constantly being added and removed during cellular processes, this makes it even harder to study lipid domains (Mukherjee and Maxfield, 2000). Even though, the domains in model membranes are much larger and stable than those in live cells, they still provide relatively useful information which can be related to smaller natural rafts (London, 2002; Samsonov *et al.,* 2001). There is clear evidence for lipid rafts in live cells being on the small side, usually around 10-100nm, and since they are transient, this makes it harder to observe them (Lingwood and Simons, 2010). If model systems are used however, lipid domains are more easily observed since they are larger in size. More information can also be

obtained depending on the methodology used and based on the lipid composition of the models which can be easily manipulated. Studying the physicochemical properties of artificial lipid systems, where the lipid composition and the environmental conditions (such as temperature, pH and ionic strength) are controlled, can provide information on the behaviour of certain lipid systems (Samsonov *et al.,* 2001). Moreover, if one uses the appropriate technique, it is almost possible to study any size domains in artificial membranes. For example, under a confocal microscope, only large (micron size) domains can be observed in suitable ternary systems, but if more sensitive techniques such as EPR and fluorescence are used instead, domains in the range of approximately 10 to 40 nm can be more effectively probed (London, 2002).

1.4 Lipid rafts and the myelin membrane

The myelin membrane is quite different from most plasma membranes due to its unusually high lipid composition. Since myelin's lipid composition is made up of approximately 30% cholesterol and a high concentration of glycophingolipids, which have been shown to promote lipid order, this would suggest that rafts may be a major component of myelin (Taylor *et al.,* 2002). This high raft content has been proposed to play an important role in the formation, maintenance and proper function of the myelin membrane (Brown and London, 1998; Taylor *et al.,* 2002). Studies have shown that raft structures are usually resistant to solubilisation by detergents at cold temperatures and for this reason, rafts are usually isolated from the myelin membrane using differential extraction methods using detergents such as CHAPS, Triton-X100 and Brij-96 amongst others (Brown and London, 1998; Taylor *et al.,* 2002). The resistance of lipid rafts to being solubilised has earned them

the commonly used term detergent resistant membranes (DRM) complexes in literature. These DRMs complexes are in a L_o state when isolated and should contain proteins that prefer partitioning in rafts. Over the years, much research has been done on isolating and analysing DRMs from myelin in an attempt to learn more about the types of microdomains present in the membrane as well as the proteins associated with them. Most of the myelin specific proteins associated with the extracted DRMs are usually separated and analysed using gel electrophoresis techniques. Among the proteins that have been shown to associate with the rafts, MAG, PLP and CNP were found to be the most predominant proteins present (Simon *et al.*, 2000; DeBruin and Harauz, 2007). However, since myelin microdomains are developmentally regulated, the protein composition would fluctuate over time as the cells mature (DeBruin and Harauz, 2007). Although a lot of studies have been carried out to determine the structure and composition of myelin, there still remains a lot to be done when it comes to characterizing the membrane's complex microdomain architecture.

1.5 Purpose of study

Lipid rafts have been shown to be involved in a number of diseases such as Parkinson's disease, Alzheimer's and autoimmune diseases, amongst others (Michel and Bakovic, 2007). Rafts have distinctly been shown to participate in various cellular processes such as signaling and provide the required environment for proteins such as members of the tyrosine kinase Src family, G-proteins and various receptor proteins, to come together and carry out these functions. Since the cholesterol content of the myelin membrane has been shown to increase during MS, this would imply that the raft environment would change, thereby affecting the

proper functioning of these proteins and hindering or even completely disrupting their normal interactions. For this reason, I was interested in studying what the effects of an increase in cholesterol would have on the lipid raft domains in the myelin membrane and if possible, determine how the resulting change in lipid environment would affect protein structure and function. Using myelin mimicking model membranes (described in Chapter 2, section 2.1.2) and FRET, the microdomain profile in each of these systems was characterized so that I could assess to what extent the increased levels of cholesterol affected lipid raft structures.

Studying lipid-protein interactions is of particular importance since a cell has the ability of varying the lipid composition of its membrane in response to a variety of stress and stimuli, thus changing the environment and the activity of the proteins in its membrane. Therefore, in the second part of this project, I focused on studying the effects of different lipid compositions on the structural conformations of a model peptide (melittin) and a PLP derived peptide. Since the lipid composition of myelin changes during demyelination, this would suggest that not only should the microdomains be affected but that protein-lipid interactions also could suffer a change which could possibly lead to proteins malfunctioning. By adding melittin to each of the two myelin systems, it can be determined how the presence of the peptide would affect the inherent physical properties of the domains, as well as determining how the peptide's secondary structure is affected in each system. This information would suggest by how much protein structures are affected during demyelination as well as how much the lipid rafts differ from each other in the presence of proteins. Once melittin's interactions had been characterized, I studied the interactions of a

peptide derived from the C-terminus of PLP, with the model membranes. This peptide segment is located on the cytoplasmic side of the myelin membrane and has theoretically been described as being a loop that could potentially act as a membrane anchor or even has the ability to bind other surrounding proteins. Furthermore, this peptide has not been previously characterized and thus this study examined how the structure of this peptide and its binding affinity changed with the various model membrane systems. By comparing the peptide's structural changes and interactions with the healthy and diseased myelin models, some light may be shed on how the proteins' structures within the myelin membrane are affected during MS and what the possible consequences could be.

CHAPTER 2

BIOPHYSICAL TECHNIQUES FOR THE STUDY OF PEPTIDE-LIPID INTERACTIONS AND LIPID DOMAIN FORMATION

2.1 Model membranes

The complexity of cell membranes makes them very difficult to use for studying specific interactions. For this reason, model membranes are extensively used to mimick simple membrane bilayers where protein-lipid interactions as well as lipid domain formations can be more easily studied. There exist a number of different types of membrane models that are currently used, such as the supported lipid bilayers (SLB), tethered bilayer lipid membranes (t-BLM) and lipid vesicles or liposomes. Vesicles, structures enclosing a small amount of an aqueous solution, are the most widely type of lipid systems used in membrane studies due to their spherical similarity to the cell where the inner environment is separated from the outside environment by the lipid barrier (Lasic, 1998). These vesicle structures arise due to the physical properties of the large number of lipids that make up the cell membrane. Most membrane lipids have a polar head group attached to two hydrophobic hydrocarbon chains which gives them an amphiphilic character (Nelson and Cox, 2008). These lipids are usually only soluble in organic solvents such as chloroform and methanol, and when placed in an aqueous environment, will spontaneously fold into vesicles and enclose some of the solution they were found in. This folding process allows the lipids to reposition themselves so that their polar head groups are exposed to the aqueous environments, both on the inside of the vesicle as well as outside, whereas the extremely hydrophobic hydrocarbon chains are shielded from the aqueous environments in what is known as the vesicle's hydrophobic core (Nelson and Cox, 2008, 2004; Kaier *et al*., 2011).

2.1.1 Size-dependent vesicle preparation

Vesicles are not only used for basic research purposes but are also applied in real life situations where they are used as vehicles for drug application, for gene transfer in medical therapy and genetic engineering, and as microcapsules for proteolytic enzymes in the food industry (Moscho *et al.*, 1996). For these applications, a number of methods have been developed to prepare vesicles different sizes, membrane compositions, and layer structures. Vesicles are easily made since they form spontaneously as a result of unfavourable interactions between water and phospholipids. However, the real challenge lies in controlling their size and structure. Depending on the size of vesicles to be made, there exist a number of different methods that can be used. Lipids are usually first dried down in a thin film before being resuspended in an appropriate buffer, suitable for the type of studies that it will be used for. Upon rehydration, the lipids initially swell and then self assemble to form multilamellar vesicles (MLVs). These MLVs are often broken down into unilamellar vesicles since they make excellent model systems for studying the dynamics and structural features of many cellular processes, including viral infection, endocytosis, exocytosis, cell fusion, and transport phenomena. Unilamellar vesicles are also much easier to study with and provide a simpler working platforms compared to MLVs. Small unilamellar vesicles (SUVs), which are usually around 30nm in size, are often produced by high energy probe sonication of the suspension of MLVs which causes them to break down and form SUVs (Huang, 1969). Large unilamellar vesicles (LUVs), ranging from around 100nm to 500nm in size, are the preferred type of vesicles used in most studies, since they are more stable than SUVs owing to their lower curvature which puts less strain on the lipids. These vesicles are often produced by

freeze-thawing followed by extrusion which forces the MLVs through membranes with a specific pore size so that they break down and form uniform unilamellar vesicles of a defined size. Giant unilamellar vesicles (GUVs) on the other hand can reach sizes of up to 100µm and are much harder to prepare. These vesicles are usually produced by the application of a static (DC) electric field to the lipid suspension in order to generate the growth of GUVs. All these different vesicles have many applications, but for this study, the focus was put on the preparation and study of 100nm LUVs that were prepared though extrusion.

2.1.2 Characterization of myelin domains using model membrane systems

For this thesis, six different lipid systems (see Table 2.1) were selected to study lipid microdomain formation and peptide-lipid interactions. Since I was interested in characterizing the differences between healthy and diseased myelin, two model membranes to represent these conditions were used. These model systems have previously been used to study the impact of MS on myelin's lipid composition (Lee *et al.,* 2011), and will therefore be useful for our purpose. Each of the lipid systems used were chosen for very specific reasons and their unique physical traits. An unsaturated phospholipid 1-palmitoyl-2-oleoyl-sn-glycero-3-phosphocholine (POPC) system was selected to represent a liquid disordered (L_d) system since its gel to liquid crystalline phase is below 0^oC, which would imply that at room temperature, the system should be fully fluid and disordered. This system would theoretically contain only a slight amount of ordered lipids, if any, and will therefore serve as a control raft-free system. The second system composed of equimolar concentrations of sphingomyelin, POPC and cholesterol, is commonly known as the "canonical raft mixture" in

literature and has been shown to be in the liquid-ordered (L_o) state common for the development of lipid rafts (Veatch and Keller, 2003) and will thus represent a control for lipid rafts. By properly characterizing the POPC and the raft systems which define the two extremes of the fluidity scale, I can thus establish the relative fluidity of most systems since they should lie somewhere in between these two points. Four other systems (See Table 2.1) were used to represent i) the plasma membrane (Lamarche *et al.,* 2007), ii) a cytosolic myelin membrane model containing a high level of cholesterol and negatively charged lipids (Inouye and Kirschner, 1988), and iii) two myelin models representing the differences between the healthy and the diseased forms of myelin (Lee *et al.,* 2011). Each of these systems will be characterized using FRET to establish their microdomain profiles and then probed with melittin and a PLP peptide to study how the protein-lipid interactions influenced changes in these domains.

Table 2.1: Lipid composition and content of model membranes investigated

POPC (PC), POPE (PE), POPS (PS), POPI (PI), sphingomyelin (SM) and cholesterol dissolved in chloroform were all mixed in appropriate amounts to give the following lipid composition in each systems.

Lipid system	***Membrane model***	***Lipid Composition (%mol)***
1	Fluid model	PC only
2	Raft Model	PC/SM /Cholesterol (33.3:33.3:33.3)
3	Plasma membrane model	PC /PE/PS/Cholesterol (44:25:10:20)
4	Cytosolic myelin model	PC/PE /PS /SM/ PI / Cholesterol (11:27:13:2:3:2:44)
5	Healthy myelin model	PC/PS/PE/SM/Cholesterol (25.9:7.3:29:6.2:31.6)
6	Diseased myelin model	PC/PS/PE/SM/Cholesterol (20.1:7.4:32.9:2.2:37.4)

2.2. Protein lipid interactions and consequential secondary conformational changes

In the second part of this project, I focused on peptide-lipid interactions involving the model membranes and a model peptide or a myelin specific protein peptide. The myelin peptide was derived from the C-terminus of PLP, which according to PLP structural models in literature, indicated that it should have a tendency to associate with the cytosolic side of the myelin membrane. By combining these peptides with the lipid systems, it can be determined how they interact with the microdomains present by measuring FRET as well as circular dichroism (CD) spectroscopy to determine any conformational changes that might occur in the different membrane environments.

2.2.1 Melittin as a model peptide

Melittin is the major protein component of the venom of the honey bee *Apis melifera* and it has both haemolytic as well as antimicrobial properties (Terilligert and Eisenbergg, 1982). It is one of the most widely studied peptide in terms of its conformational properties and its action of mechanism, which is precisely why it was selected as a model peptide for this study. Melittin is a small protein containing 26 amino acids (Gly-Ile-Gly-Ala-Val-Leu-Lys-Val-Leu-Thr-Thr-Gly-Leu-Pro-Ala-Leu-Ile-Ser-Trp-Ile-Lys-Arg-Lys-Arg-Gln-Gln-NH_2), and usually adopts a random coil conformation in solution but spontaneously forms an alpha helix when it comes in contact with lipid membranes and thus can induce lysis of the cell (Klocek *et al.,* 2009; Hartings *et al.,* 2008). Since melittin is positively charged (pI=12.3), binding to anionic lipid vesicles is usually induced by the electrostatic interactions which then results in chemical adsorption where melittin inserts itself into the lipid bilayer (Hartings *et al.,* 2008). The polypeptide backbone of melittin usually has a kink in it due to the bulky presence of an imine side group from the proline residue and the resulting shape in a bent alpha helix with an angle of around 120^{o}. Residues 1-10 form an α-helical structure which is connected, through the bend at residues 11 and 12, to a longer α -helix containing residues 13-26 (see Figure 2.1) (Klocek *et al.,* 2009; Hartings *et al.,* 2008).

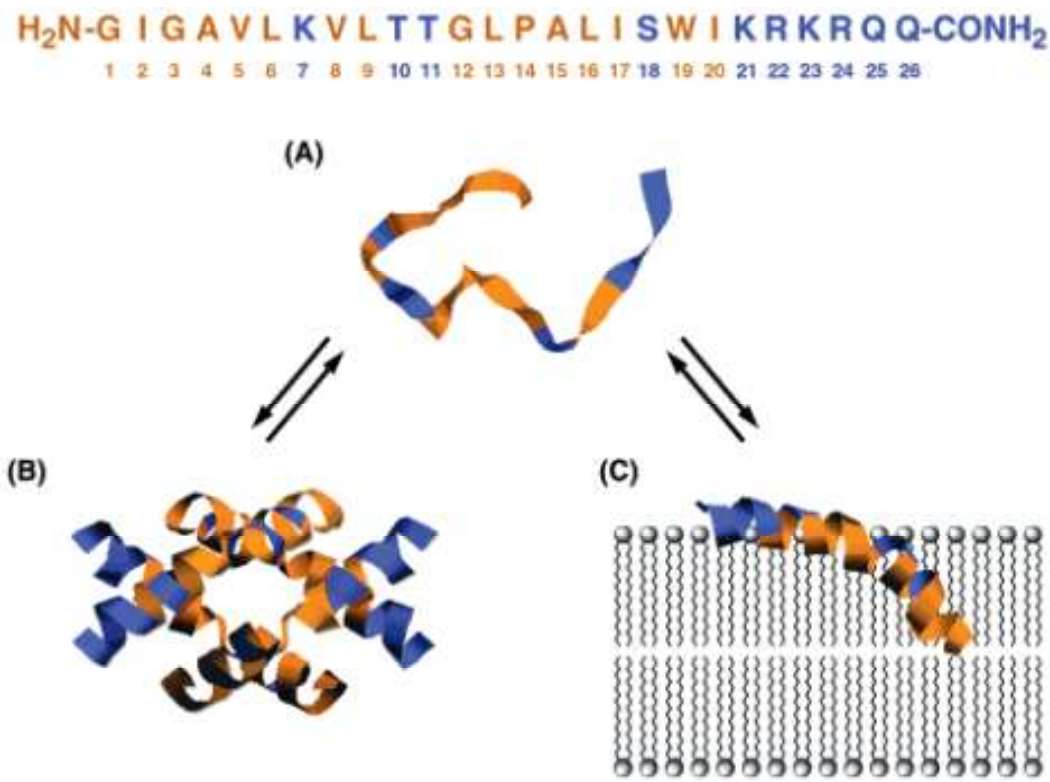

Figure 2.1: The secondary structures of melittin in buffer and lipid environments

Secondary structural change of melittin going from a random coil structure to either a monomeric and tetrameric conformation when lipid bound. Polar residues are shown in blue and hydrophobic residues are shown in orange. Reprinted with permission from the American Chemical Sopciety (ACS) (Niemz, A. and Tirell, D.A. (2001) Self-association and membrane-binding behavior of melittins containing trifluoroleucine. *J. Am. Chem. Soc. 123*:7407–7413) Copyright 2001.

It should be noted that the alpha helix formed is an amphipathic one where one side is polar and the other is more hydrophobic because the side chains of residues 1-6 are all hydrophobic, one side of the helix is somewhat more hydrophobic then the other in this region. While the bulky side chains of Ile-2, Val-5, and Leu-6 are all positioned towards the "inner" side, the opposite face of the helix has only one small Ala-4 chain (Hartings *et al.,* 2008). The same ensues for residues 7 to 20 where the apolar and polar residues are almost

completely segregated from each other as they located on opposite sides of the helix. While Val-8, Leu-9, Leu-13, Leu-16, Ile-17, Trp-19, and Ile-20 which are all hydrophobic are all aligned on one side of the helix, Lys-7, Thr-10, Thr-11, and Ser-18 which are hydrophilic are located on the other side as shown in the helical wheel for melittin (see Figure 2.2). The last 6 residues on the C-terminus are highly hydrophilic, with 2 Lys and 2 Arg residues which confers an overall positive charge to this part of the helix (Terilliger and Eisenbergg, 1982). The melittin chain can thus be divided into three regions based on the distribution of polar and apolar side chains: 1) a hydrophobic NH_2-terminal region, 2) a central section with hydrophobic and hydrophilic faces, and 3) an entirely hydrophilic C-terminal region.

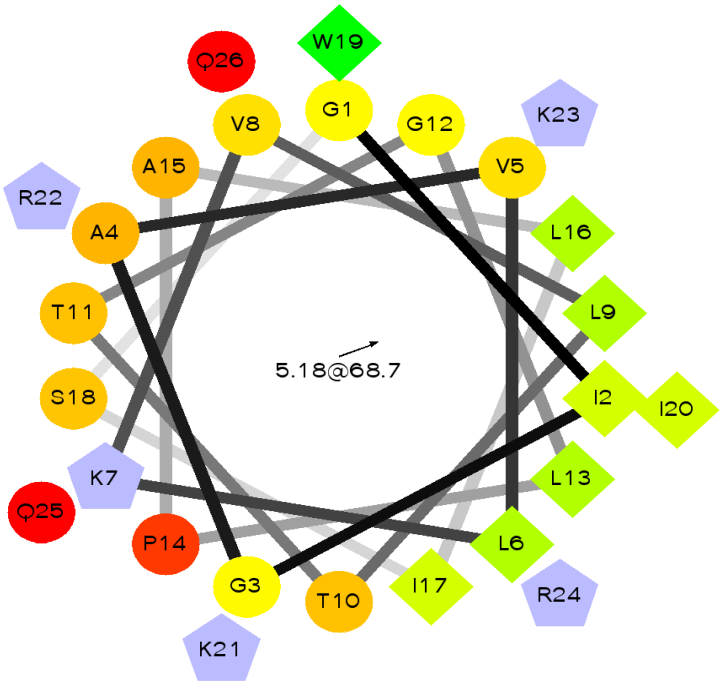

Figure 2.2: Helical wheel of melittin showing the amino acid arrangement in the helical structure

Melittin has the following amino acid sequence GIGAVLKVLTTGLPALISWIKRKRQQ. By default the output presents the hydrophilic residues as circles, hydrophobic residues as diamonds, potentially negatively charged as triangles, and potentially positively charged as pentagons. Hydrophobicity is color coded as well: the most hydrophobic residue is green, and the amount of green is decreasing proportionally to the hydrophobicity, with zero hydrophobicity coded as yellow. Hydrophilic residues are coded red with pure red being the most hydrophilic (uncharged) residue, and the amount of red decreasing proportionally to the hydrophilicity. The potentially charged residues are light blue. The hydropbic moment indicate the general direction in which most of the hydrophobic residues is located once the peptide has folded into an alpha helix. (Created using Don Armstrong and Raphael Zidovetzki's helical wheel script. Version: Id: **wheel**.pl,v 1.4 2009-10-20 21:23:36 don Exp.)

The secondary structure of melittin can be affected by a number of factors, including by the environment it is found in. Depending on the pH and ionic strength of the solution as well as the peptide concentration, melittin can aggregate and form a tetramer which makes it soluble in buffer solutions. The four melittin chains in the tetramer are nearly identical in conformation (see Figure 2.1) and it has been suggested that they can form torroidal pores in

cell membranes and phospholipid vesicles that cause leakage of cellular contents (Niemz and Tirell, 2001).

In this study, melittin was introduced into each of the lipid systems (described in section 2.1.2), in order to determine how the conformation of the peptide is affected in each and how this in turn affects the microdomain profile of the model membranes. FRET was used to monitor changes in the microdomains' properties whereas CD was used to determine the peptide's overall secondary structure. By analysing the results of these experiments, one can determine the microdomain fluctuations in each lipid system as well as the conformational changes induced in melittin. This may subsequently lead to a better understanding of the potential effects that changes in the composition of myelin can have on the structure and function on its membrane proteins.

2.2.2 Myelin proteolipid protein

The myelin proteolipid protein (PLP), which is a hydrophobic integral membrane lipoprotein, is one of the most abundant proteins found in CNS myelin. The function of PLP is still relatively unknown but it has been proposed that it could be involved in several functions such as membrane adhesion and compaction of myelin, maturation of oligodendrocytes, involvement in early stages of oligodendrocyte/axon interactions and wrapping of the axon, and finally in the maintenance and survival of axons (Greer and Lees, 2002). Its exact function has not yet been determined due to its physical properties, namely its extreme hydrophobicity, which makes it difficult to work with. Human PLP is a highly basic (pI= 9.3)

intrinsic membrane protein consisting of 276 amino acids. PLP is believed to form four transmembrane helices which span the myelin membrane (see figure 2.3) and its N-terminus and C-terminus should be found on the cytoplasmic side of the membrane (Greer and Lees, 2002; Hudson, *et al.,* 1989)

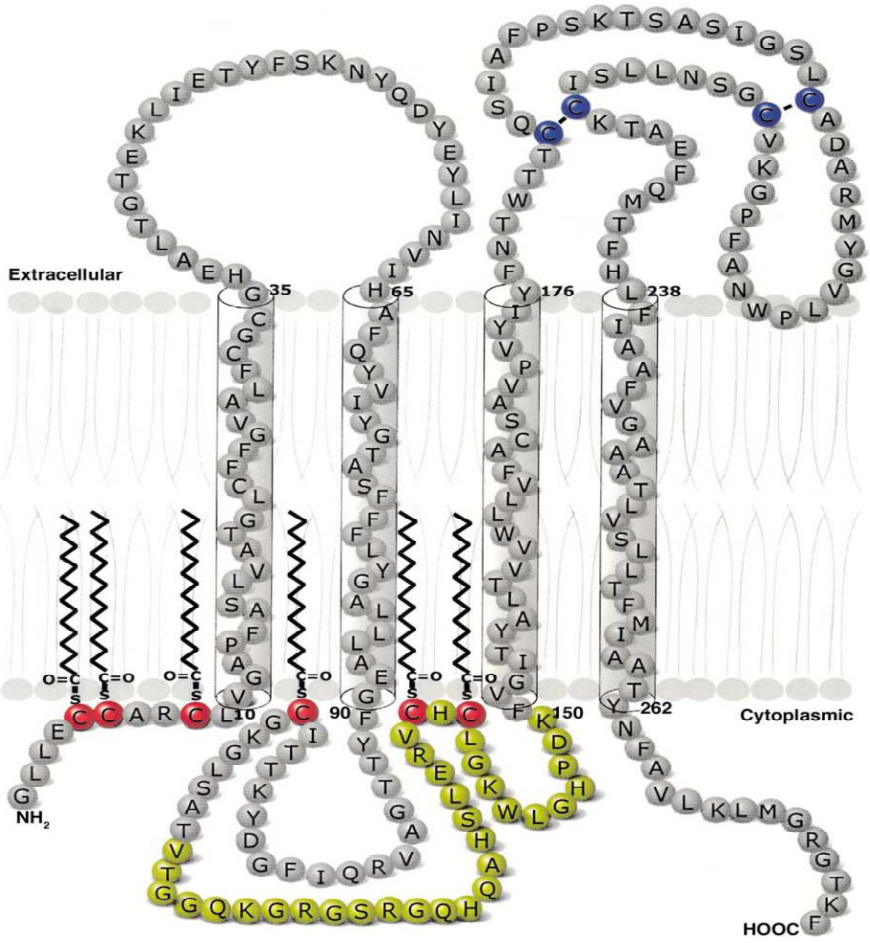

Figure 2.3: Probable structure and orientation of PLP in the myelin membrane

PLP is a tetraspan protein, with four transmembrane helices spanning the myelin membrane, and with the NH_2 and COOH termini both located on the cytoplasmic face of the membrane. The yellow region represents the sequence that is missing in DM20 (isoform). The red Cys residues represent the possible sites of acylation which could act as membrane anchors. Reprinted with permission from Elsevier Science Ltd (Greer, J.M. and Lees, M.B. (2002). Myelin Proteolipid protein- the first 50 years. Int. J. Biochem. Cell Biol. 34: 211–215) Copyright 2002.

Since PLP is so abundant in the white matter of the brain, it is also believed that it might play a very important role in neurological disorders such as MS. As a major component of CNS myelin, PLP is a candidate target antigen for autoimmune attack in demyelinating diseases. It has been shown that the injection of PLP in experimental animals, can induce an autoimmune demyelinating disease known as experimental autoimmune encephalomyelitis (EAE), which displays similar features and pathology to MS (Greer and Lees, 2002; Hudson, *et al.,* 1989; Werner *et al.,* 2007). Since PLP could be a major factor in triggering MS and because there is still so much to learn about this protein, I decided to select a PLP peptide and study its interactions with different model membranes in this study. In this case, I selected the C-terminus of human PLP (residues 258-277), located on the cytoplasmic side of the membrane and having the following amino acid sequence Ile-Ala-Ala-Thr-Tyr-Asn-Phe-Ala-Val-Leu-Lys-Leu-Met-Gly-Arg-Gly-Thr-Lys-Phe. This peptide was selected after careful analysis of some of the loop regions present in PLP using online secondary structure prediction softwares such as Yaspin, Jpred and the Protein Predict software, as well as the level of difficulty in synthesizing these loops in the lab. Several sections of the PLP protein were anaylsed and among these were the loop regions with residues 131-157, 198-220 and the C-terminus containing residues 258-277. Not only did the C-terminus appear to be relatively easy to chemically synthesize under the right conditions but it also predicted to be alpha helical in structure. The C-terminus peptide could potentially be acting as a membrane anchor or even as a site of binding for other membrane proteins. By introducing this PLP peptide into the model membrane systems, one can determine its structural conformation as well as its binding affinities to different membrane lipids. Figure 2.4 shows the helical wheel

of the PLP peptide and conveniently shows that it has the properties to adopt the structure of an amphipathic alpha helix.

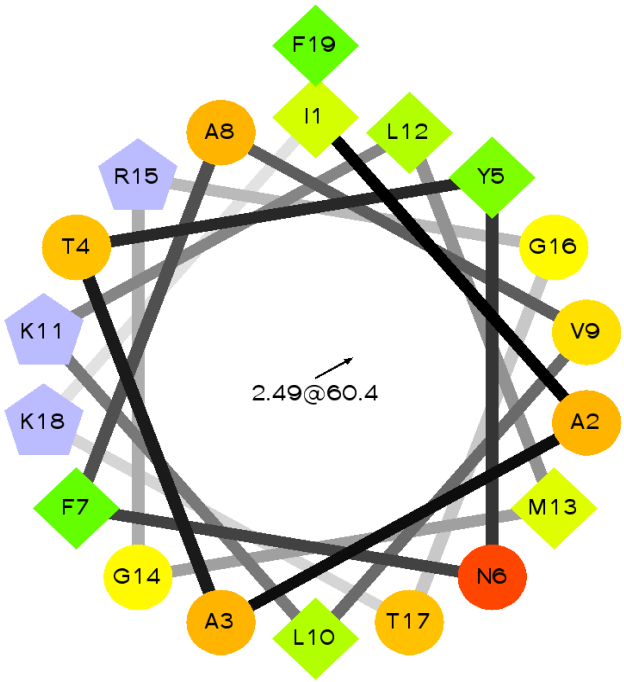

Figure 2.4: Helical wheel of C-terminus PLP (258-277) showing the amino acid arrangement in the helical structure

The C-terminus PLP peptide has the following amino acid sequence IAATYNFAVLKLMGRGTKF. By default the output presents the hydrophilic residues as circles, hydrophobic residues as diamonds, potentially negatively charged as triangles, and potentially positively charged as pentagons. Hydrophobicity is color coded as well: the most hydrophobic residue is green, and the amount of green is decreasing proportionally to the hydrophobicity, with zero hydrophobicity coded as yellow. Hydrophilic residues are coded red with pure red being the most hydrophilic (uncharged) residue, and the amount of red decreasing proportionally to the hydrophilicity. The potentially charged residues are light blue. *(Created using Don Armstrong and Raphael Zidovetzki's helical wheel script. Version: Id: **wheel**.pl,v 1.4 2009-10-20 21:23:36 don Exp.)*

2.3 FRET as a method to monitor changes in microdomain formation

In order to monitor changes in the microdomain profile of each of our model systems, FRET was used to investigate each of them. FRET is an extremely sensitive technique that has

been widely used to probe membrane microdomains within the 10 to 40 nm range (Loura *et al.,* 2009). FRET is a photophysical process that causes fluorescence quenching of a donor molecule in an excited state through non-radiative transfer of energy (via long-range dipole-dipole coupling) to another acceptor molecule in the ground state, provided that the acceptor's absorption spectrum overlaps with the emission spectrum of the donor (Lakowicz, 2006). In most biological studies where FRET is involved, only one pair of molecules interacts, which makes the transfer kinetics simpler to understand, thereby enabling easy determination of distances at the molecular scale (Loura *et al.,* 2009; Jares-Erijman and Jovin, 2003). The commonly used experimental observable obtained is the FRET efficiency, E, and this can be calculated from the ratio of intensity of donor steady-state emission in the presence (I_{DA}) and absence (I_D) of the FRET acceptor as described in the equation below (Loura *et al.,* 2009, Jares-Erijman and Jovin, 2003):

$$E = 1 - \frac{I_{DA}}{I_D} \quad \text{..... Equation 2.1}$$

FRET can be very useful in studying membrane microdomains, if the proper probes are used. The most common procedure would be to use two probes with one having a higher affinity for the L_o domains and the other for the L_d phase. Once the probes are incorporated in the lipid bilayer, their FRET efficiency can be measured and it is expected that an increase in the lateral heterogeneity (L_o and L_d) will result in a decrease of FRET efficiencies (E) when both donor and acceptor molecules segregate to their preferred lipid domains (Jares-Erijman and Jovin, 2003; Sengupta *et al.,* 2007). This is a direct result of the average distance

between the two molecules increasing, therefore making it harder for energy transfer to occur. However, if both probes prefer the same domains, this will lead to an increase in the values of E since the probes are in very close proximity to each other (see Figure 2.5).

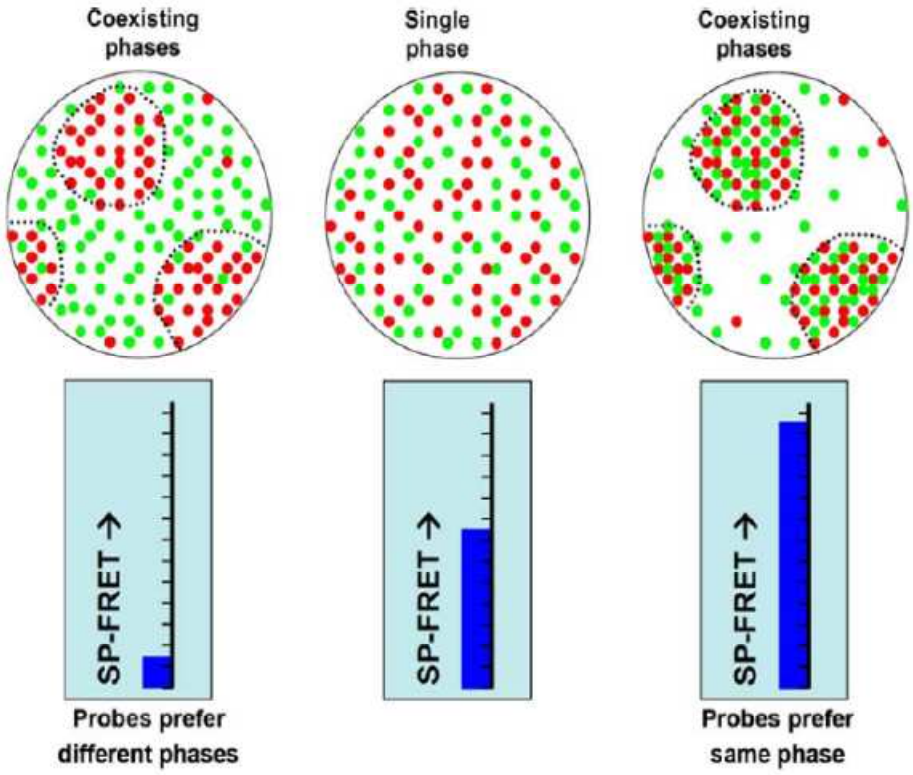

Figure 2.5: Schematic representation of the effect of phase separation and probe partition on the FRET efficiency.

D and A molecules are represented by green and red dots, respectively. In a single-phase membrane, an intermediate FRET signal intensity is observed. In the presence of coexisting phases, however, the probes can partition preferentially between alternative environments, causing their local concentrations to rise or fall. If the probes prefer different phases, they are effectively separated, reducing FRET. If the probes prefer the same phase, they are effectively clustered and the FRET signal increases. Reprinted with permission from European Biophysics Journal (Loura, L.M.S., Fernandes, F. and Prieto, M. (2010). Membrane microheterogeneity: Förster resonance energy transfer characterization of lateral membrane domains. *Eur. Biophys. J.* 39:589–607) Copyright 2010.

The probes selected for this study are very commonly used in FRET studies, namely 1,2-dipalmitoyl-*sn*-glycero-3-phosphoethanolamine-N-7-nitro-2-1, 3-benzoxadiazol-4-yl (NBD-DPPE) as the donor probe and 1,2-dioleoyl-*sn*-glycero-3-phosphoethanolamine-N-lissamine rhodamine B sulfonyl (Rhod-DOPE) as the acceptor probe. Depending on the degree of saturation of their acyl chain, this will cause the probes to either favour the L_d or the L_o phase. In this case, NBD-DPPE has two long saturated acyl chains which allow it to partition into the L_o phases whereas, Rhod-DOPE has two acyl chains each of which contains a double bond, causing it to partition in the L_d phase. The structures of the donor and acceptor probes are shown in Figure 2.7.

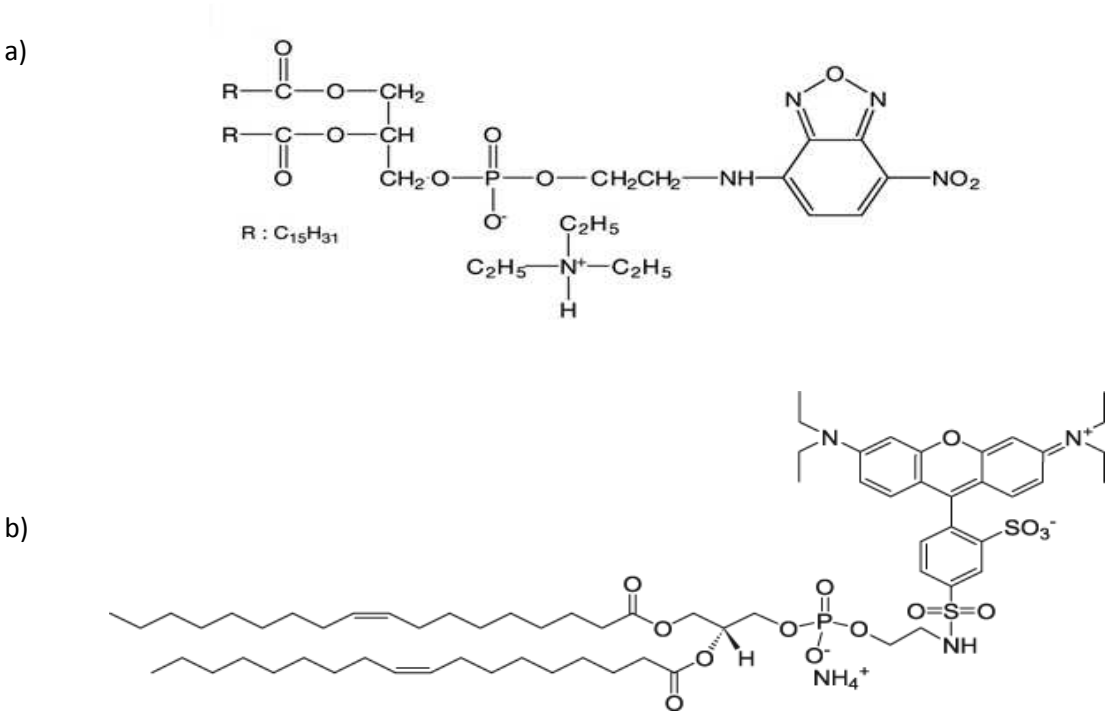

Figure 2.6: Structure of the donor and acceptor probes used in FRET studies

The figure shows the structure of a) NBD-DPPE and b) Rhod-DOPE. These probes acted as donor-acceptor pairs in the FRET studies used to study lipid raft formation. NBD-DPPE preferentially partitions into the L_o phase, whereas Rhod-DOPE prefers the L_d phase.

2.4 Tryptophan fluorescence and melittin

Tryptophan fluorescence is commonly used in membrane studies to study the degree of interaction between a protein or peptide with the lipid bilayer. Usually proteins or peptides containing tryptophan residues will exhibit changes in its fluorescence emission intensity and in the wavelength of its emission maximum, depending on the type of environment they are found in. Tryptophan typically displays a blue shift upon going from an aqueous environment to a more hydrophobic one with a smaller dielectric constant such as in membrane bilayers (De Kroon *et al.,* 1990). The emission fluorescence of tryptophan, ranging from around 308nm to 355nm, is sensitive to its local environment and is dependent on the degree of solvent exposure of the chromophore (Vivian and Callis, 2001). This interesting property makes tryptophan fluorescence useful for estimating the degree of binding of peptide or proteins to membranes of different lipid composition. The model peptide melittin is intrinsically fluorescent due to the presence of a single tryptophan residue, Trp-19, which makes it a sensitive probe to study the interaction of melittin with membrane-mimetic systems (Raghuraman and Chattopadhyay, 2004). This property of melittin is particularly useful because there are no other intrinsically fluorescent aromatic amino acids in melittin and this makes interpretation of fluorescence data less complicated due to lack of interference and heterogeneity.

2.5 Circular dichroism (CD) spectroscopy for the determination of protein secondary structure

In the second part of this project, I focused on peptide-lipid interactions involving the PLP peptide and the model peptide melittin were investigated. The study of lipid-protein interactions is of particular importance because cells have the ability to vary the lipid composition of their membrane in response to a variety of stress and stimuli, thus changing the environment and the activity of the proteins associated with the membrane. By combining melittin and the PLP C-terminus peptides with different lipid systems, I would like to determine how they interact with the microdomains present by measuring FRET. Circular dichroism (CD) spectroscopy was also used to determine if there were any conformational changes that might result due to changes in the membrane environments. Generally, CD spectroscopy measures differences in the absorption of left-handed polarized light versus right-handed polarized light which results from the protein's structural asymmetry. If the protein has an ordered structure, it will generate a specific signal that can either be positive or negative or both. The secondary structure of proteins are usually determined in the far UV region (190-250nm) for at these wavelengths the peptide bond acts as the chromophore giving rise to specific signals for the alpha-helix, beta-sheet, and random coil structures in the protein (see figure 2.7) (Kelly *et al.,* 2005).

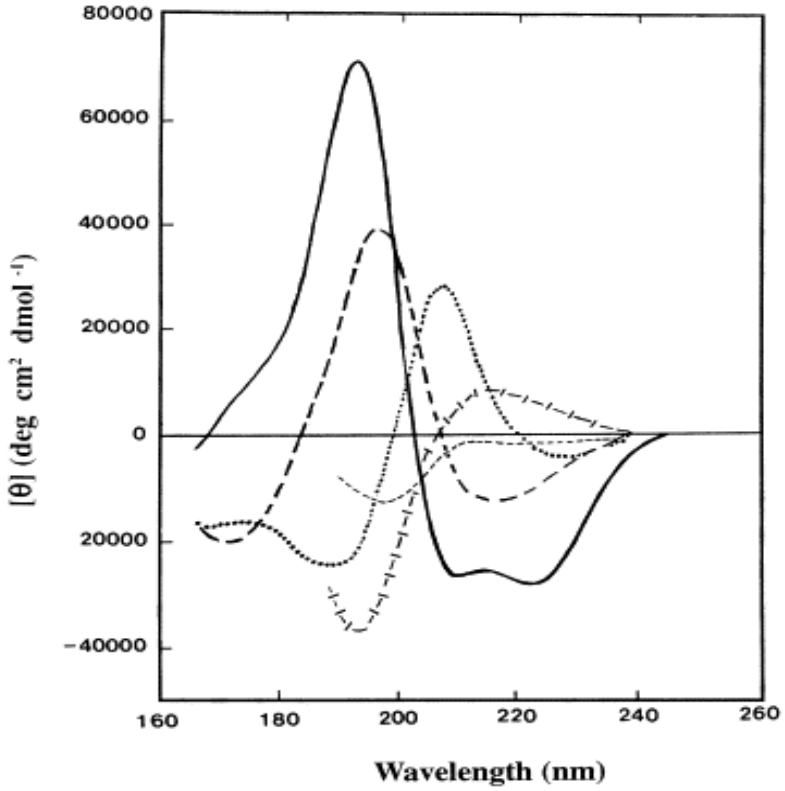

Figure 2.7: Far UV CD spectra of various protein secondary structures

Solid line, α-helix; long dashed line, anti-parallel β-sheet; dotted line, type I β-turn; cross dashed line, extended 3_1-helix or poly (Pro) II helix; short dashed line, irregular structure. Reprinted with permission from Elsevier (Kelly, S.M., Jess, T.J., and Price, N.C. (2005) How to study proteins by circular dichroism. *Biochim. et Biophys. Acta* 1751: 119 – 139) Copyright © 2005, Elsevier.

2.6 Isothermal titration calorimetry (ITC) for the determination of binding affinities

Studying how biomolecules interact with other molecules is key for understanding biological functions. Consequently, a number of factors, such as the strength and specificity of the interactions, have to be taken into consideration. Isothermal titration calorimetry (ITC) is commonly used as a direct and efficient method to measure the energy associated with a chemical reaction, triggered by the mixing of two components (Leavitt and Freire, 2001). The thermodynamics of interactions between different molecular species are

determined by the number and types of bonds that are made by the component molecules. For this reason, ITC experiments are usually carried out through injections of a ligand, such as a lipid suspension, into a solution containing the peptide solution as shown in Figure 2.8. Upon interaction of the two reagents, a heat of reaction is either released or absorbed depending on the type of reaction taking place. The heat profile observed is proportional to the amount of lipids that binds to the peptide in each injection and the heat of reaction is obtained by calculating the area under each peak generated so that the sum total of these will give the enthalpy (ΔH) of the reaction (Leavitt and Freire, 2001, Ladbury and Chowdhry, 1996). As the reaction goes to completion, the peptide solution will become saturated, and further injections will only give small heat peaks indicative of either mechanical or dilution effects that need to be subtracted from all the injection peaks before analysis (Leavitt and Freire, 2001). Calorimetric measurement is the only method available for the direct determination of thermodynamic parameters associated with an interaction, since the enthalpy change will showcase the extent of an interaction (Ladbury and Chowdhry, 1996). By effectively comparing the measurements for the interaction of the PLP peptide with specific lipid systems, one can determine which lipid interactions are favoured by this peptide. Since so little is known about the structure and the interaction of this peptide, measuring ITC will help to shed some light on whether the peptide-lipid interaction is entropy driven or more dependent on electrostatic interactions.

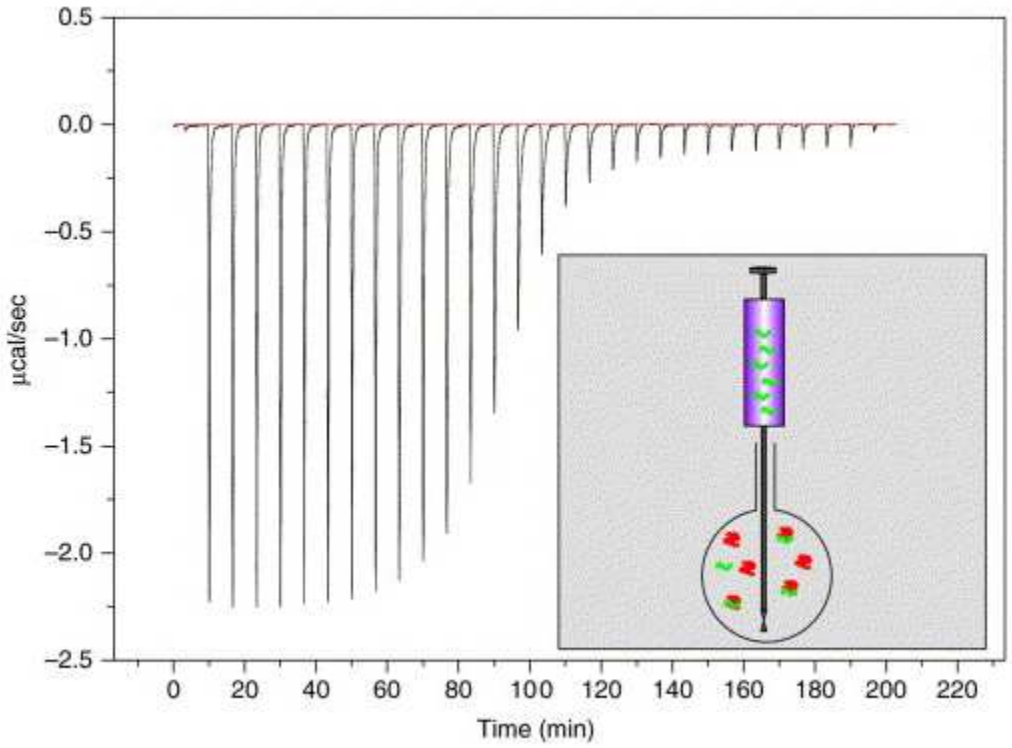

Figure 2.8: The experimental setup and typical profile for ITC

A typical ITC experiment showing the titration of a ligand into a cell that contains a peptide solution. As the solution in the cell becomes saturated, the residual heat effects originate from dilution of the peptide and also from mechanical effects associated with the injection. These effects need to be subtracted before thermodynamic analysis.Reprinted with permission from Elsevier (Leavitt, S. and Freire, E. (2001). Direct measurement of protein binding energetics by isothermal titration calorimetry. *Curr. Opin. Struc. Biol*. 11:560–566) Copyright 2001.

CHAPTER 3

MATERIALS AND METHODS

3.1 Materials

The lipids that were used to make model membrane vesicles are palmitoyl-oleoyl-phosphatidylcholine (POPC), palmitoyl-oleoyl-phosphatidylethanolamine (POPE), palmitoyl-oleoyl-phosphatidyinositol (POPI), palmitoyl-oleoyl-phosphatidylserine (POPS), egg sphingomyelin (SM), and cholesterol (Avanti Polar Lipids, AL, USA). Buffers were prepared using 2-amino-2-hydroxymethyl-propane-1,3-diol (Tris), 4-(2-hydroxyethyl)-1-piperazineethanesulfonic acid (HEPES), sodium chloride (NaCl), sodium fluoride (NaF). Once prepared, the vesicles were resuspended in a 5mM HEPES, 150mM NaCl, pH 7.4 buffer for FRET and ITC measurements. For CD experiments, the vesicles were resuspended in 100mM Tris, 10mM NaF buffer pH 7.4 to minimize any absorption interference. The fluorescent probes used were 1,2-dipalmitoyl-*sn*-glycero-3-phosphoethanolamine-N-7-nitro-2-1, 3-benzoxadiazol-4-yl (NBD-DPPE) and 1,2-dioleoyl-*sn*-glycero-3-phosphoethanolamine-N-lissamine rhodamine B sulfonyl (Rhod-DOPE) (Avanti, Polar Lipids, Alabama USA). The peptides used were: Melittin (5mg, Sigma-Aldrich, Oakville, ON) with an HPLC purity of greater than 85% and PLP's C- terminal (258 to 277) peptide IAATYNFAVLKLMGRGTKF (20mg) with an HPLC purity of over 95% (aappTEC, KY, USA). Both peptides were dissolved in Milli-Q water to make up stock solutions. The concentrations of the peptides in solution were then determined by measuring their absorbances at 280nm and using the extinction coefficients of their aromatic residues.

3.2 Methods

3.2.1 Vesicle preparation

LUVs were used throughout this project to study lipid microdomain formation and their ensuing interactions with melittin and the PLP peptide. LUVs, with a diameter of a 100nm, were selected since they are similar in size to many intracellular membranes such as the mitochondria. These vesicles are very nearly unilamellar and they offer a reasonable radius of curvature which is closer to what is found in natural membranes unlike SUVs. Even though MLVs would better represent the myelin sheath, both in dimension and composition, I started off using unilamellar vesicles since they offer a well-defined single bilayer which would give better measurement readings and would also be easier for interpretation. The LUVs were prepared by first dispensing the appropriate volumes of the lipid stocks into round bottom flasks. For FRET measurements, NBD-DPPE and Rhod-DOPE were added so that their final concentrations were at 0.8 and 0.2 %mol, respectively. Stock solutions of each lipid (POPC, POPS, POPE, POPI, SM and cholesterol) were previously prepared in chloroform at a concentration of 25mg/ml and were stored in the dark, at -20°C. Aliquots of these stock solutions were mixed and dried under reduced pressure by passing a gentle stream of nitrogen over them to promote evaporation of the solvents. The resulting thin lipid film was then further dried overnight in a vacuum dessicator in order to remove of any traces of residual solvent. The following morning, the lipids were hydrated in buffer solution and briefly exposed to a bath sonicator to ensure that all the lipids were resuspended. It should be noted that for all fluorescence and ITC measurements, lipids were resuspended in 5mm HEPES 150mM NaCl pH 7.4 buffer whereas 100mM Tris, 10mM NaF pH 7.4 buffer was used

for vesicles prepared for CD measurements. The lipid suspensions were then frozen and thawed five times before being passed 19 times through a 100nm polycarbonate membrane using a syringe extruder (Avestin, Ottawa, Canada) to give uniform LUVs. Vesicles were prepared fresh on the day of the experiment to minimize the possibility of lipid oxidation.

3.2.2 FRET measurements

For FRET measurements, the donor and acceptor probes in chloroform/methanol (4:1) were added to the lipid system at a probe to lipid concentration of 1:125 (0.8 %mol) and 1:500 (0.2 %mol) respectively. The vesicles were allowed to equilibrate for about an hour at 25^{o}C before measurements were taken. The acceptor, Rhod-DOPE, which has a maximum excitation wavelength of 560nm, was expected to partition into L_d phase whereas the donor NBD-DPPE which has a maximum excitation wavelength of 460 nm, was expected to partition into the L_o (rafts) phase based on the saturation of their acyl chains. With the partitioning of the probes, characterization of the domains can be completed in each of the systems. For each lipid system, four preparations were used, each of which contained a different combination of the probes. The first lipid preparation contained no probes and was used as the blank to establish a base line. The second preparation contained only the donor probe while the third one contained the acceptor only and both of these systems were used as controls for concentration corrections. The last preparation contained both donor and acceptor probes and was used to monitor energy transfer.

Steady-state fluorescence emission spectra were obtained using a Varian Eclipse spectrofluorometer and the temperature was controlled by a circulating water bath. FRET

measurements were carried out at room temperature (25^{o}C) using a quartz cuvette with a 1cm pathlength. Three different sets of excitation and emission wavelengths were used:

1) Excitation at 428nm and emission at 450nm

2) Excitation at 465nm and emission at 475nm

3) Excitation at 560nm and emission at 570nm

The two excitation wavelengths at 428nm and 465nm were used to ensure that the acceptor probe, which has an excitation wavelength of 560nm, was not being directly excited. Excitation at 560nm was performed as a control to determine the emission spectrum of the acceptor and was used for concentration corrections. Once the vesicle systems had been characterized, a small aliquot of melittin was added at a final concentration of 10µM (1 mol%), mixed by quick vortexing and allowed to equilibrate for about 5 minutes before FRET measurements were taken again at the same conditions described above. The FRET efficiency was then calculated, both in the presence and absence of melittin, to establish a microdomain profile for each of the lipid systems, using equation 2.1 (see section 2.3) below where I_{DA} is the intensity in the presence of both donor and acceptor and I_D is the intensity of the donor only.

$$E = 1 - \frac{I_{DA}}{I_D} \qquad \text{..... Equation 2.1}$$

3.2.3 Tryptophan Fluorescence Measurement

Melittin contains only one tryptophan residue and which makes it possible to determine location of the residue in the lipid membrane by measuring its intrinsic fluorescence. Steady-state fluorescence was measured on a Varian Eclipse spectrofluorometer using a 1-cm pathlength quartz cuvette. Melittin was added in small aliquots to the prepared LUVs and allowed to equilibrate for about 5 minutes before fluorescence measurements were taken. The samples were excited at 280nm and the emission spectra were collected from 300nm to 450nm at room temperature (25^{o}C) with the excitation and emission slits set at a nominal bandpass of 5 nm. Samples containing no melittin were used as blanks and their intensity spectra were subtracted from each sample spectrum containing melittin to cancel out any contribution due to the solvent Raman peak and other scattering artefacts.

3.2.4 CD spectroscopy

For CD measurements, the vesicles were prepared as described above using 10mM Tris 100mM NaF buffer pH 7.4. Most of the information for protein structure studies is obtained in the far UV range (190-260nm), but unfortunately, many buffers, as well as proteins themselves, might absorb too strongly in this range thus making it difficult to obtain a clean signal. For this reason, when measuring CD, vesicles were resuspended in 10mM Tris, 100mM NaF pH 7.5 buffer since this buffer containing fluoride ions, has been shown to have the least amount of interference unlike buffers containing chloride ions. Once the vesicles are prepared, the peptides were added and mixed by vortexing and allowed to equilibrate for approximately 5 minutes before readings were taken. Melittin was added to the vesicles at

concentrations of 5µM, 10µM, 20µM, and 40µM at which point the peptide started to aggregate and form a tetrameric structure in most of the lipid systems. The PLP peptide was used at 10µM, 20µM, 40µM and 60µM concentrations where it finally started to show signs of aggregation. All measurements were taken in an Aviv 215 spectropolarimeter using a quartz optical cell with a pathlength of 1 cm. The spectra were recorded in 0.5 nm increments with a 1-s response and a bandwidth of 1nm. An average of 4 scans was taken per sample and after subtraction of the appropriate blank; the spectra were manipulated to give smoothed spectra without critically altering the original ones using the AVIV software provided with the CD instrument. All data were represented as mean residue ellipticities and were calculated using equation 3.1 below.

$$[\theta] = \frac{\theta_{obs}}{10Cl} \quad \text{..... Equation 3.2}$$

where θ_{obs} is the observed ellipticity in mdeg, l is the pathlength in cm, and C is the concentration of peptide bonds in mol/L (Raghuraman and Chattopadhyay, 2004).

3.2.5 Isothermal titration calorimetry (ITC) measurements

ITC measurements were carried out using a VP-ITC micro calorimeter for the PLP peptide at varying concentrations in order to determine the best possible interactions. Lipid into peptide titrations were performed at 25^{o}C by injecting 10µl aliquots of 5mM lipid vesicles into the calorimeter cell containing 1.5ml of the peptide solution a specific concentration.

The heats of dilution were determined in the control titrations by injecting the lipid solution into pure buffer and were subtracted from the final analysis.

CHAPTER 4

CHARACTERIZATION OF LIPID MICRODOMAINS USING FLUORESCENCE RESONANCE ENERGY TRANSFER (FRET)

4.1 Fluorescence resonance energy transfer (FRET) for the study of lipid rafts

The presence of lateral inhomogeneities or lipid domains in the cell membrane is an issue of great interest as well as controversy. Lipid rafts, ordered regions of the cell membrane, are known to be important in cellular function. Since the lipid composition of the myelin membrane has been shown to change during demyelination, this would suggest that the lipid rafts present in the membrane would be affected. In order to investigate the effects of demyelination on the myelin membrane microdomains, fluorescent lipid probes were introduced into myelin mimicking model membrane so as to characterize these domains through FRET. The donor (NBD-DPPE) and acceptor (Rhod-DOPE) probes used in this study contained alkyl chains that differed from each other in terms of the saturation of their carbon chain (See chapter 2, Figure 2.6). This property allows the probes undergo differential partitioning into L_o or L_d environments in the lipid bilayer. While NBD-DPPE prefers to partition into the L_o domains, Rhod-DOPE on the other hand prefers to partition into the L_d phase due to the presence of a double bond in its alkyl chain. The presence of the double bond would introduce a kink into the hydrocarbon chain thereby preventing it from properly stacking itself with the other saturated lipids and thus promoting its partitioning into the L_d phase. By monitoring donor quenching in the presence of the acceptor, quantitative measurements of the energy transfer efficiency in different membrane models can be obtained. The capacity of FRET measurements to discriminate between laterally separated molecules is predicted to be the greatest when the distance between the two probes is approximately equal to one to four times the Forster distance (R_o) of a particular donor/acceptor pair (Dewey and Hammes, 1980; Zimet *et al.,* 1995). The R_o for NBD-DPPE

and Rhod-DOPE is estimated to be between 4.5-7 nm (Wu and Brand, 1994; Thomas *et al.,* 1978) and more recently, FRET studies performed in DOPC vesicles have shown that the Forster distance between NBD-PE and Rhod-PE was determined to be 6.4 nm which would make them sensitive for studying lipid rafts which usually have dimensions in the tens of nanometers (Loura *et al.,* 2000).

4.2 FRET characterization of model membrane systems

4.2.1 Fluorescence of donor probe in model membrane systems

For this study, FRET measurements were carried out using the model lipid systems previously described in Chapter 2, Section 2.1.2. The NBD-DPPE and Rhod-DOPE probes were incorporated during vesicle preparation and the concentrations used, 0.08 %mol and 0.02%mol respectively, were kept relatively low to ensure that the probes did not interfere with lipid stacking and that the natural bilayer structure was preserved. FRET experiments were carried out in the absence and presence of melittin to determine how the presence of the peptide-lipid interactions affected the microdomains in each lipid system. The donor probe was first added to each of the lipid systems to determine its emission spectra at excitation wavelengths of 428nm, 465nm and 560nm. NBD-DPPE has a maximum excitation at around 465nm and should not absorb at 560nm. The emission spectra of the acceptor probe Rhod-DOPE was also measured at the same wavelengths to ensure that there were no significant emissions at excitation wavelengths of 428nm and 465nm which would interfere with the donor probe's absorption. The emission spectra of the acceptor probe at excitation wavelengths of 560nm in the different model membranes are shown in Appendix A. Rhod-

DOPE absorbs most strongly around 560nm and should therefore have a negligible direct excitation at 428nm which was the wavelength used to monitor the FRET efficiency. Lipid systems containing only the acceptor probe therefore served as controls to ensure that the acceptor did not absorb in the same range as the donor. NBD-DPPE on the other hand has a maximum emission around 535nm if excited at a wavelength of 465nm. While fluorescence readings were taken at this wavelength, measurements that were considered in this study were taken at 428nm to ensure no direct excitation of the acceptor probe in systems that contain both probes (Lamarche *et al.,* 2007). The emission spectra of the donor probe NBD-DPPE measured at an excitation wavelength of 428nm, in the presence and absence of melittin, in each of the model membrane systems, is shown in Figure 4.1.

a)

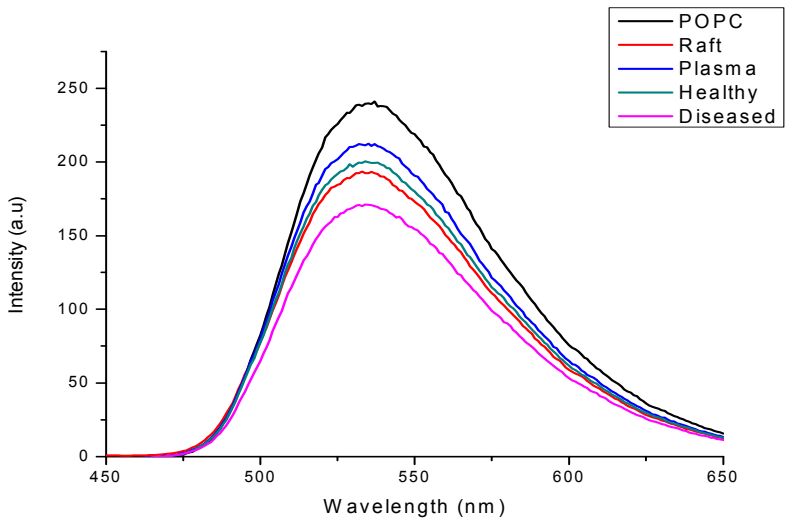

b)

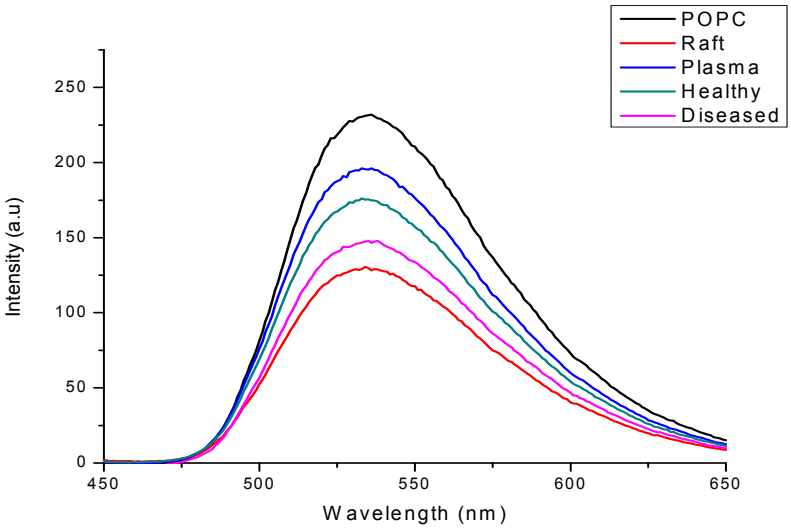

Figure 4.1: Typical fluorescence emission spectra of NBD-PE in the various model membranes

Fluorescence emission was measured at an excitation wavelength of 428nm to determine the difference in intensity between each of the lipid systems used and in the presence and absence of melittin. LUVs were prepared in 5mM HEPES, 150mM NaCl, pH 7.4 buffer and NBD-DPPE was added to the lipid systems at a concentration of 0.8 %mol (1:125 donor: lipid). The emission spectra for NBD-DPPE in a) the lipids system alone and b) in the presence of 10 µM melittin were recorded between 450nm to 650nm for one of the trials conducted in each system.

Although the concentration of the donor probe NBD-DPPE was the same in each lipid system (0.8 %mol), it was observed that the fluorescence emission intensity differed in each system. This phenomenon was also observed in the emission of the acceptor probe

Rhod-DOPE (see appendix A) and could be due to the lipid composition of the systems. In Figure 4.1, it was observed that the POPC system exhibited the highest fluorescence emission intensity whereas the other lipid systems containing cholesterol showed slightly lower intensities (summarized in Table 4.1). An interesting observation was that as the cholesterol content of the model membranes increased, the fluorescence emission of the donor and acceptor probe decreased in turn. While the plasma model and the POPC lipid systems exhibited the highest emission intensity, the higher cholesterol content present in the other lipid systems resulted in a decreased in intensity. The greatest decrease in fluorescence intensity was observed in the raft system and the diseased myelin model. A similar trend was also observed upon the addition of melittin.

Table 4.1: NBD fluorescence emission maxima in the absence and presence of melittin

The donor probe was added to the systems at a concentration of 0.8 %mol and fluorescence was measured at an excitation wavelength of 428nm. Melittin was mixed into the systems after vesicle preparation at a final concentration of 10μM.

Lipid systems	%mol Cholesterol	Fluorescence emission intensity (a.u)	
		Lipids only	Lipids + melittin
POPC	0	235	225
Raft	33.3	193	130
Plasma membrane	20	212	196
Healthy myelin	31.6	200	175
Diseased myelin	37.4	171	148

The NBD moiety, which is relatively photostable, has previously been shown to be weakly fluorescent in aqueous environments but upon transfer to more hydrophobic environments, it fluoresces more brightly. This shows that NBD is highly sensitive to the environment it is in, thus making it ideal for this type of study (Rukhmini *et al.,* 2001; Lin and Struve, 1991).

Previous studies have shown that NBD labeled phospholipids often rearrange themselves in membrane bilayers so that the polar NBD group is located near the interfacial region. However, in the presence of cholesterol, NBD has been shown to be buried almost 5-6 Å from the center of the bilayer (Mukherjee and Chattopadhyay, 1996). One possible explanation for this phenomena, could be that the stereochemical rigidity of the sterol ring prevents the NBD group from looping back to the membrane interface upon vesicle preparation despite the latter's polar nature (Chattopadhyay, 1990). The acceptor probe Rhod-DOPE is believed to suffer the same effects as NBD-DPPE, and the increasing levels of cholesterol only serve to bury the rhodamine head group deeper into the membrane (MacDonald, 1990). Although this effect should technically increase the fluorescence emission of the probes which are now buried in a very hydrophobic environment, the emission spectra obtained instead showed a decrease in fluorescence intensity as the cholesterol content increases. The reason for this could be due to the clustering of these probes into very small lipid domains that would bring them very close to each other. Cholesterol as well as other membrane condensing lipids such as sphingolipids, would promote the formation of lipid domains into which the probes would partition based on the saturation of acyl chains. Separation of lipid phase leads to an increase in the local concentrations of NBD or rhodamine in the bilayer, and their close proximity would promote self quenching which would result in a decrease in the fluorescence intensity observed in each of these systems (Kaur and Sanyal, 2010; Raghuram *et al.,* 2007, MacDonald, 1990).

Upon addition of 10μM melittin to each of the systems containing the donor probe (and the acceptor probe, as shown in Appendix A), the fluorescence intensity of NBD decreased in comparison to the system without the peptide (See Table 4.1). Cholesterol has been shown to modify the physical properties of lipid bilayer since it can intercalate between the long carbon chains of lipids and hold the molecules tightly together, hence increasing membrane rigidity. This would decrease the fluidity of the membrane and make it harder for peptides such as melittin to penetrate into the bilayer. In this case, melittin may only bind to the surface of the bilayer without being able to penetrate too deeply into the hydrophobic core. This could explain the decrease in the emission intensity of NBD upon the introduction of melittin into the systems. Since NBD can easily relocate to the surface in the fluid POPC vesicles, the slight decrease in NBD emission can be attributed to small interactions between the cationic peptide and the donor probe's polar head group. In the model membranes containing cholesterol, the decrease in fluorescent emission was much more significant and it could be possible that the peptide is somehow increasing the clustering of the NBD probe by promoting reorganization of the lipidic assembly and hence leading to self quenching as described above.

4.2.2 Energy transfer in model membranes

In order to study the lipid microdomains in the model membranes, the resonance energy transfer was measured and in this case both NBD-DPPE (donor) and Rhod-DOPE (acceptor) were added to the lipids upon vesicle preparation. When excited at 428nm, the FRET systems containing both probes were expected to show a decrease in fluorescence of

the donor while the acceptor probe would show an increase in emission due to resonance energy transfer. It is assumed that most of the Rhod-DOPE would have partitioned into the L_d phase whereas the NBD-DPPE would partition mostly into the L_o phase. Probes were excited at 428nm and the emission spectra was collected between 450-650nm. As an example, Figure 4.2 shows the fluorescence emission of the donor and acceptor probes at an excitation wavelength of 428nm in the raft system followed by their combined emission in the FRET system. All other spectra for each of the lipid systems can be found in Appendix A. To compare the energy transfer phenomenon taking place in each of the lipid systems both in the presence and absence of melittin, their FRET profiles were overlaid and are shown in Figure 4.3 while the maximum emission intensity of the two probes, have been tabulated and are shown in Table 4.2.

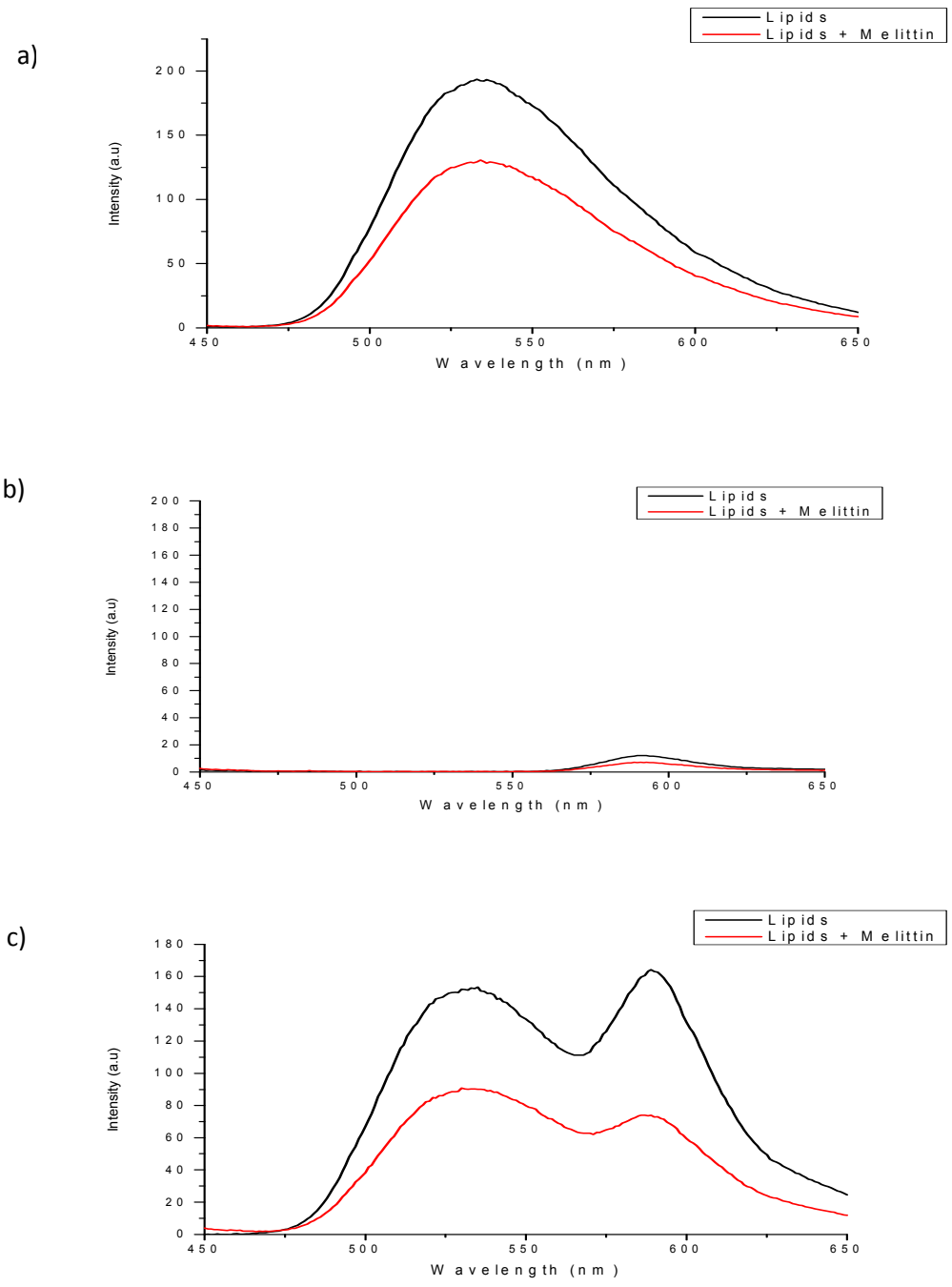

Figure 4.2: Fluorescence of donor and FRET Transfer in the raft lipid system

The emission spectra of a) NBD-DPPE fluorescence b) Rhod-DOPE fluorescence c) FRET emission were obtained at an excitation wavelength of 428nm. Melittin was added at a final concentration of 10µM and briefly allowed to equilibrate before measurements were taken.

a)

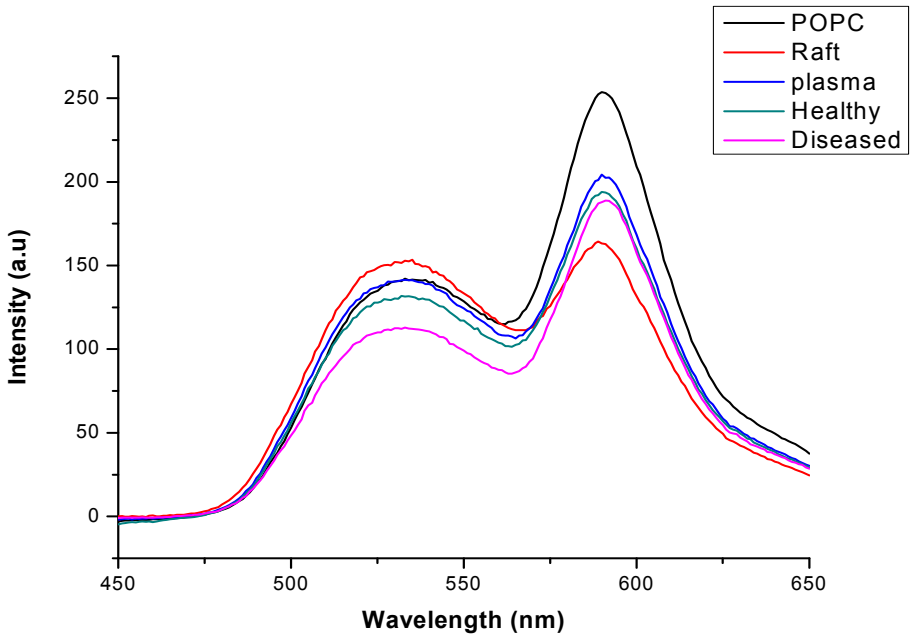

b)

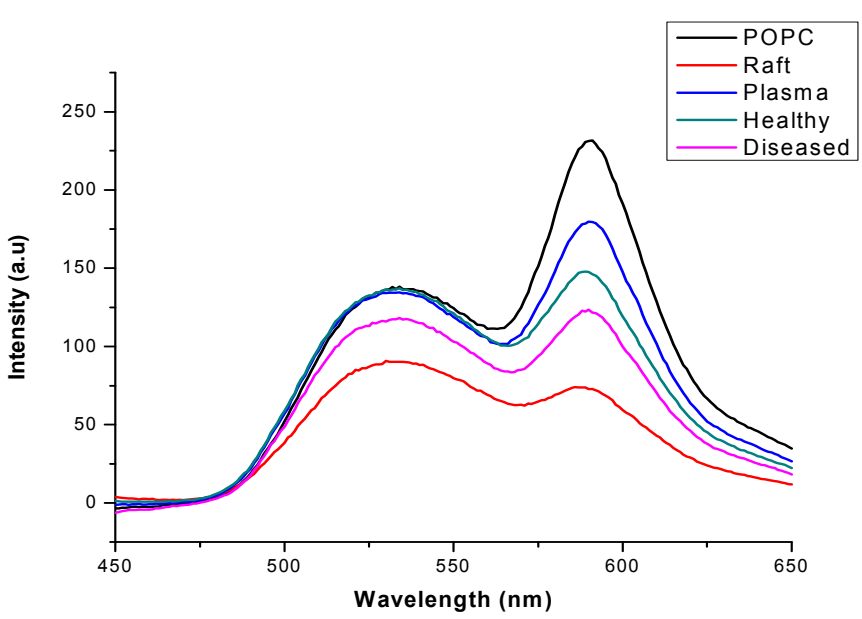

Figure 4.3: Comparison of FRET profiles for donor NBD-DPPE and acceptor Rhod-DOPE pair in the various lipid systems

The resonance energy transfer in each of the five model systems was measured at an excitation wavelength of 428nm, both in a) the absence and b) presence of melittin. LUVs were prepared in 5mM HEPES and 150mMNaCl, pH 7.4 buffer and NBD-DPPE was added to the lipid systems at a concentration of 0.8 %mol (1:125) whereas Rhod-POPE was added at 0.2 %mol (1:500).

Table 4.2: FRET emission intensity in the absence and presence of melittin

Donor and acceptor probes were added at a concentration of 0.8%mol and 0.2%mol respectively and FRET was measured at an excitation wavelength of 428nm. Values listed were obtained from one of the three trials conducted for FRET measurements. The fluorescence intensities are given in arbitrary units (a.u).

Lipid system	Fluorescence emission intensity (a.u)			
	NBD-DPPE emission at 530 nm		Rhod-DOPE emission at 590 nm	
	Lipids Only	Lipids+ Melittin	Lipids Only	Lipids + Melittin
POPC	142	138	254	232
Raft	153	91	164	74
Plasma membrane	141	134	204	178
Healthy myelin	131	137	194	148
Diseased myelin	113	118	189	123

4.3 FRET analysis and characterization of lipid domains in model membranes

The results obtained show that energy transfer was more prominent in some of the systems compared to others. The POPC system appeared to have the largest energy transfer as shown in Figure 4.3 where its NBD peak was significantly decreased in the presence of the acceptor, compared to its emission intensity in the absence of Rhod-DOPE as shown in Figure 4.1. The emission peak of the acceptor in the presence of the donor, concurrently, showed an increase in intensity compared to its emission profile shown in Figure 4.1, which would be indicative of resonance energy transfer taking place. The raft system on the other hand,

showed the least amount of energy transfer as shown by the emission maxima intensities of the donor and acceptor probe which were almost similar in value. In order to better quantify the energy transfer in each of the systems, the energy efficiency (E) was calculated and provided an estimation of the fluidity of each of the lipid systems. FRET experiments were carried out in triplicate for each system, and the average efficiency and standard deviation were calculated (using equation 2.1) and plotted as a bar graph shown in Figure 4.4.

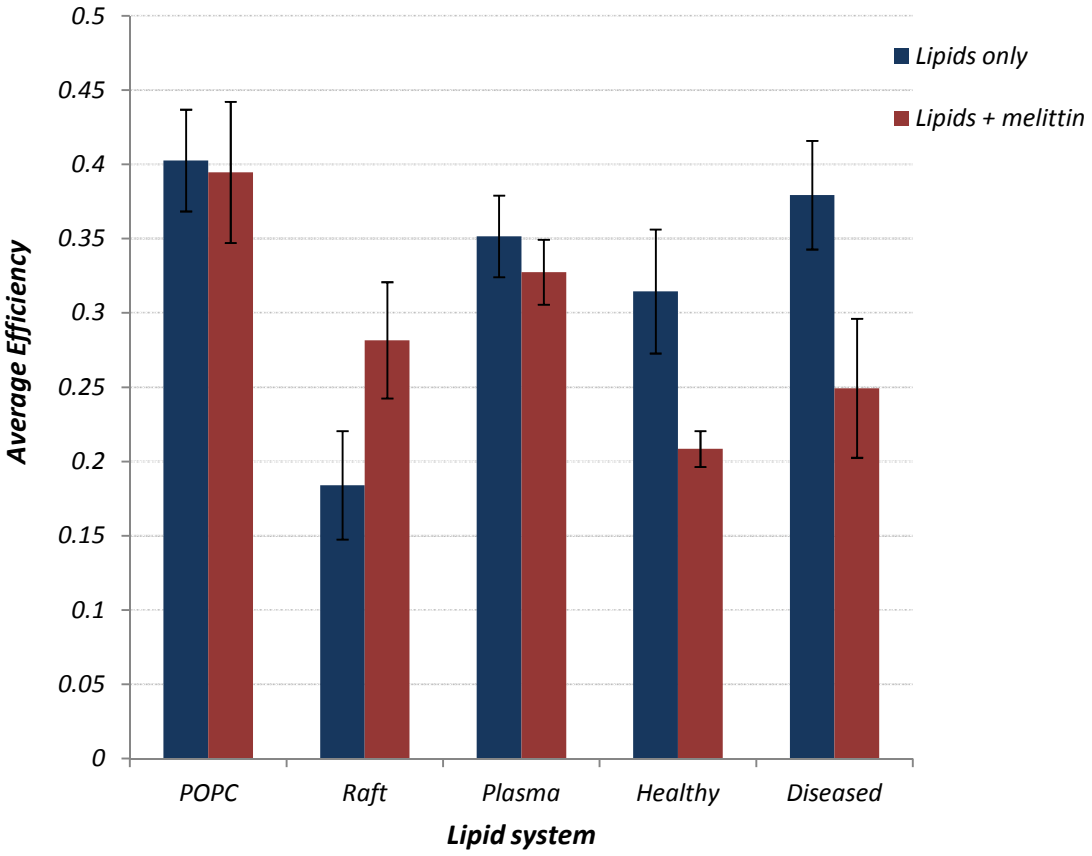

Figure 4.4: Average energy transfer efficiency (E) in various lipid systems

The average efficiency was computed from three trials performed for each lipid system. The blue bars represent E for the lipid systems in the absence of melittin while the red columns show E in the presence of melittin.

The computation of the energy efficiency (E) for each system gave an indication of the fluidity and the approximate size of lipid domains present in each system. At first glance, it would appear that both the POPC system and the diseased myelin system had similar high efficiencies in the absence of melittin. While these results were expected for the POPC system which is very fluid, it was quite surprising for the diseased myelin system to exhibit such high amounts of energy transfer, given that it contains a significant amount of cholesterol (37.4 %mol) which should promote domain formation and hence probe segregation. POPC is known to be in fluid the L_d phase at room temperature and since no other components were present, the lipids did not self associate to form microdomains. As such, the distance between the donor and acceptor probes was very small since the whole system was in a mostly L_d phase. This would result in a high rate of energy transfer given the proximity of the probes. When melittin was added to the POPC system, the energy efficiency went down only slightly which would imply that the presence of the peptide did not significantly impact the lipid arrangement of the bilayer. One reason for the unusually high efficiency of the diseased myelin model could potentially be due to the formation of very small lipid microdomains, since this system contains only a small amount of saturated sphingomyelin and a high level of cholesterol. The formation of smaller lipid domains would cause the donor and acceptor probes to be relatively close to each other even though they partitioned themselves into different phases (see Figure 4.5). Furthermore, since the myelin mimicking systems used in this study are complex five lipids systems, it could be possible that the bilayer would maintain the coexistence of a gel phase as well as the liquid phase which includes the L_o and L_d phases. This type of lipid phase coexistence is believed to exist in

complex cell membranes, albeit only transiently, due to interactions between certain sphingolipids, including sphingomyelin and is also promoted at lower temperatures (Loura *et al.,* 2009). When it comes to the FRET results obtained for the diseased myelin systems, the increased efficiency could be a result of the coexistence of a gel phase and the more fluid liquid phases which would bring the donor and acceptor probes closer to each other in the fluid liquid phases. Both NBD-PE and Rhod-PE have been shown to have an affinity for the fluid liquid phases, and the presence of the gel phase reduces the area into which these probes can partition, hence bringing them closer to each other resulting in an increase in the FRET efficiency (Loura *et al.,* 2001). Since the myelin mimicking systems used in this study are complex lipid systems, their phase diagrams are still unknown and this makes it difficult to confirm the results obtained in terms of fluid and gel phases of the bilayer. The addition of melittin to the diseased myelin model caused a significant drop (~35%) in the energy efficiency which could be attributed to the peptide-lipid interactions favouring the formation of larger microdomains as shown in Figure 4.5. In this case, it could be possible that melittin would promote the fusion of smaller lipid domains into larger ones that would cause the distance between the probes to increase, hence explaining the drop in the FRET efficiency. Melittin has previously been reported to induce lipid reorganization in membrane bilayers which would further serve to explain these results (Wessman *et al.,* 2008). Moreover, the clustering of the donor probe into these larger domains could potentially favour the self quenching of NBD which would lead to reduced efficiency as well, since less resonance energy is transferred to the acceptor probe.

The two systems having the next highest efficiency were the plasma membrane model and the healthy myelin model. The plasma membrane had a slightly higher efficiency (~9%) which may be attributed to a lower cholesterol concentration (20 %mol), whereas the healthy myelin system contained 31.7 % cholesterol. The cholesterol level in the systems would dictate the degree of ordered lipid arrangement in the systems since it has previously been shown to intercalate between the saturated acyl chains of membrane lipids to promote lipid order and hence domain formation (London, 2002; Dupree and Pomicter, 2010). The higher cholesterol content of the myelin system, as well as the presence of sphingomyelin, in this system would promote a higher fraction of L_o domains compared to the plasma membrane which lacked sphingomyelin. The reduced efficiency in the myelin system can thus be attributed to a greater distance between the probes which would hinder energy transfer. Upon the addition of melittin, both the plasma and the myelin system showed a decreased efficiency which would suggest that the peptide somehow affected the lipid arrangement in the systems such that the distance between the probes increased in its presence. This would once again imply that the introduction of melittin into the systems could induce the formation of slightly larger lipid domains. Lastly, the raft system exhibited the lowest FRET efficiency out of all the systems used in this study; the raft model system is known to be in a mostly liquid ordered phase, which would make it less fluid. Previous studies have also shown that at room temperature (25^{o}C), the lipid domains in this system are usually fairly large and are around 75-100nm in size (Almeida *et al.,* 2005). The strictly ordered lipid arrangement would cause the probes to be held in place, preventing them from getting close to each other, hence explaining the very low energy transfer. The addition of

melittin however showed some novel results. Unlike the other systems where the FRET efficiency decreased in the presence of the peptide, the raft model instead showed an increase in efficiency. It would seem that melittin had in this case promoted the formation of smaller domains which, decreased the distance between the donor and acceptor probes and thus leading to an increased efficiency. Furthermore, based on the FRET spectra shown in Figure 4.3, it was observed that the fluorescence intensity of both the donor and the acceptor decreased significantly in the presence of melittin. One plausible explanation could be that melittin causes lipid rearrangement into smaller microdomains thus concentrating the two probes into different local areas. The close proximity of similar probe molecules to each other could once again trigger a self quenching process which could contribute to the loss of fluorescence intensity shown in Figure 4.3.

Lipid system	*Lipid domains*	*Lipids domains in the presence of melitin*
POPC	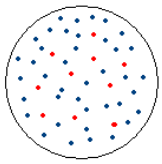	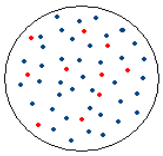
Raft	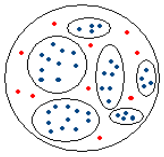	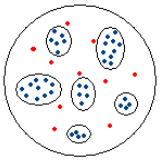
Plasma Membrane	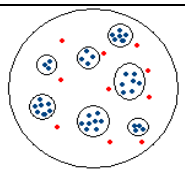	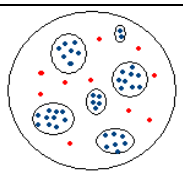
Healthy Myelin	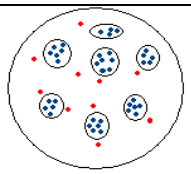	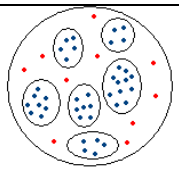
Diseased Myelin	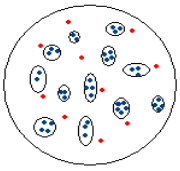	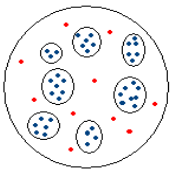

Figure 4.5: Proposed lipid domain properties and probe segregation in various lipid systems

The diagram gives a representation of the shape and size of the lipid domains that could be present in the lipid systems studied in this work as well as the segregation of the donor NBD-DPPE (blue) and Rhod-DOPE (red) from each other. The POPC system represents a L_d system with no microdomains whereas the raft system is represented as being mostly L_o. The remaining systems contain L_o domains within the fluid L_d area. The addition of melittin seemed to increase the L_o domain size in the plasma membrane, healthy and diseased myelin systems. Conversely, the addition of melittin to the lipid raft system lead to a decrease in the L_o domain size.

4.4 The impact of cholesterol levels on membrane domains

Cholesterol–lipid interactions have long been recognized as an important element in membrane structure. Studying cholesterol-containing model membranes has deepened our understanding of how cholesterol contributes to the formation and the organization of lipid rafts. While this molecule prefers to intercalate between the long chains of sphingolipids and induce the formation of laterally segregated domains, it can also migrate across a lipid bilayer much faster than any other membrane lipids thereby affecting the microdomain distribution (Silvius, 2003). Fluorescence resonance energy transfer experiments have greatly extended the knowledge behind the principles of lipid raft organization previously detected in detergent-insolubility studies. Determining how cholesterol interacts with membrane lipids, would improve the understanding of the basic principles behind raft formation. The FRET results obtained suggest that the increase in cholesterol during the demyelination process, does affect the size and formation of lipid domains in the myelin membrane and potentially its interactions with membrane proteins. When compared to the plasma membrane model, the lipid domains in the myelin mimicking models appear to be much more susceptible to variations in their size and composition due to high levels of cholesterol. The FRET results obtained indicate that the size of the lipid domains in the diseased system, are smaller compared to the healthy myelin model. Cholesterol is probably the most important lipid when it comes to controlling the size and functions of L_o domains in membranes and consequently its presence in the cell membranes should be tightly regulated to ensure the proper function of membrane rafts and the proteins associated with them. Any fluctuations in the cholesterol levels could lead to changes in the topology of membranes, hence affecting

the proper function of membrane proteins. If the basic structure of membrane rafts is compromised, this would in turn impact cellular processes modulated by these rafts such as signal transduction. Proper understanding of how the lipid rafts in the myelin are affected during MS could prove useful in determining how protein function is affected during MS and what the possible repercussions could be.

Chapter 5

Peptide–lipid interactions of melittin and the myelin specific PLP peptide

5.1 The effects of lipid composition on the secondary structure of melittin

Melittin, a bee venom peptide, is one of the most widely studied amphiphatic, membrane-lytic, helical peptide (See section 2.2.1). The peptide usually targets eukaryotic membranes containing cholesterol, and although it is too cytotoxic to be used as an antibiotic, melittin is often used as a model peptide in peptide-lipid interactions studies. Melittin is a positively charged (+6), 26-amino acid peptide with the following sequence; (+)Gly-Ile-Gly-Ala-Val-Leu-Lys(+)-Val-Leu-Thr-Thr-Gly-Leu-Pro-Ala-Leu-Ile-Ser-Trp^{19}-Ile-Lys(+)-Arg(+)-Lys(+)-Arg(+)-Gln-Gln-NH_2 (Vogel, 1987), and its crystal structure shows that it is a bent α-helical rod. This crystal structure has been shown to differ slightly when the peptide is in a lipid environment, with the bilayer lipid composition affecting its overall structure (Anderson *et al.,* 1980). The helical structure of melittin is strongly amphiphatic with one side of the helix consisting of the hydrophobic side chains whereas the other side consists of hydrophilic side chains. Just like other antimicrobial peptides, at high enough concentrations, melittin is known to induce membrane lysis through the formation of a tetramer structure which can induce the formation of transmembrane pores in the bilayer. Studying the conformations of melittin in different lipid environments can provide information about binding mechanisms as well as information on how lipid composition of model membranes dictates the overall secondary structure of peptides. In order to study the effects of different lipid compositions on the structure of melittin, circular dichroism (CD) spectroscopy (see section 2.5, Figure 2.8) was used to determine its secondary structure while fluorescence techniques were used to investigate the binding affinity of the peptide into different membrane bilayers. Since melittin is known to be monomeric at low

concentrations and tetrameric at high concentrations, four different concentrations (5, 10, 20 and 40 μM) were used to determine the potential aggregation point of the peptide and the subsequent effects on its secondary structure in different lipid systems. In most cases, melittin has been shown to self-associate at concentrations as low as 13μM depending on the type of lipid systems it is found in (Wessman *et al.,* 2001; Terwilligert and Eisenberg, 1982)

5.1.1 Concentration-dependent structure of melittin in buffer

Analysis in the far UV region can provide useful information in terms of protein structure. Melittin has been shown to have a mostly random coil structure in solution and this was verified by CD measurements of different concentrations of melittin in 10mM Tris, 100mM NaF buffer pH 7.4 before CD measurements were taken between 190 and 260nm. All readings were taken at 25^{o}C and the concentration-dependent spectra are shown in Figure 5.1. The spectra obtained confirmed that the peptide was mostly in a random coil state in buffer solution at concentrations of 5μM and 10μM as shown by the presence of a minimum at 202nm which is usually indicative of mostly random coiled structures. While the 5μM and 10μM melittin spectra appeared to be mostly random coiled, the spectra for increasing concentrations of melittin began to show the development of an alpha helical structure as shown by the appearance of a second small minimum at around 222 nm which is typical of an alpha helical signal. A CD spectrum of a helical peptide or protein is typically characterized by a double minima; one at 208nm and a second minimum of nearly equal intensity at 222nm. This would be indicative of an oligomerization process of the alpha helices which

started to occur at concentrations as low as 20µM in solution. As the concentration of melittin goes from 5µM to 40µM, it is very likely that the peptide goes through a number of different association processes. At very low concentrations, melittin is usually monomeric but as the gradually concentration increases the peptide could initially self-associate into a dimeric structure consisting of two α-helices before finally forming a tetrameric structure (dimer of dimers) at higher concentrations (Schubert *et al.,* 1985). The self-association of the peptide into a tetrameric structure consisting of four helices which are nearly identical in conformation, could take place through hydrophobic interactions since melittin is known to form amphipathic α-helices.

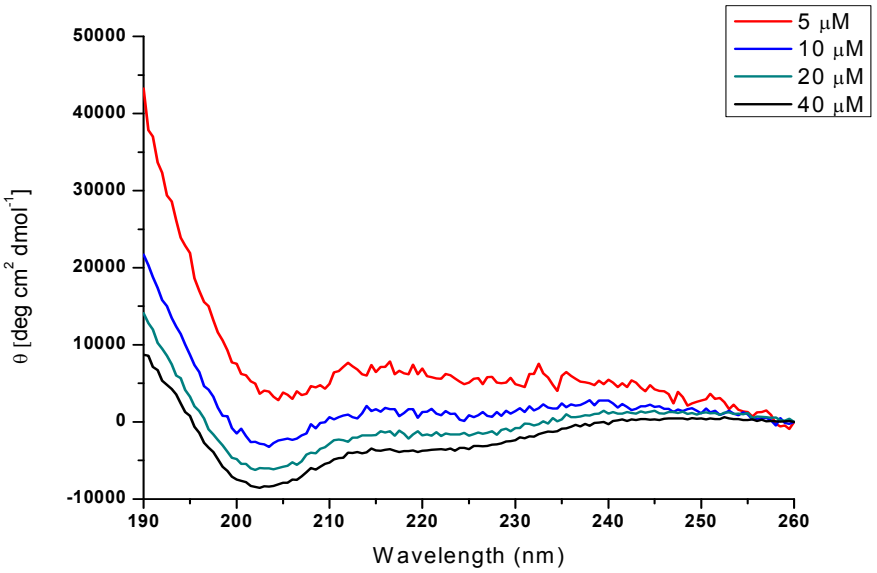

Figure 5.1: Concentration-dependent far UV CD spectra of melittin in buffer

Melittin was added 10mM Tris, 100mM NaF buffer pH 7.4, approximately 3 minutes before the scan was started, vortexed and then briefly centrifuged (<10s) down before scanning. Four scans were taken for each sample and all measurements were carried out at 25^{o}C in a 1mm pathlength cuvette. The final averaged spectra were converted to molar ellipticities and further smoothed using the AVIV CD software.

The structure of the tetrameric melittin thus seems ideally suited for conferring a high aqueous solubility to this small peptide which has predominantly apolar residues. Most of the charged and polar amino acid side chains are spread out over the surface of the tetramer and along with the polypeptide backbones of the four chains, these residues form a hydrophilic coat which shields the central hydrophobic core from the solvent. Additionally, since the melittin tetramers contain only positive charges, the electrostatic repulsion between them probably contributes to melittin's aqueous solubility and prevents the peptide from precipitating out of the solution (Terwilliger and Eisenberg, 1982).

5.1.2 Concentration-dependent structure of melittin in POPC

Phosphatidylcholines are zwiterrionic phospholipids found abundantly in the cell membrane. POPC is often used in peptide-lipid interaction studies to represent simple lipid bilayers. In this project, POPC was initially used to represent a fluid liquid disordered (L_d) system in FRET experiments where lipid domains were mostly absent and melittin was added to characterize the effects of the peptide on lipid rearrangement and domain formation in this simple bilayer. In order to determine the effects of POPC on the structure of melittin, CD measurements were taken at increasing concentrations of the peptide to determine its overall secondary structure.

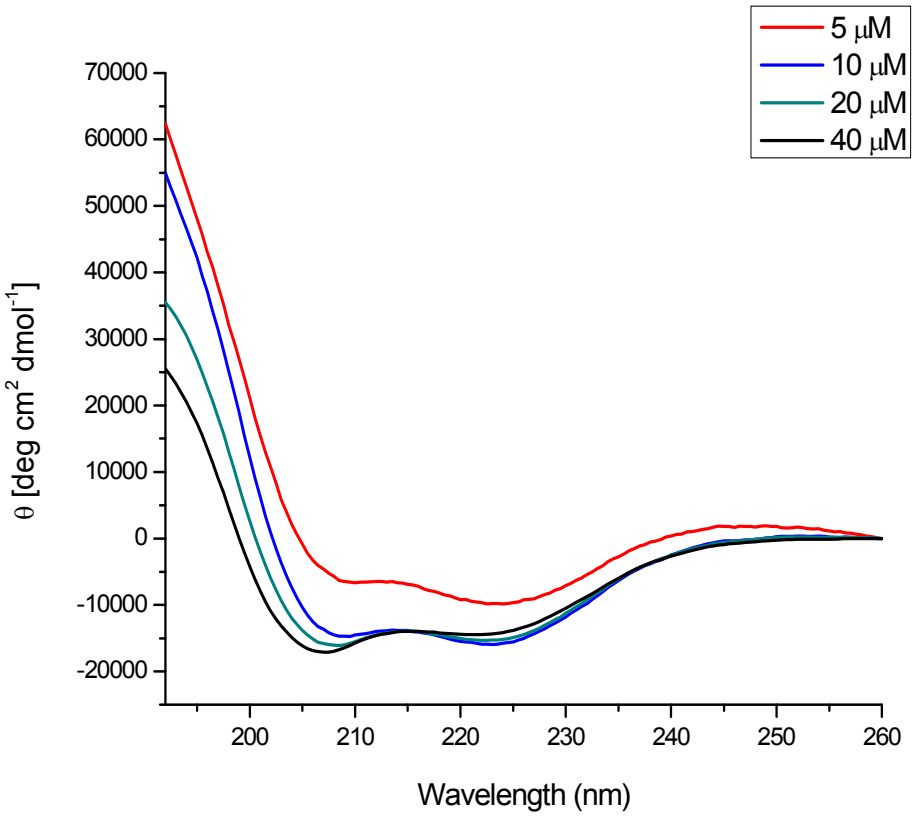

Figure 5.2: Concentration-dependent far UV CD spectra of melittin in POPC

Melittin was added to 1mM POPC LUVs, approximately 3 minutes before the scan was started, vortexed and then briefly centrifuged (< 10s) before scanning. Four scans were taken for each sample and all measurements were carried out at 25°C in a 1mm pathlength cuvette. The final averaged spectra were converted to molar ellipticities and further smoothed using the AVIV CD software.

The results indicate that the interaction of melittin with POPC vesicles caused the peptide to adopt a mainly α-helical structure (see Figure 5.2). As the concentration of the peptide increased, the interaction with the lipids seemed to increase as well, as shown by the increase in depth of the minima at approximately 207nm. However, as the concentration increased, this minimum started to shift left towards shorter wavelengths. This small blue shift is most prominent at the 40μM concentration and could suggest the emergence of a

slightly higher fraction of random coil structure with the major structural component is still an α-helix. At this point it is highly likely that self-association of the peptide could promote a coiled-coil structure. Furthermore, the presence of an isodichroic point at 267nm for the 10, 20 and 40μM CD spectra, could indicate the presence of mixture of different structural species. As the concentration of melittin steadily increases, it is likely that the peptide self associates, going from being a monomer to a dimer and eventually a tetramer. While the self-associated form of melittin still interacts with the membrane bilayer, it should also be noted that at high concentrations, melittin can potentially lyse membranes that do not contain cholesterol since they are more fluid and easier to penetrate. Previous studies have shown that the tetrameric structure of melittin can induce pore formation in membrane bilayers that are cholesterol-free. Since Figure 5.2 indicates a loss in the helical signal at concentrations higher than 5μM as shown by the blue shift of the minima at around 208nm, it is possible that melittin could have ruptured the vesicles. The loss in interaction with the lipid bilayer would in turn cause a change in the helical structure of the peptide.

5.1.3 Concentration-dependent structure of melittin in the raft "canonical mixture" membrane model

The canonical raft mixture is known to be in a mostly liquid ordered phase (L_o) and consists of equal amounts of POPC, SM and cholesterol (Almeida *et al.,* 2005; Goni *et al.,* 2008). Cholesterol has been shown to increase the rigidity of cell membranes and promote lipid order in lipid bilayers. The high degree of cholesterol in this system therefore prevents melittin from binding and penetrating too deeply into the lipid bilayer. Since melittin is not

deeply embedded and is more exposed to the polar environment in this lipid system, this could explain why the peptide appears to have a higher random coil content. The loss in helicity in the raft system compared to the POPC system (Figure 5.2) could be due to a reduced amount of peptide-lipid interactions.

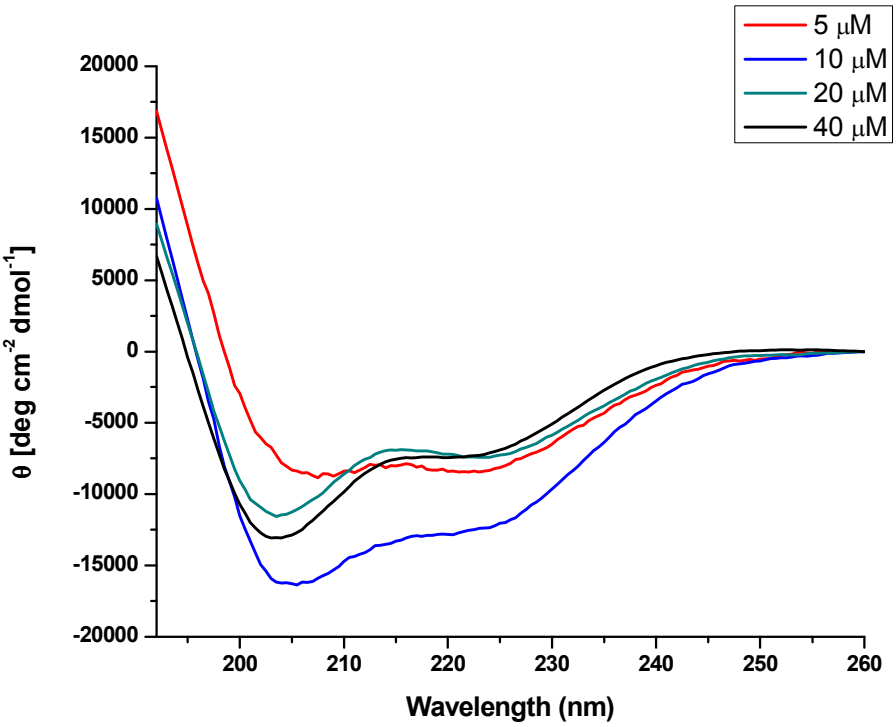

Figure 5.3: Concentration-dependent far UV CD spectra of melittin in raft membrane model system

Melittin was added to 1mM raft LUVs (1:1:1 SM/PC/Cholesterol), approximately 3 minutes before the scan was started, vortexed and then briefly centrifuged (< 10s) before scanning. Four scans were taken for each sample and all measurements were carried out at 25^{o}C in a 1mm pathlength cuvette. The final averaged spectra were converted to molar ellipticities and further smoothed using the AVIV CD software.

At 5μM, melittin appeared to have the highest α-helical content as shown in Figure 5.3. For this spectrum, the first minimum was located at 207nm and the second at around 223nm which would indicate that the peptide is mostly helical at this concentration. At very low

concentrations, it is thought that the peptide might become adsorbed to the surface of the membrane bilayer even though it is unable to penetrate it, hence the low molar ellipticities observed at 5μM. As the concentration increased, the structure started to change from a helix to a more random coiled configuration. This is demonstrated by the blue shift of the local minimum at 207nm to around 202nm, a property often observed in the presence of random coils. The presence of the local minima at 222nm however, would indicate that at concentrations of 10μM and above, melittin contained a mixture of helix and random coil structures, a feature that was not very visible in buffer (see Figure 5.1). The presence of a high amount of cholesterol makes the bilayer structure of this system very rigid, which in turn would make it difficult for the peptide to insert itself deeply into the bilayer. Since melittin cannot properly interact with the lipids in the bilayer, it cannot form fully helical structures at low concentrations. It should also be noted that the lower molar ellipticities observed at the 202nm minima compared to the POPC measurement, shows that the peptide did not have strong peptide-lipid interactions especially in the case of the 20μM and 40μM peptide concentrations. From the CD spectra, it can be seen that as the concentration increases from 5μm to 10μM there is a significant increase in terms of the interaction of the peptide with the lipids as shown by the increase in depth of the local minima at 202 nm and 222nm. However, as the concentration increases, the spectra for the 20μM and 40μM peptide concentrations show an upward shift which would suggest that the peptide-lipid interactions have been considerably weakened. This would suggest that, at these concentrations, melittin is no longer interacting as effectively with the bilayer but is instead favoring the formation of either dimeric or tetrameric structures consisting for two and four

alpha helices respectively that could allow it to go into solution. This information would indicate that the presence of high levels of cholesterol in membrane bilayers could make it harder for melittin to penetrate them hence favoring a self-association process.

5.1.4 Concentration dependent structure of melittin in plasma membrane model system

Melittin has previously been shown to have a strong affinity for eukaryotic membranes that contain cholesterol (Wessman *et al.,* 2008). This information is somewhat paradoxical given that cholesterol has been shown to inhibit the lysis of cell membranes and lower the interaction of such antimicrobial peptides with the lipid bilayer. It has been suggested that the rigid ring system and perpendicular orientation of the sterol molecule with respect to the plane of the membrane, make an attractive target for many bacterial toxins and antibiotic peptides (de Krujjif, 1990). The presence of tryptophan in melittin further increases its binding properties to cholesterol containing membranes by forming stable complex with the rigid ring system. The tight lipid packing induced by cholesterol, however, could account for the inhibition of the lytic properties of melittin, making it harder for the peptide to penetrate the surface of the bilayer and promoting pore formation (Raghuram and Chattopadhyay, 2004). Furthermore, melittin is known to interact selectively with negatively charged lipids since it has an overall net charge of +6 at physiological pH, which would promote electrostatics interactions with the negatively charged bilayers, hence increasing binding. In order to study the effects of cholesterol and negatively charged lipids on melittin, the peptide was introduced into a plasma model membrane system which

contained around 20% cholesterol and 10% POPS which carries a negative charge. CD measurements were carried out and the results are shown in Figure 5.4.

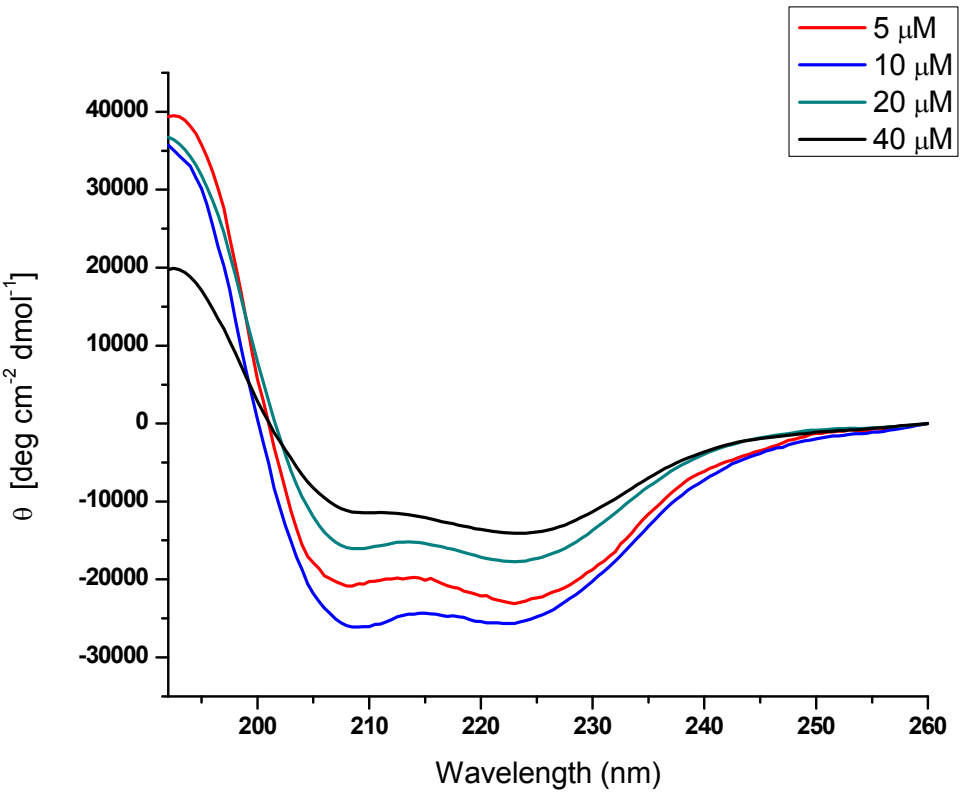

Figure 5.4: Concentration-dependent far UV CD spectra of melittin in plasma membrane model

Melittin was added to 1mM plasma membrane (PC/PS/PE/SM/Chol at 20.1:7.4:32.9:2.2:37.4 %mol) LUVs, approximately 3 minutes before the scan was started, vortexed and then briefly centrifuged (< 10s) before scanning. Four scans were taken for each sample and all measurements were carried out at 25^{o}C in a 1mm pathlength cuvette. The final averaged spectra were converted to molar ellipticities and further smoothed using the AVIV CD software.

When melittin was added to the plasma membrane model system, the spectra indicated the peptide adopted a mostly helical structure. As the concentration increased from 5μM to 10μM, the peptide lipid interactions seemed to increase as shown by the downward shift of the spectra. However, this interaction decreased when the concentration increased from

20μM to 40μM, and the spectra started to shift upwards. When compared to the spectra for POPC and the raft model systems, the overall interactions of melittin with this bilayer appeared to be significantly higher which could be due to the presence of the negatively charge phospholipid POPS which increases electrostatic interactions between the lipid bilayer and the cationic peptide. While the CD spectra indicated that the peptide was predominantly alpha helical, comparison of the $\theta_{222nm}/\theta_{208nm}$ ratio indicated that melittin still contained some coiled coil structure. This ratio is often use to distinguish between the helical and coiled coil structures present in peptides and a value ≤1 usually indicates the presence helices while values ≥ 1 indicate a mix of coiled coil structures and helices (Ybe *et al.,* 2009). At 5μM and 10μM the CD spectra had a ratio of 1.09 and 0.98 respectively, which would indicate a mostly helical structure with a small amount of a random coil structure present. However, as the concentration increased to 20μM and 40μM, the ratio also increased which would indicate that the coiled coil structure is increasing while the helical content decreases. This could imply that at these higher concentrations the peptide is starting to aggregate, a process also indicated by the upward shift of the CD spectra and the slight loss in the spectra's helical definitions. In this case it might be possible that the presence of the negatively charged POPS would compensate for the presence of cholesterol in the lipid bilayer and promotes the binding of melittin, thus allowing the peptide to self-associate within the lipid bilayer.

5.1.5 Concentration-dependent structure of melittin in cytosolic myelin model

The cytosolic myelin model membrane has been used in many studies to represent the cytosolic leaflet of the myelin sheath. This system contains about 44% cholesterol which is very high for a cell membrane and 13% POPS and 3% POPI which would confer an overall negative charge to the bilayer. POPC, POPE and SM make up the rest of this bilayer and are present at 11%mol, 27%mol and 2%mol respectively. Since most of the proteins found in the CNS are predominantly basic and hence positively charged at physiological pH (net charge of +6 at this pH), melittin made an ideal model to study the interactions of such proteins with the myelin model. Initial CD measurements carried out, showed that increasing concentrations of the peptide only resulted in progressively decreased level of interactions with the lipids as shown by the upward shift of the spectra shown in Figure 5.5. When compared to the spectra in the POPC and raft systems, the peptide-lipid interactions appeared to be significantly higher and this could be a result of increased electrostatic interactions due to the presence of the negatively charged phospholipids POPS and POPI. The 5µM melittin spectrum appeared to have the highest degree of interactions with the lipid bilayer. At this concentration, the $\theta_{222nm}/\theta_{208nm}$ was equal to one and this information combined with the general structural of the spectrum would suggest a predominantly helical content. As the concentration increased, the spectra started to show a decrease in its interactions with the bilayer as demonstrated by the upward shift of the spectra. At 40µM melittin, the spectra appeared to have lost most of its helical definition, which would imply that at this point, the peptide is self-associating. The main reason for the decrease in

interaction and start of the aggregation process could most likely be related to the high amount of cholesterol present in this system which would prevent penetration of the peptide into the bilayer. As the peptide failed to properly interact with the lipids, it is more than likely that it started to self associate in order to shield its hydrophobic residues rather than forcing its penetration into the rigid bilayer. At this point, it would appear that even the high negative charge of the bilayer could not negate the bilayer effects induced by the high amount of cholesterol present, and hence promoting self association of melittin at higher concentrations which would take place both on the surface of the bilayer as well as within.

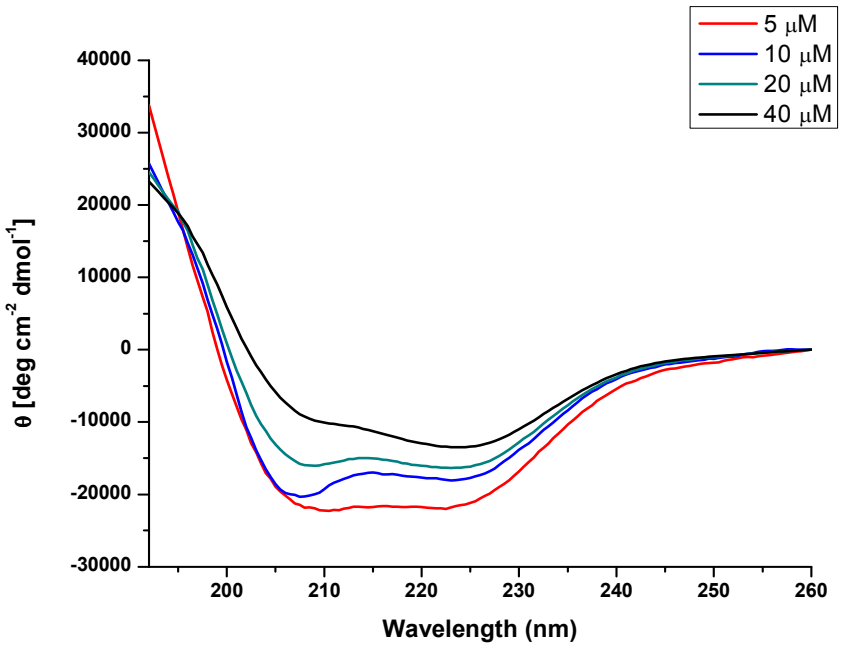

Figure 5.5: Concentration-dependent far UV CD spectra of melittin in cytosolic myelin membrane model

Melittin was added to 1mM cytosolic myelin (PC/PS/PE/PI/SM/Chol at (11:13:27:3:2:44 %mol) LUVs, approximately 3 minutes before the scan was started, vortexed and then briefly centrifuged (< 10s) before scanning. Four scans were taken for each sample and all measurements were carried out at 25^{o}C in a 1mm pathlength cuvette. The final averaged spectra were converted to molar ellipticities and further smoothed using the AVIV CD software.

5.1.6 Concentration dependent structure of melittin in healthy and diseased myelin model systems

The cholesterol level has been shown to increase during the demyelination process involved in MS (Banguy *et al.,* 2011). This change in the lipid composition, which also includes a decrease in the sphingomyelin content, has the potential of affecting the structure and thus the function of myelin membrane proteins. In order to study the effects of the change in lipid composition on protein structure and interactions, melittin was introduced in the two model lipid systems representing a healthy and a diseased myelin model. CD measurements were taken at 25^{o}C to determine any fluctuations in secondary structure induced by the difference in lipid composition between the two systems and the results are shown in Figure 5.6. The healthy myelin model used in this study contained approximately 31.6% cholesterol and 6% SM. When CD measurements were taken at 5μM, 10μM, 20μM and 40μM melittin, it was observed that the peptide adopted a mostly helical structure as shown by the presence of the two minima at 207 nm and 222nm which correlate to a typical α-helical signal shown in Figure 2.7. Unlike any of the other spectra analysed so far, the 5μM and 10μM melittin spectra in this model, exhibited a deep inflection at the 207nm mark. The reason behind this phenomenon is still unclear but it indicated that melittin had a strong interaction with the bilayer. The presence of the negatively charge lipid POPS (13 %mol) could have further increased the electrostatic interactions between the positively charged peptide and the bilayer. As the concentration of peptide increased, an aggregation process seemed to take place as denoted by the upwards shift of the spectra. Furthermore the loss in spectral features would suggest that aggregation took place at concentrations of 20μM and above

and could be attributed to the system's high cholesterol levels which would promote self-association on the bilayer and even cause the peptide to go into solution.

a)

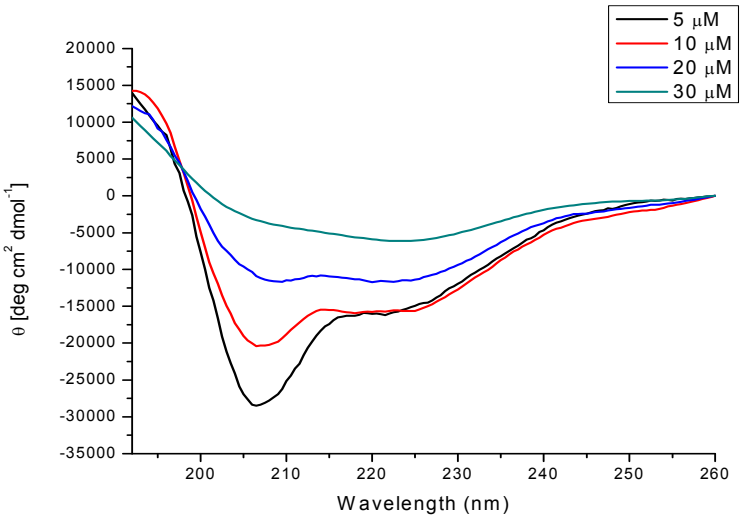

b)

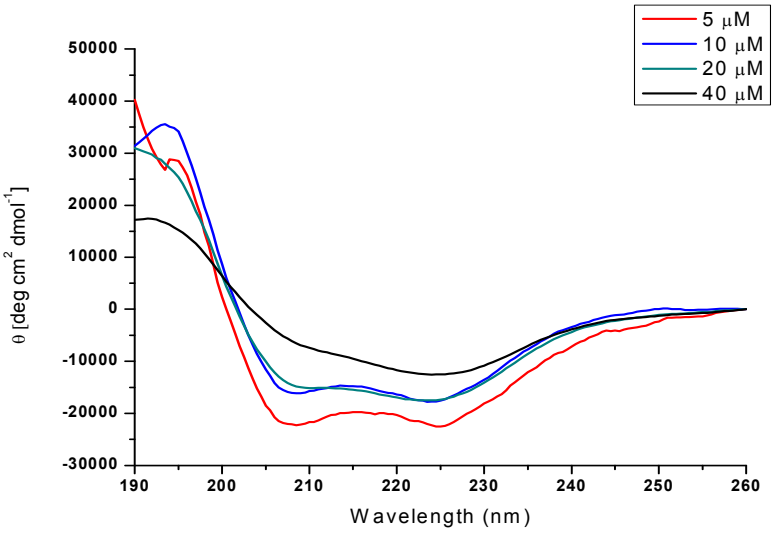

Figure 5.6: Concentration-dependent far UV CD spectra of melittin in healthy and diseased myelin models

Melittin was added to 1mM of a) healthy myelin (PC/PS/PE/SM/Chol at 25.9:7.3:29:6.2:31.6 %mol) b) diseased myelin (PC/PS/PE/SM/Chol at 20.1:7.4:32.9:2.2:37.4 %mol) LUVs, approximately 3 minutes before the scan was started, vortexed and then briefly centrifuged (< 10s) before scanning. Four scans were taken for each sample and all measurements were carried out at 25^{o}C in a 1mm pathlength cuvette. The final averaged spectra were converted to molar ellipticities and further smoothed using the AVIV CD software.

The diseased myelin model used in this study contained around 37.4% cholesterol and only 2% SM. The lower concentration of SM present in this system would suggest that the lipid bilayer would be slightly less rigid than the healthy myelin system since the SM to cholesterol ratio is now smaller. Our FRET study has shown that this system may contain small lipid domains which in the presence of melittin, could fuse together to form larger domains. When analyzing the spectrum for each concentration of melittin, it appeared that the 5μM peptide concentration had the greatest interaction with the bilayer as shown in Figure 5.6(b). As the concentration increased, the lipid bilayer interaction also decreased as indicated by the CD spectra which started to lose their definition. This would suggest that there could be peptide aggregation taking place on the surface of the lipid bilayer which would result in decreased peptide-lipid interactions. When compared to the healthy myelin model, the diseased model's spectra seem to have an overall lower negative molar ellipticity which could be explained by the higher level of cholesterol present. High amounts of cholesterol can promote the formation of a crystalline structure which would affect the bilayer's physical properties. This property of the bilayer would cause the peptide to aggregate on its surface hence accounting for the loss in definition of the 40μM CD spectrum. All in all, it would seem that the increase in the cholesterol content caused a decrease in the peptide-lipid interactions and helical content (>5 μM) when compared to the healthy lipid system. These findings would imply that the process of demyelination could cause certain membrane proteins in the myelin sheath to lose their functional structure which would result in the interruption of certain cellular processes thus leading to the symptoms experienced during MS.

5.2 Studying the partitioning of melittin into model membrane systems using tryptophan fluorescence

Melittin is intrinsically fluorescent due to the presence of a single tryptophan residue (W19), which makes it a sensitive probe for studying the interaction of the peptide with membrane bilayers. The tryptophan residue in melittin is located between the basic C-terminus and the hydrophobic N-terminus as shown in Figure 2.1. The of interaction of melittin with the lipid bilayer can be determined by the blue shift or red shift of the emission maximum upon binding to lipid vesicles. A blue shift would imply that the tryptophan is located in a more hydrophobic environment and suggests that the greater the shift is, the more embedded the peptide is into the lipid bilayer. The fluorescence emission spectra of melittin in each of the model systems were first obtained by mixing 10μM of melittin with 1mM of the lipid LUVs. The spectra were then overlaid, shown in figure 5.8, in order to compare for any shift in the emission maxima which would be indicative of how deeply melittin binds to the bilayer in each system. Comparing the tryptophan localization of melittin in the healthy and the diseased myelin model would provide an indication of how the peptide interactions are affected by the effects of demyelination on the lipid composition of myelin.

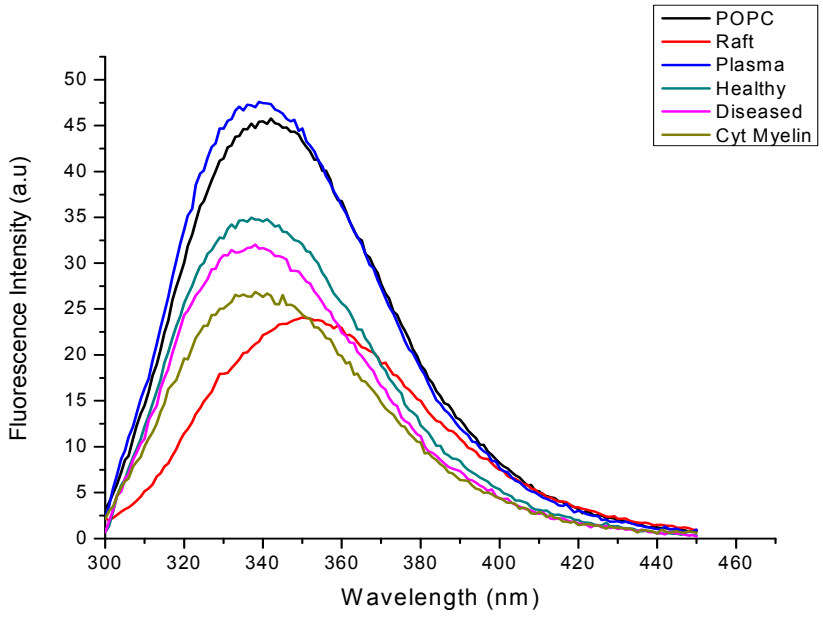

Figure 5.7: Tryptophan fluorescence of melittin in various lipid systems

The average tryptophan fluorescence of 10µM melittin was measured at an excitation wavelength of 280nm and calculated from 2 trials in order to determine the degree of interaction of the peptide in each of the lipid systems.

Table 5.1: Fluorescence emission maxima of 10µM melittin in six different lipid systems

The wavelength of the emission maxima of tryptophan was determined by taking the median the maximum values since the emission spectra were broad. A blue shift would indicate that the Trp residue is located in a more hydrophobic environment, whereas a red shift would indicate that the Trp is more exposed to the polar environment. In this case all wavelength shifts were taken relative to the maxima wavelength of the POPC system.

Lipid System	**Tryptophan Fluorescence**		
	Fluorescence Intensity (a.u)	Maxima Wavelength (median)	Deviation (nm)
POPC	45.8	342	± 2 nm
Raft	24.0	351	± 4 nm
Plasma membrane	47.3	336	± 4 nm
Healthy myelin	34.9	337	± 3 nm
Diseased Myelin	31.7	338	± 2 nm
Cytosolic Myelin	26.6	335	± 3 nm

Since the POPC system contained no cholesterol, it served as control to which the other systems could be compared. At first glance, it would appear that melittin had the greatest blue shift in the cytosolic myelin model and a red shift in the canonical raft system compared to the POPC system as shown in Table 5.2. Since the cytosolic myelin model contains negatively charged lipids POPI and POPS, this would make it the most negatively charged system of all six systems being used. Melittin has a +6 charge at neutral pH and this would cause the peptide to be highly attracted to the negatively charged bilayer therefore promoting the peptide's interaction with the bilayer, despite the system's high cholesterol content. Since the raft model is the only other uncharged lipid system after POPC, it was the only one to exhibit a red shift which would imply less penetration by melittin. It is known that cholesterol changes the physical property of the lipid bilayer by intercalating between the long acyl chains of sphingolipids and acting like glue to hold the lipids tightly together. This would explain why melittin interacts the least with the raft model which has previously been shown to be in a highly liquid ordered (L_o) state, thereby preventing the peptide from properly penetrating the surface of the bilayer. The blue shifts for the plasma membrane, healthy myelin and diseased myelin systems on the other hand were all very close to each other as shown in Table 5.2. Although the healthy and the diseased myelin as well as the plasma membrane all contained cholesterol, they still showed a blue shift compared to the POPC system. One possible explanation for this shift could be due to the fact that these systems also contain the negatively charged lipid POPS which would increase the electrostatic interactions between the peptide and the bilayer. Since the diseased system contains a higher amount of cholesterol than the healthy myelin and plasma membrane

models, it does appear to have the smallest blue shift compared to the other two whereas the plasma model which contains the lowest amount of cholesterol out of the three system showed the largest blue shift. Taking these results into consideration, it would appear that the interaction of melittin with the bilayers is mainly dictated by electrostatic interactions, followed by the amount of cholesterol present.

The fluorescence emission intensity appeared to decrease with increasing amount of cholesterol present in the bilayer. When looking at Figure 5.8, the rigid raft model which contained equimolar concentrations of POPC, cholesterol and SM, had the lowest emission intensity while the POPC system containing no cholesterol showed the highest intensity. Since the cholesterol content of the healthy and diseased model only differed by 6%, their emission intensity were very close to each other, whereas the cytosolic myelin model which contained 44% cholesterol appeared to have a lower intensity. The effects of cholesterol on the fluorescence intensity could possibly be due to both specific as well as general bilayer effects induced by cholesterol which could put melittin's tryptophan in close proximity to cholesterol and hence favouring some specific interactions between the two molecules. Tryptophan fluorescence is also known to be sensitive to the presence of water in its immediate environment and therefore a decrease in fluorescence intensity could be due to increased water penetration in the interfacial region (where the tryptophan residue in membrane-bound melittin is localized) of the membrane induced by cholesterol. Since the peptide cannot embed itself too deeply into the lipid bilayer, this would result in an increased amount of water molecules in the vicinity of the tryptophan residue which would

in turn cause a decrease in the tryptophan fluorescence. Melittin has also previously been shown to be able to exhibit red edge excitation shift (REES) Chattopadhyay and Rukmini, 1993). A shift in the wavelength of maximum fluorescence emission towards higher wavelengths, caused by a shift in the excitation wavelength toward the red edge of the absorption band, is termed REES. This effect is usually observed when fluorophores are located in motionally restricted environments. The ability of melittin Trp to exhibit REES could depend on a number of factors including its location in the membrane. REES studies combined with NMR and fluorescence quenching studies have shown that, melittin Trp partitions close to the interfacial region. More often than not, the lipid composition (negatively charged) had an effect on the REES for membrane bound melittin but cholesterol levels did not seem have an effect on this shift (Haldar *et al.,* 2011; Chattopadhyay and Rukmini, 1993). Taking this into consideration along with the results, it maybe concluded that while the level of cholesterol affects the physical properties of membrane bilayers, preventing melittin from embedding itself too deep; the negative charges associated with the bilayer manage to compensate for this decrease in interaction by allowing melittin to bind closer to the interfacial region. Since melittin is located so close to the interfacial region, the presence of cholesterol would push it even closer to the polar environment hence explaining the decrease in emission intensity in the presence of high levels of cholesterol. As such, most of the myelin mimicking systems used in this study exhibited the highest degree of peptide binding since their bilayers are negatively charged, whereas the raft system which contained no charge had the lowest amount of melittin binding.

5.3 Studying the interaction of melittin in myelin model membranes using Trp fluorescence

In the second part of the Trp fluorescence emission experiment, the melittin concentration was varied from 5µM to 40µM in the healthy and the diseased myelin model as well as the cytosolic myelin membrane model. Changes in the fluorescence emission maxima were analysed in order to determine the strength of the peptide binding in each of the system and the results are shown in Figure 5.9.

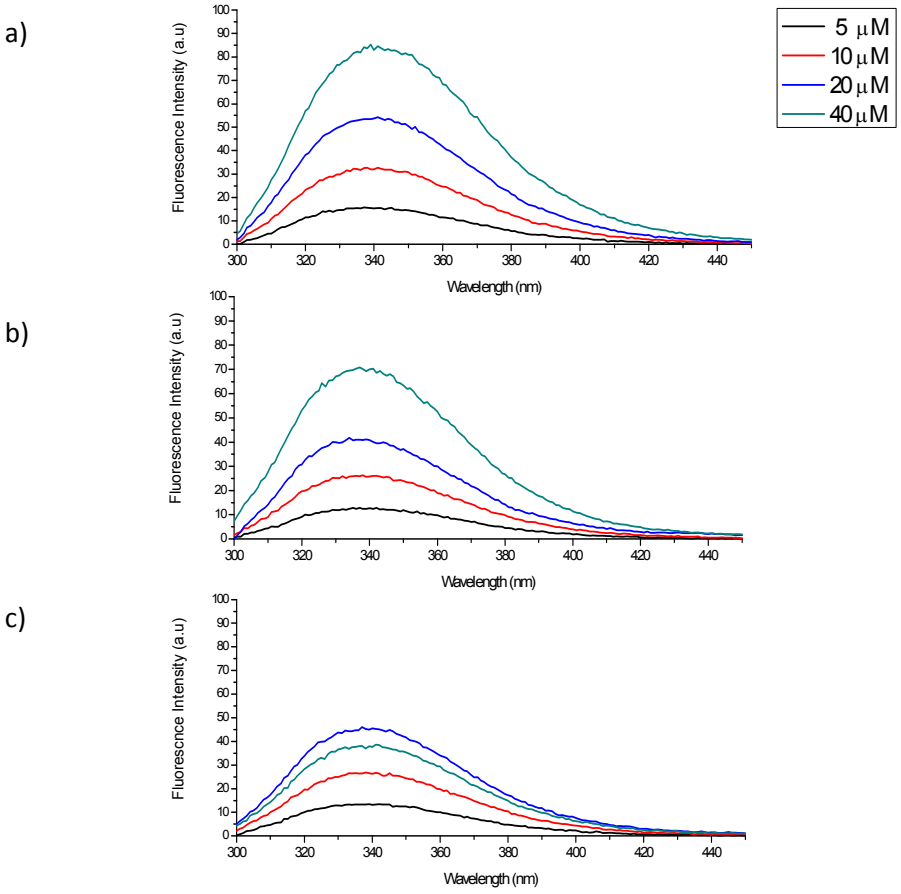

Figure 5.8: Concentration dependent Trp fluorescence in myelin model membranes

The emission spectra of increasing concentrations of melittin in a) healthy myelin model, b) diseased myelin model, and c) cytosolic myelin were measured at an excitation wavelength of 280nm to study possible fluctuations in peptide-lipid interactions at 25^{o}C.

Table 5.2: Concentration-dependent normalized intensities in the myelin mimicking membrane models

Melittin Concentration (μM)	*Normalized Fluorescence Intensity*		
	Healthy Myelin	*Diseased Myelin*	*Cytosolic Myelin*
5	0.19	0.18	0.29
10	0.38	0.37	0.58
20	0.62	0.58	1.00
40	1.00	1.00	0.84

As expected, the emission intensity seemed to increase proportionally with the increase in peptide concentration in both the healthy and diseased system. However, according to Figure 5.8, it would appear that melittin had an overall higher emission intensity in the healthy myelin system compared to the diseased myelin system. In this case, it is highly likely that the higher cholesterol level present in the diseased myelin system (37.4%) would hinder the binding of the peptide as compared to the healthy myelin system which contains less cholesterol (31.6%). The lower emission intensity in the diseased system would indicate that the tryptophan residue is located closer to the interfacial region where water molecules can come into closer contact with it. The cytosolic myelin model on the other hand (Figure 5.9 (c)), showed an increase in emission intensity as the concentration increased from 5μM to 20μM, but decreased at the 40μM mark unlike the healthy and diseased myelin models. As previously mentioned tryptophan emission is known to be sensitive to the presence of water in its immediate environment and therefore a decrease in emission intensity could also be due to an increase in water molecules surrounding the Trp residue (Raghuram and

Chattopadhyay, 2004). This information could suggest that at the 40μM concentration mark, the peptide has likely started to self-associate which would result in reduced interactions with the lipid bilayer despite the presence of a large amount of negative charge on the membrane. The high cholesterol content of the cytosolic myelin model (44%) would favour the self would increase the bilayer's rigidity, making it harder for the peptide to penetrate deeply. It should also be noted that the emission intensity of melittin in this cytosolic myelin model system is much lower than in the healthy and the diseased myelin model which contained a lower amount of cholesterol. This information is further confirmed by Table 5.2 which shows the normalized emission intensities of melittin in each of the myelin mimicking systems and it would appear that melittin could indeed undergo a self-association process at higher peptide concentrations and this process is further enhanced by the concentration of cholesterol present in the bilayer. The increase in the cholesterol level during demyelination resulted in decreased binding of the melittin peptide, which would suggest that when it comes to the proteins in the myelin membrane, the change in lipid composition could potentially affect protein function since the peptide-membrane interaction is perturbed.

5.4 Secondary structure determination of the myelin C-terminus PLP peptide

The PLP peptide used in this project was derived from the C-terminus of the myelin proteolipid protein (PLP) and has the following amino acid sequence Ile-Ala-Ala-Thr-Tyr-Asn-Phe-Ala-Val-Leu-Lys-Leu-Met-Gly-Arg-Gly-Thr-Lys-Phe. In putative the structural model for PLP, this peptide has been represented as being part of the fourth transmembrane α-helix

making up this multi-spanning protein, while the remaining segment is shown as ending up in a loop on the cytosolic side of the myelin membrane (See section 2.2.2). This loop segment of the peptide could serve to interact with other myelin proteins such as MBP or even act as a membrane anchor guiding the protein into the membrane so as to position the protein properly in the development of the myelin membrane. In order to better understand the functions of this loop region of PLP, CD measurements were initially carried out, between peptide concentrations of 10μM and 60μM, in the different model systems used in this project to determine its secondary structure.

5.4.1 Concentration-dependent structure of PLP peptide in buffer

The buffer used in the CD measurements was 10mM Tris and 100mM NaF buffer pH 7.4. The PLP peptide was added in at concentrations of 10, 20, 40 and 60μM and scans were taken in the far UV region (190-260 nm). Unlike melittin which was mostly random coiled in buffer, the PLP exhibited some interesting properties in buffer as shown in Figure 5.9.

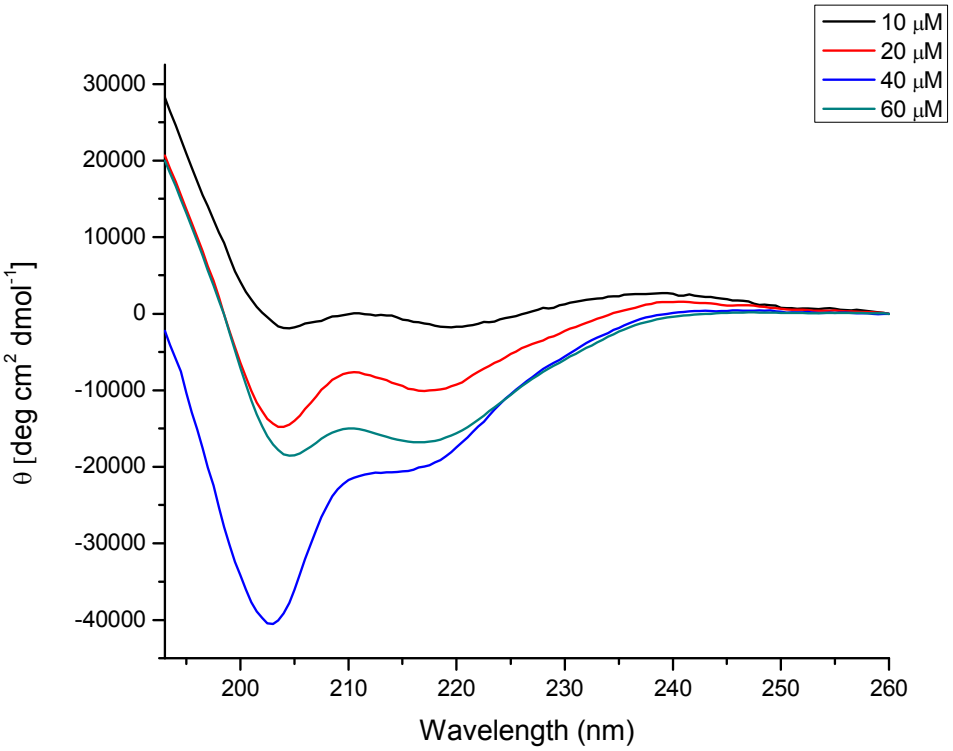

Figure 5.9: Concentration-dependent far UV CD spectra of PLP peptide in buffer

The PLP peptide was added to the 10mM Tris, 100mM NaF buffer pH 7.4, approximately 3 minutes before the scan was started, vortexed and then briefly centrifuged before scanning. Four scans were taken for each sample and all measurements were carried out at 25°C in a 1mm pathlength cuvette. The final averaged spectra were converted to molar ellipticities and further smoothed using the AVIV CD software.

The overall structure of the PLP peptide seemed to indicate that it contained some degree of an alpha helix even at its lowest concentration of 10μM. As the concentration increased from 10 to 40μM, the interactions of the peptide seemed to be increasing and its CD spectra exhibited a mostly random coiled signal (minima at ~203nm) with a small amount of helical structure present as shown by the local minima at around 220nm. The 40 μM spectra was quite different from that observed at the other concentrations and had a very high negative molar ellipticity at around 203nm which was surprising. At this point it would appear that the

peptide is mostly random coiled but the presence of a slight minima at around 220nm would indicate the presence of a small amount of a helical structure. At 60µM the peptide interactions seemed to decrease as shown by the upward shift of the spectrum, and the overall shape of the spectrum changed to show a mostly helical structure with the first local minima previously seen at 203nm now shifting to around the 205 nm mark. These changes would indicate that the PLP peptide, which is slightly less amphipathic than melittin, with a smaller hydrophobic moment of 2.49 (see Figure 2.4, Chapter 2) and only has a net charge of +3, had more tendency to self associate to shield its hydrophobic residues. As the concentration increased, the peptide seemed to undergo a structural change from a partly helical structure with a small amount of a random coil structure to a predominantly helical structure.

5.4.2 Concentration-dependent structure of PLP peptide in 80% TFE

The C-terminus peptide selected for this study has never been studied before, but prediction studies showed that this peptide should exhibit a small amount of helical structure in most membrane environments. To further analyse the peptide's structure, CD measurements were taken in 80% trifluoroethanol (TFE) solution. Measurements were also taken in 20% and 50% TFE solution and the results are shown in appendix B. In most cases, TFE enhances the helicity of peptides that are already helical in solution or induces helicity in peptides that are mostly random coiled (Rajan and Balaram, 1996). TFE is often used as a membrane mimetic solvent to induce secondary structures similar to those produced in membrane environments. The structure stabilising property of TFE is thought to arise mainly

due to its hydrophobicity which is due to the presence of the trifluoromethyl group which allows TFE to interact with the hydrophobic side chains of peptides, as well as hydrogen bonding. TFE can form better H-bonds than ethanol or water and interact with carbonyl groups to stabilize secondary structures. In the case of the PLP peptide, TFE was successful in inducing an almost perfect alpha helical structure at the higher concentrations as shown by its CD signal which was very similar to the alpha helical CD signal shown in Figure 2.8. This information would suggest that the PLP peptide has the propensity to form amphipathic α-helices in membrane environments similar to those used for the melittin study. The spectra obtained even showed the presence of an isodichroic point at around 200nm which would indicate the transition of the peptide from a mixture of random coil and helical structure to a predominantly helical structure. However, the questions remain, is whether the PLP peptide will interact with the model membranes in the same way as melittin did, or if its interaction and structural shape would differ largely from that of melittin.

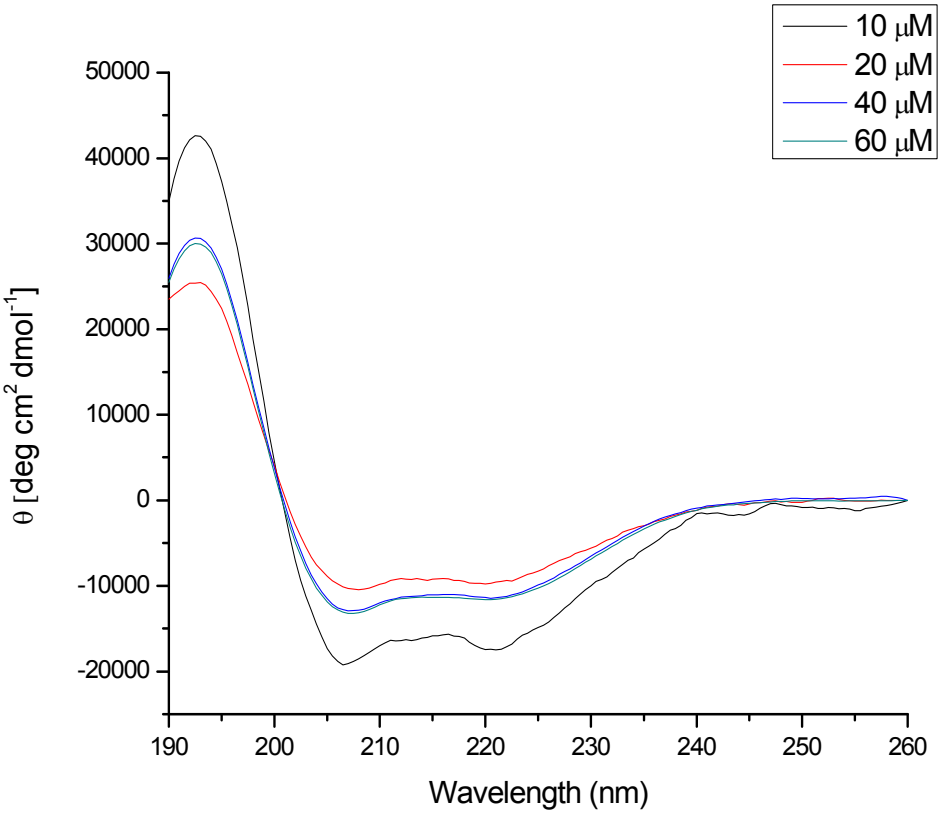

Figure 5.10: Concentration-dependent far UV CD spectra of PLP in TFE solution

The PLP peptide was added to the 80% TFE solution, approximately 3 minutes before the scan was started, vortexed and then briefly centrifuged before scanning. Four scans were taken for each sample and all measurements were carried out at 25^{o}C in a 1mm pathlength cuvette. The final averaged spectra were converted to molar ellipticities and further smoothed using the AVIV CD software.

5.4.3 Concentration-dependent structure of PLP peptide in POPC

CD measurements were also taken in zwitterionic POPC LUVs which is the simplest model system used in this project and the results are shown in Figure 5.11. As the concentration increased from 10μM to 20 μM, the interaction of the peptide with the lipid vesicles increased as shown by the greater negative ellipticities observed. Both spectra seemed to indicate that the peptide had adopted a helical structure which still contained

some random coil structure as shown by the shift of the local minima at around 204 nm. At 40μM, the overall shape of the spectra changed, and the minima at the 205 nm decreased while the minima at the 220 nm mark increased significantly. Similar to the structure of the PLP peptide in buffer, the 40 μM spectra appeared to undergo some unusual change compared to the 5 μM and 10 μM spectra. In this case instead of showing a mostly random coiled structure as was the case in the buffer measurement, the peptide seemed to adopt a mostly helical structure as indicated by the presence of two minima at 206nm and 222nm. However, unlike a typical alpha helical signal, the spectra observed had a shallower minimum at 206 nm, which would indicate the presence of a different type of helical structure such as a 3_{10} helix. Further research will have to be conducted to confirm this hypothesis in order to determine the specific type of structural change the peptide is going through. Since the PLP peptide can readily self-associate it could also be possible that the association of the peptide molecules could give rise to this unusual signal. At 60μM the overall shape of the spectrum was lost which would indicate an aggregation process taking place. Since the sample used for the measurement turned cloudy, it is possible that the peptide could have caused the lipid vesicles to fuse together and undergo an aggregation process which would cause to be precipitated out of the buffer solution.

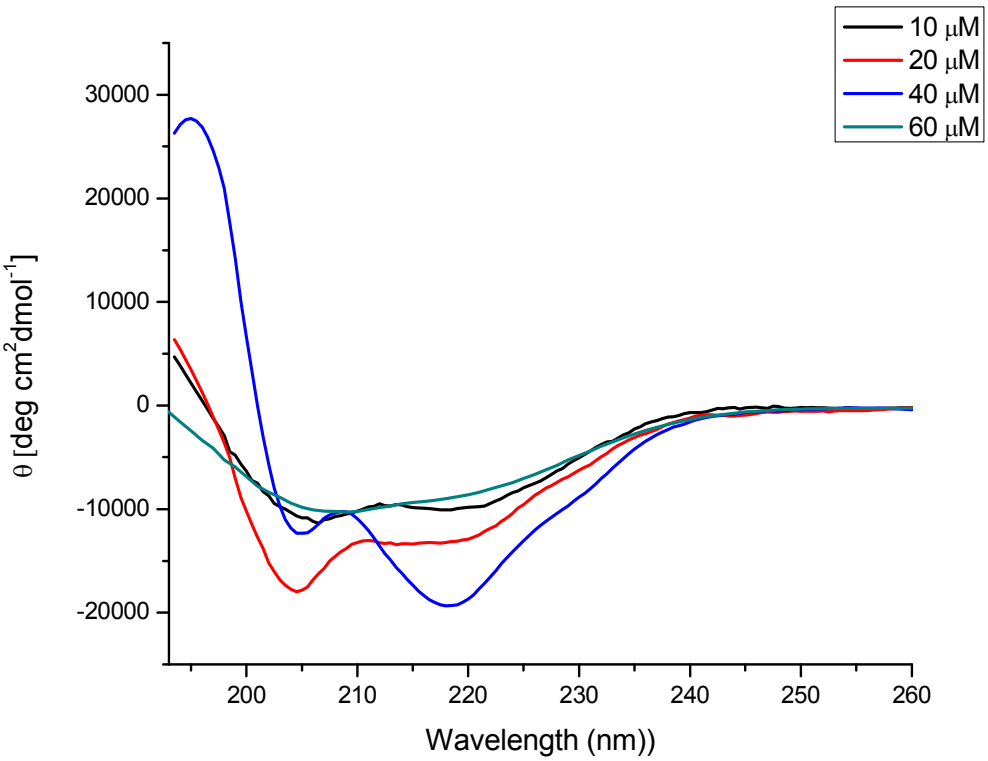

Figure 5.11: Concentration-dependent far UV CD spectra of PLP in POPC

The PLP peptide was added to 1mM POPC LUVs, approximately 3 minutes before the scan was started, vortexed briefly and briefly centrifuged before scanning. Four scans were taken for each sample and all measurements were carried out at 25^{o}C in a 1mm pathlength cuvette. The final averaged spectra were converted to molar ellipticities and further smoothed using the AVIV CD software.

5.4.4 Concentration-dependent structure of PLP peptide in raft model LUVs

The raft system which contains equimolar concentrations of sphingomyelin, POPC and cholesterol is mainly in a liquid ordered (L_o) phase at room temperature. The high cholesterol and sphingomyelin content confers a very rigid structure to the bilayer making it harder for peptides to bind strongly to its surface. The PLP peptide was introduced into this system at concentrations going from 10μM to 60μM and CD measurements were taken in

the far UV region. The spectra obtained at each concentration were overlaid for comparison and are shown in Figure 5.12.

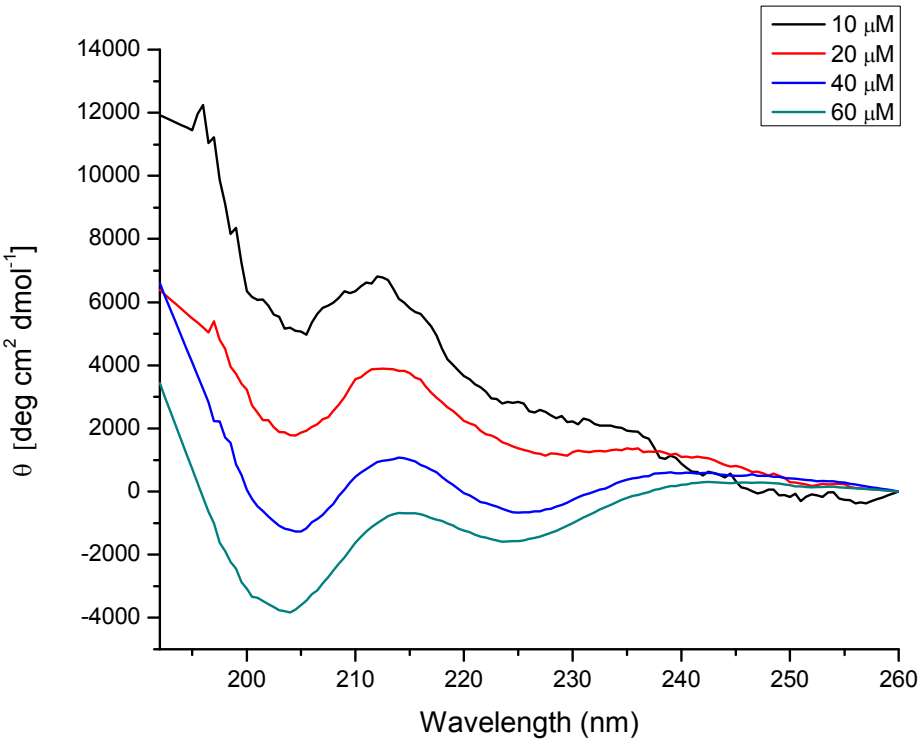

Figure 5.12: Concentration-dependent far UV CD spectra of the PLP peptide in the raft model

The PLP peptide was added to the raft (PC/SM/Chol 1:1:1) LUVs, approximately 3 minutes before the scan was started, and centrifuged briefly before scanning. Four scans were taken for each sample and all measurements were carried out at 25°C in a 1mm pathlength cuvette. The final averaged spectra were converted to molar ellipticities and further smoothed using the AVIV CD software.

The CD spectra indicate that the peptide did not have a strong interaction with the vesicles at the 10μM and 20μM concentrations since their spectra had no well defined structure as well as very low ellipticities. However as the concentration increased, the interactions with the lipid vesicles also increased as shown by the downwards shift of the spectra and the development of a more helical structure. The 40μM and 60μM both seemed to contain

predominantly random coiled structures with a small amount of an alpha helical content as indicated the presence of the local minima at 225nm. Unlike its interaction with POPC, the PLP peptide in this raft system had lower ellipticity values which would indicate that the peptide had a very small affinity for this membrane bilayer. Since the raft bilayer is extremely rigid, this would make it harder for the peptide to properly interact with the lipid bilayer, hence its mostly random coiled structure. In this case it is possible that the peptide had a minimum amount of interaction with the bilayer and was therefore acting more as mobile loop.

5.4.5 Concentration dependent structure of PLP peptide in plasma membrane model

The plasma membrane model used in this project contained around 20 %mol cholesterol, 44 %mol POPC, 25 %mol POPE and the negatively charge phospholipid POPS at a concentration of 10 %mol which conferred an overall negative charge to the bilayer. Given that the PLP peptide has a net positive charge of +3 at neutral pH, the negative charge on the plasma membrane bilayer should promote strong electrostatic interactions with the peptide. The concentration dependent CD measurements taken revealed that the peptide had no real structure at around 10μM but adopted a mostly helical structure at 20μM and 40μM (Figure 5.13). As the concentration of the peptide increased, the overall interactions with the lipids also seemed to increase as shown by the greater negative ellipticities observed, which is indicative of strong peptide-lipid interactions. Finally, at 60μM the spectra started to lose its definition which would indicate the start of an aggregation process where the PLP peptide caused the lipid vesicles to fuse. These results show that the combination of cholesterol and

negative charge in the membrane bilayer, greatly helped in increasing the interaction of the peptide with the bilayer compared to the POPC and the raft model. The increased interaction with the lipids, allowed the peptide to achieve a more helical structure at higher concentrations, a feature that was not observed in the raft model membrane system.

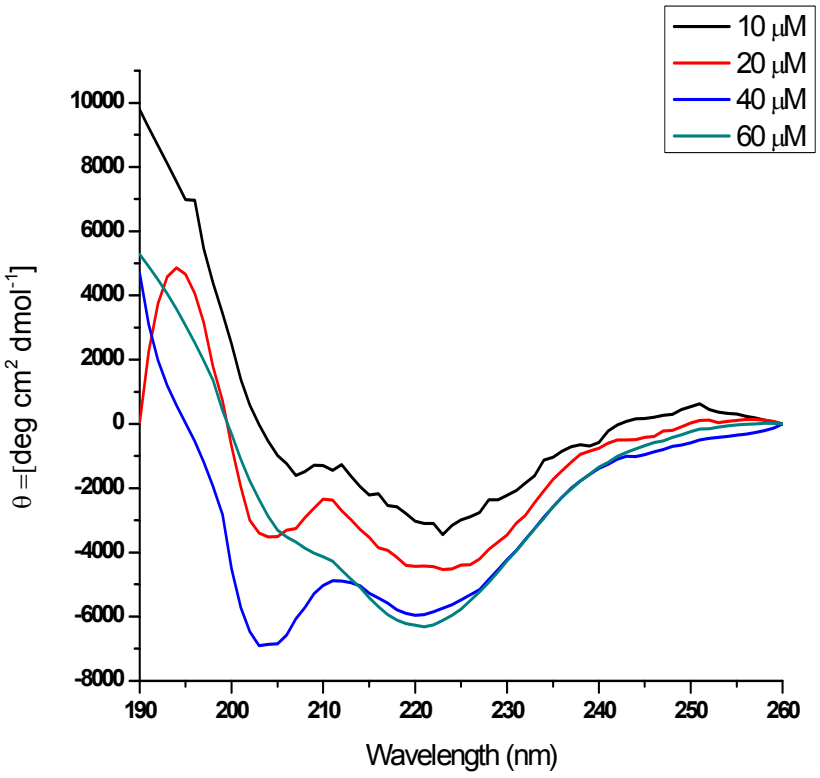

Figure 5.13: Concentration-dependent far UV CD spectra of the PLP peptide in the plasma membrane model

The PLP peptide was added to the plasma membrane (PC/PE/PS/Chol at 44:25:10:20 %mol) LUVs, approximately 3 minutes before the scan was started, and centrifuged briefly before scanning. Four scans were taken for each sample and all measurements were carried out at 25^{o}C in a 1mm pathlength cuvette. The final averaged spectra were converted to molar ellipticities and further smoothed using the AVIV CD software.

5.4.6 Concentration dependent structure of PLP in cytosolic myelin membrane model

The cytosolic myelin model used in this project contained 44% cholesterol, which is unusually high for cell membranes, and would make it a very rigid bilayer capable of preventing the strong binding of peptides. However, it also contained two negatively charged phospholipids namely, POPS (13 %mol) and POPI (2 %mol), which conferred an overall negative charge to the bilayer which could thus promote the binding of the positively-charged PLP peptide in spite of the high cholesterol content. The structure of the peptide was determined by taking CD measurements in the far-UV region and the results are shown in Figure 5.14.

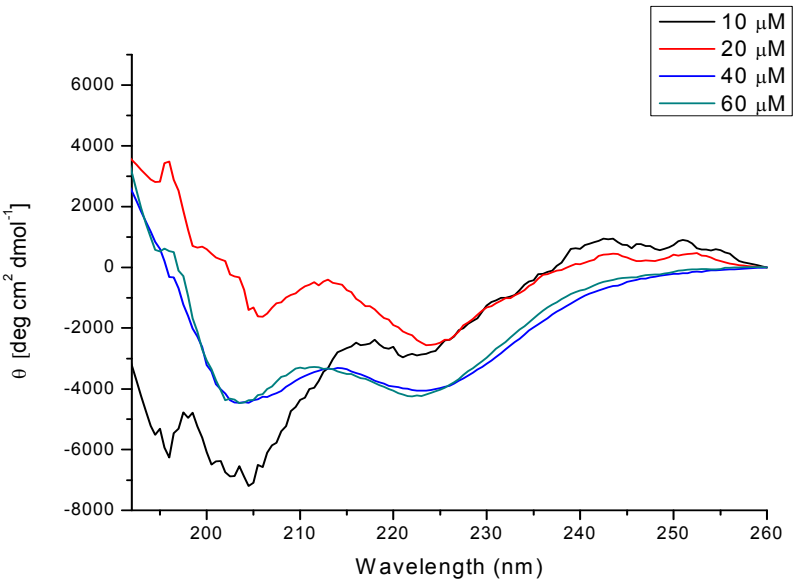

Figure 5.14: Concentration-dependent far UV CD spectra of the PLP peptide in the cytosolic myelin model

The PLP peptide was added to the cytosolic myelin (PC/PE/PS/PI/SM/Chol at 11:27:13:2:3:44 %mol) LUVs, approximately 3 minutes before the scan was started, and centrifuged briefly before scanning. Four scans were taken for each sample and all measurements were carried out at 25^{o}C in a 1mm pathlength cuvette. The final averaged spectra were converted to molar ellipticities and further smoothed using the AVIV CD software.

The PLP peptide seemed to have a relatively good interaction with the cytosolic membrane model. At concentrations of 10μM the peptide did not appear to have a strong interaction with the lipid vesicles but as the concentration increased to 20μM, the peptide started developing a small amount of an alpha helical structure but still contained a predominantly random coiled structure. As the concentration further increased to 40μM and 60μM, the peptide's spectra changed to a predominantly alpha helical signal which had a lower molar ellipticity than the 20μM concentration. At 40μM and 60μM, the CD spectra showed $\theta_{222nm}/\theta_{208nm}$ of 0.99 and 1.18 respectively which would confirm the presence of a mostly helical structure for the PLP peptide. These results are surprising since the structure of peptide does not seem to be affected by the high level of cholesterol present in the bilayer and unlike melittin which would rather self-associate rather than penetrate this rigid structure, the PLP peptide instead seemed to have favorable interactions. Although the peptide-lipid interactions were relatively weak, the results could indicate that the PLP peptide actually favours liquid ordered (lipid rafts) environments.

5.4.7 Concentration-dependent structure of PLP in healthy and diseased myelin models

The two systems used to represent healthy and diseased myelin models differed from each other mainly in terms of their cholesterol and sphingomyelin content. While the cholesterol was shown to increase by around 6% during MS, the sphingomyelin level decreased by 4%, which could lead to changes in the lipid organization in the bilayer. The FRET results have shown that the changes in lipid composition in diseased myelin, lead to the formation of smaller lipid domains compared to the healthy myelin membrane (See section

4.2.2). This change in lipid organization in the myelin membrane, could affect the structure and function of proteins in the membrane. In order to study the structural difference of the PLP peptide in both these systems, CD measurements were taken in the far UV regions, with increasing concentrations of the peptide and the results are shown in Figure 5.15.

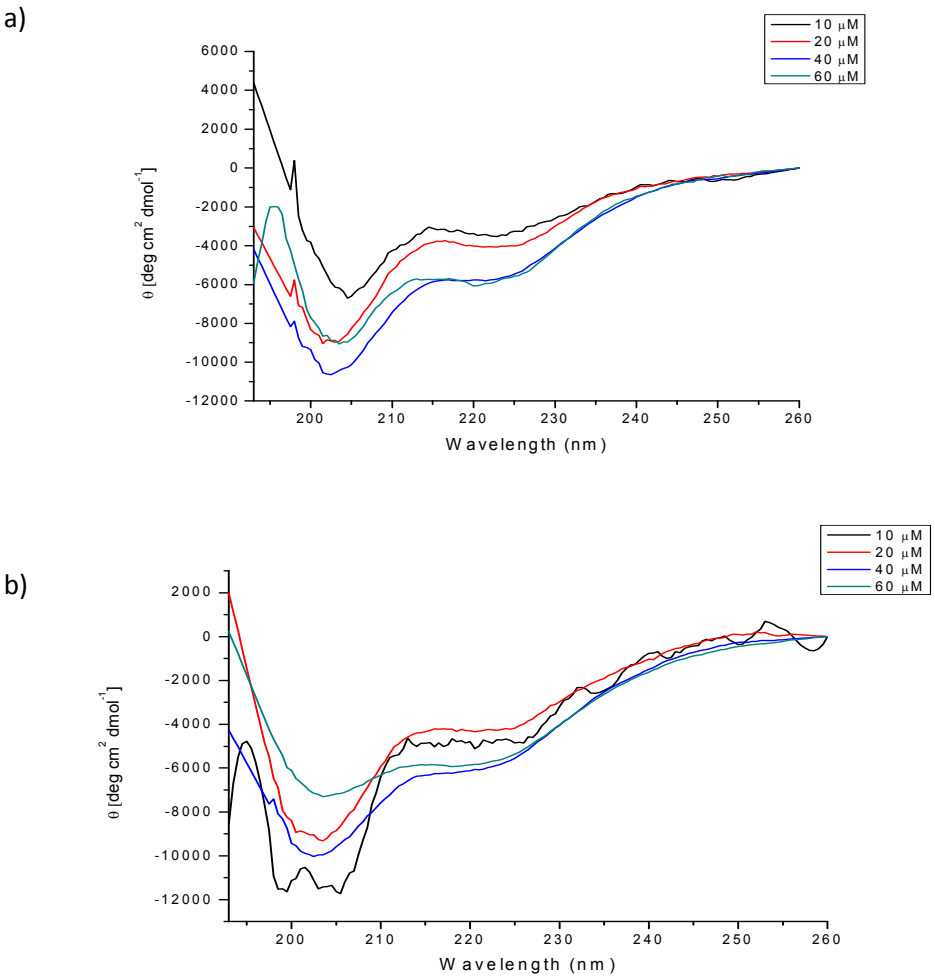

Figure 5.15: Concentration-dependent far UV spectra of the PLP peptide in the healthy and diseased myelin models

The PLP peptide was added to a) healthy myelin (PC/PS/PE/SM/Chol at 25.9:7.3:29:6.2:31.6 %mol) b) diseased myelin (PC/PS/PE/SM/Chol at 20.1:7.4:32.9:2.2:37.4 %mol) LUVs, approximately 3 minutes before the scan was started, vortexed briefly and then centrifuged briefly before scanning. Four scans were taken for each sample and all measurements were carried out at 25°C in a 1mm pathlength cuvette. The final averaged spectra were converted to molar ellipticities and further smoothed using the AVIV CD software.

At 10μM concentration, the PLP peptide appeared to have a mostly random coil structure along with some alpha helical properties in both the healthy and the diseased myelin systems but the lipid-peptide interactions seemed to be the strongest in the diseased myelin system as shown by the deeper local minima at approximately 205nm. As the concentration increased from 20 to 40μM, the spectra in both systems showed similar structural characteristics with the peptide exhibiting slightly helical structure but still containing a significant amount of random coil structure. Further increases in the peptide concentration lead to increased interactions with the lipid bilayer with the peptide maintaining some of its random coil structure. However, at 60μM, the spectra showed some differences; the healthy myelin system has a slightly stronger interaction with the peptide and a higher helical content compared to the diseased system. While the spectrum in the healthy system maintained its partly random coil structure, the 60μM spectrum in the diseased system showed a shift to a mostly helical structure but suffered a decreased in its interactions with the lipid bilayer as shown by the upwards shift of its spectrum. All in all, it would seem that the peptide is mostly random coiled in both systems with only a small amount of an alpha helical structure. As the concentration increased, however, the peptide seemed to gain a more α helical shape in the diseased system although the upwards shift of its 60μM spectra would indicate that the peptide is not interacting as efficiently with the lipid bilayer. The reason for this could due to the increased levels of cholesterol which would make it harder for the peptide to interact with the bilayer. As a result of this, it could be possible that a fraction of the PLP in the sample could be starting to aggregate. These findings would suggest that the demyelination process could end up causing a decrease in the interaction of the PLP

C terminus with the membrane which could in turn affect the proteins functions, thus leading to interrupted cellular processes.

5.5 Comparison of the effects of lipid composition on melittin and the PLP peptide structure

Melittin is a small positively charged (+6) peptide which according to our results seems to interact with lipid vesicles predominantly through electrostatic interactions at low concentrations. The PLP peptide on the other hand showed peptide-lipid interactions that were quite different although it was also positively charged (+3) and it would seem that a combination of electrostatic interactions as well as hydrophobic effects, dictated the peptide's interactions with lipid bilayers. In order to better compare the differences in structure and interactions of these two peptides, their helical content in each system was calculated while the molar ellipticity at 222 nm (θ_{222}nm) was plotted as a function of the concentration to study the effects of peptide concentration on the structure of melittin and the PLP peptide. Changes in the ellipticity at 222nm are a useful probe for visualizing varying helical content.

5.5.1 Change in helical content of melittin and the C-terminus PLP peptide in various membrane model systems

The molar ellipticities at 222nm (θ_{222nm}) were plotted as a function of the peptide concentration in order to establish the difference in the peptide-lipid interactions of melittin and the C-terminus PLP peptide. These graphs gave an indication of what concentrations of each peptide interacted the best with the lipid vesicles and at what point aggregation was

most likely to occur. According to Figure 5.16 which shows the θ_{222nm} of melittin, the peptide appeared to have the greatest peptide-lipid interactions in most of the systems at around 10μM as shown by the higher negative ellipticities obersved at that concentration. After this point, the curve in most of the lipid systems started to go up towards less negative values which would indicate the start of an association process. At this point, melittin formed its characteristic tetrameric structure consisting of four alpha helices which makes it possible for the peptide to lyse lipid vesicle lacking cholesterol. According to Figure 5.16, it would appear that melittin had the least interaction with the raft model systems which was expected, given that this system is very rigid, and had the highest interaction with the plasma model membrane which contained 20% cholesterol and 10% POPS. The θ_{222nm} of melittin at 10μM in most of the myelin model membranes were all very close to each other, with the diseased and the cytosolic myelin models having a slightly higher ellipticity than the healthy myelin model.

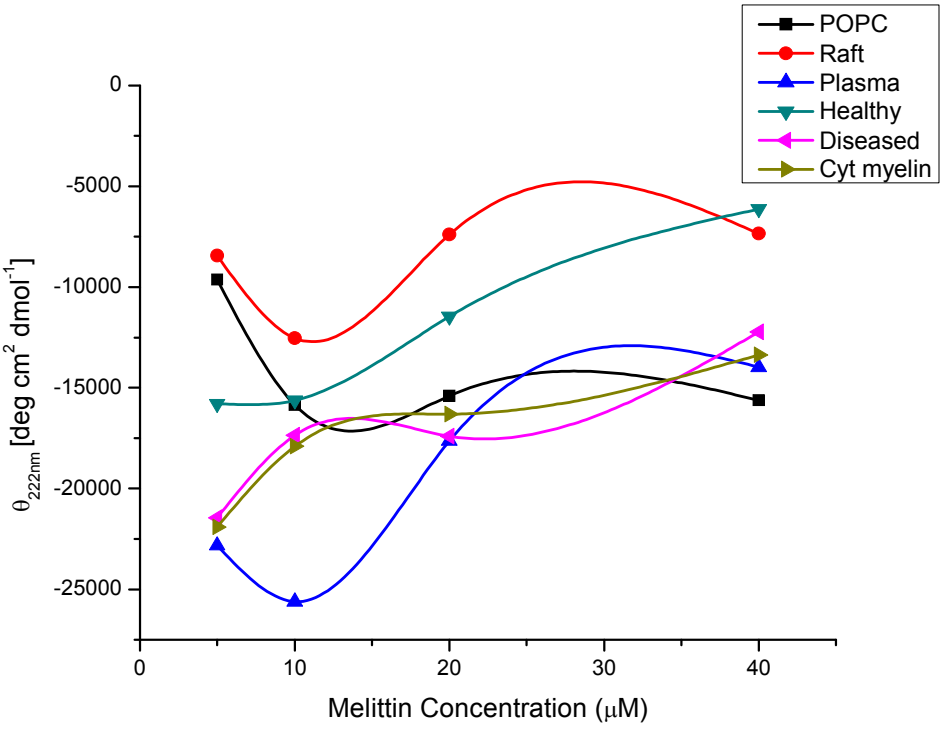

Figure 5.16: Change in helical content as a function of melittin concentration
The molar ellipticity at 222nm (θ_{222nm}) was plotted against increasing concentrations of melittin. In most of the systems, melittin appeared to have the highest peptide-lipid interaction at 10μM.

When looking at the lipid titration curves for the PLP peptide, it would appear that this peptide had the greatest interaction at 40μM concentrations as shown in Figure 5.17. Although the molar ellipticity at 60μM appeared to be slightly larger than the 40μM, this point was neglected since the peptide showed signs of aggregation of the lipid vesicles in most of the systems at this concentration. The PLP peptide appeared to have the least peptide-lipid interactions with the raft system and the highest interaction with the POPC system, whereas the other negatively charged systems had intermediate interactions. Since the raft model is extremely rigid, this could explain the lower θ_{222nm} obtained in this system compared to the others. However, it should be noted that for this raft system, the CD spectra indicated that the peptide gained more helicity as its concentration increased and this

system was the only one in which the peptide did not seem to aggregate. While the plasma membrane and the diseased and healthy myelin models all had similar θ_{222nm} at 40μM, the cytosolic myelin membrane showed a lower negative θ_{222nm} which would be indicative of reduced peptide-lipid interactions given that this system contains around 44% cholesterol and would make it harder for the peptide to interact with the bilayer. Unlike the raft system which showed increasing negative θ_{222nm} as the concentration increased, the peptide seemed to promote aggregation at 60μM in the cytosolic myelin membrane, which would suggest that, in the presence of negatively charged lipid POPI (3%) and POPS (13%), the positively charged peptide (+3) could potentially associate on the surface of the lipid vesicle, ultimately causing the vesicles to fuse and precipitate out of the solution. This information would suggest that the PLP peptide did not favour interaction with cholesterol containing lipid system while the presence of negatively charged lipids in the lipid bilayer seemed to promote peptide association.

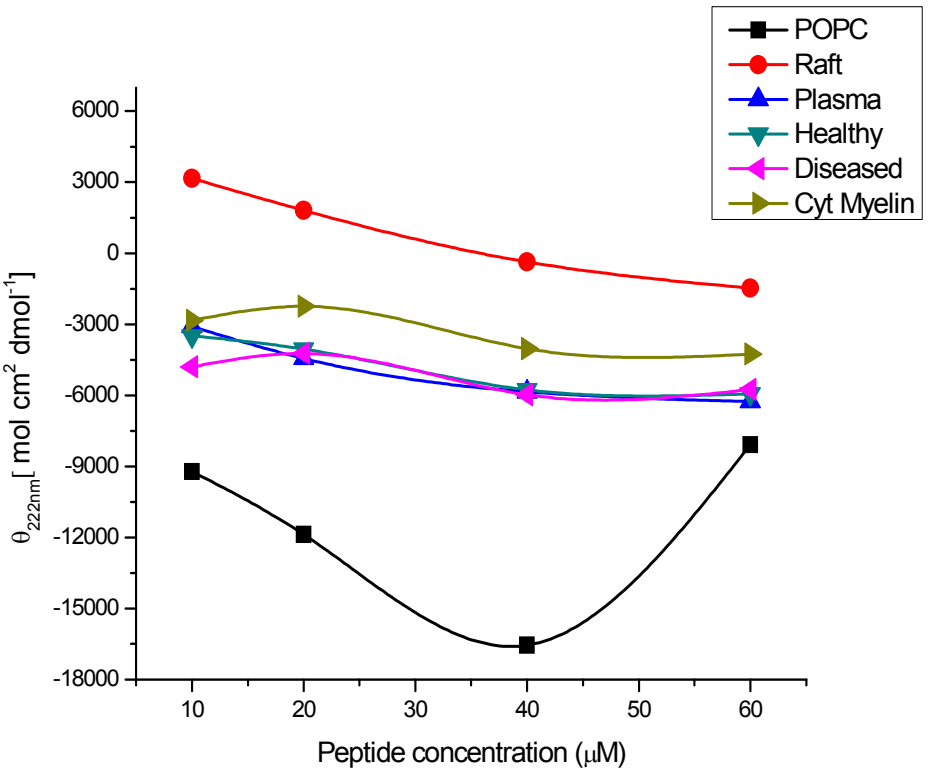

Figure 5.17: Change in helical content as a function of the PLP peptide concentration
The molar ellipticity at 222nm (θ_{222nm}) was plotted against increasing concentrations of the PLP peptide. In most of the systems, melittin appeared to have the highest peptide-lipid interaction at 10μM.

5.5.2 Comparison of structural difference of melittin and the PLP peptide in different membrane models

In order to establish a better comparison for the structure of melittin in the different model membrane systems used in this study, the 10μM CD spectra were overlaid for better analysis and are shown in Figure 5.18. The 10μM spectra were selected since they showed the highest peptide lipid interactions in most of the systems as shown in Figure 5.16. Furthermore, at 10μM, the concentration that was also used in the FRET study, the peptide was shown to be mostly monomeric.

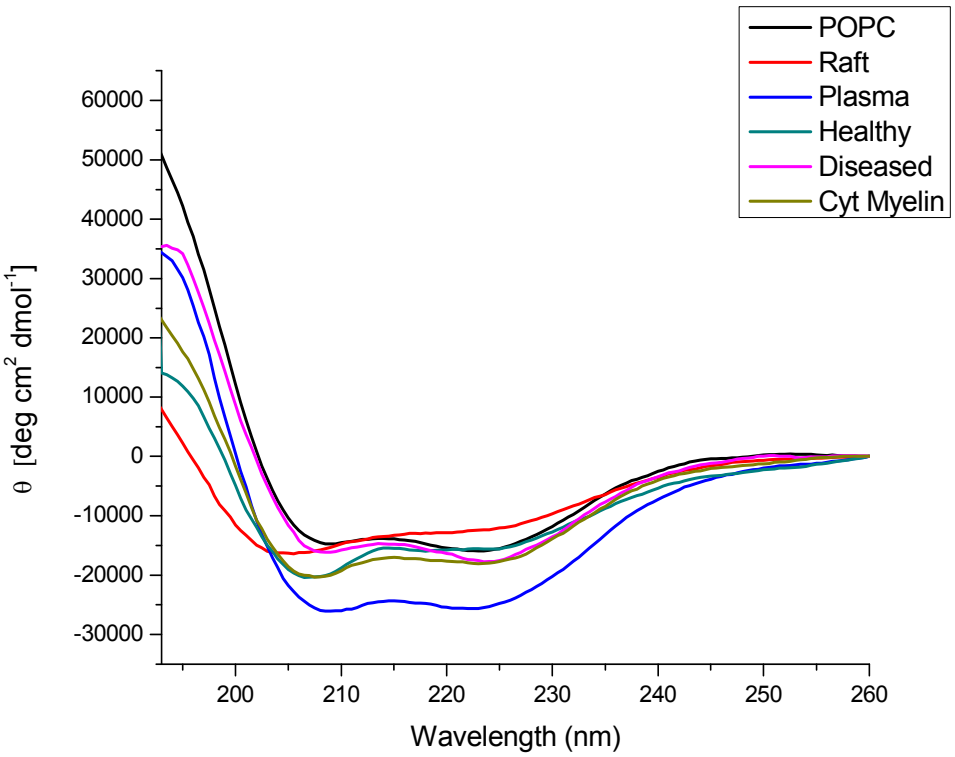

Figure 5.18: Far UV CD spectra for 10µM melittin in different model systems

Melittin was added to the LUVs, approximately 3 minutes before the scan was started, vortexed and then briefly centrifuged before scanning. Four scans were taken for each sample and all measurements were carried out at 25^{o}C in a 1mm pathlength cuvette. The final averaged spectra were converted to molar ellipticities and further smoothed using the AVIV CD software.

From Figure 5.18 it would appear that 10µM of melittin has the highest interactions with the plasma membrane model. Previous fluorescence and CD studies have shown that at low concentrations (≤ 10µM), melittin is usually monomeric and as the concentration of the peptide increases, the helical content also increases due to aggregation (Hartings *et al.,* 2008). This plasma membrane system contained a moderate amount of cholesterol (20%) compared to the other models used in this project as well as a small amount of negatively charged POPS phospholipids (10%). The cytosolic myelin membrane and the healthy myelin

model had the next highest level of peptide interactions. These two systems had a higher cholesterol content than the plasma model membrane, at 44% and 31.7% cholesterol content respectively. The slightly higher amount of POPS (13%) present in the cytosolic myelin membrane along with POPI (3%), appeared to have compensated for the high level of cholesterol in the system which could otherwise have hindered the interaction of melittin with this rigid bilayer. POPC and the diseased model had almost identical spectra, where melittin appeared to be predominantly helical with the presence of a small amount of random coil structure. Since the diseased myelin model contained a high amount of cholesterol (37.4%) and was negatively charged, it is highly like that melittin could not penetrate the bilayer but instead aggregated on the surface of the vesicles due to the presence of the negative charge. This would account for the lower peptide-lipid interactions observed since cholesterol prevents melittin from binding to tightly and forming pore structures that could rupture the lipid vesicles. Instead, it is likely that melittin self-associated on the surface and could have formed a mixture of different structural species. As the concentration of melittin increased from 5 μM to 40 μM, it could be possible that the peptide initially interacted as a monomer with the lipid bilayer, but at higher concentrations it self-associated and formed either dimeric or tetrameric alpha helical structures. The POPC model on the other hand, contained no cholesterol and it is possible that melittin could have self associated to form a tetramer structure consisting of four alpha helical structure and formed pore structure which could easily have lysed the membrane bilayer hence accounting for the lower interactions.

In order to better compare the effects of the different lipid bilayers on the structure on the PLP peptide, its 40μM CD spectra from each of the lipid system were overlaid for comparison. The 40μM spectra was selected based on the lipid titration graphs shown in Figure 5.17 which indicated that the peptide had the highest interaction with the lipid vesicles at this concentration. At this 40 μM concentration, it would seem that the POPC system had the maximum interaction with the peptide. However, this signal could also be due to the start of an aggregation process where the peptide self associates on the surface of the bilayer in order to shield its hydrophobic residues from the polar environment it is in. The secondary structure of the peptide in the other cholesterol containing systems seemed to have more of a random coil structure with a local minimum in the 203nm region but also contained a small degree of an alpha helical structure as shown by the shallow minima at around 223nm. The plasma membrane model which contains 20% cholesterol and 10% POPS, was the only system exhibiting more of an alpha helical structure with only a small amount of random coil present. The diseased and healthy myelin model both showed spectra that were very close in shape but the cytosolic myelin membrane which contains almost 44%mol of cholesterol along with a significant amount of negatively charged lipids showed an interaction which was very close to that of the raft model membrane. This would suggest that the negative charge of the bilayer only plays a small role in the binding of the peptide which depends more on the level of cholesterol present. While electrostatic interactions would guide and allow the peptide to bind to the surface of the bilayer, it is the amount of cholesterol present in the bilayer that would dictate the depth of penetration of the peptide.

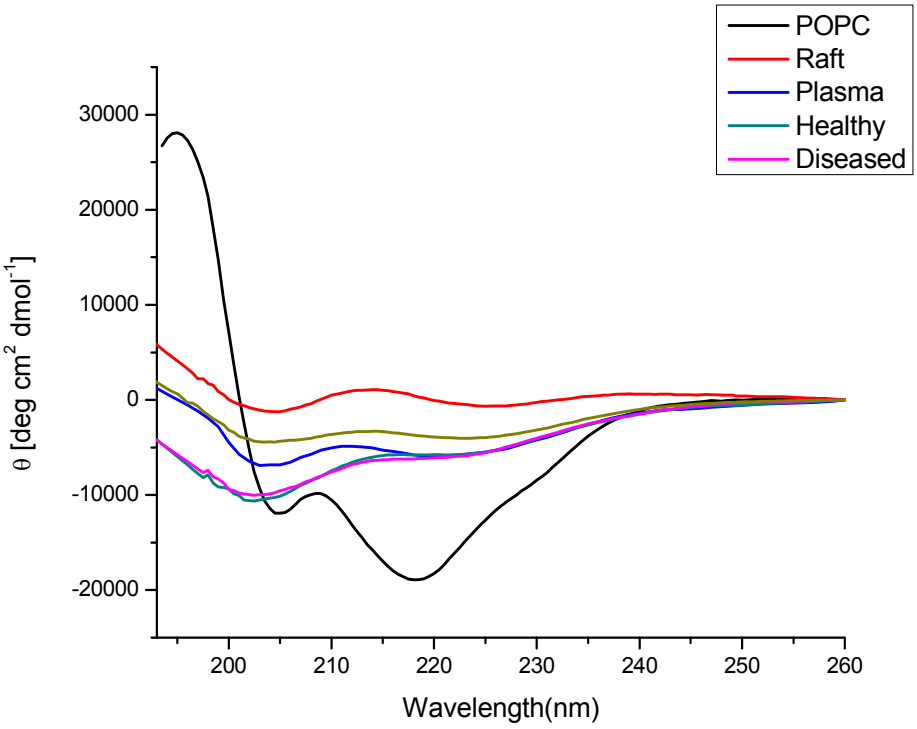

Figure 5.17: Far UV CD spectra of 40µM of the PLP peptide in the different lipid systems

The 40uM CD spectra of the PLP peptide measured in each of the lipid systems were aligned for comparison purposes.

To further analyse the alpha helical content of 10 µM melittin and 40µM PLP peptide in each of the system, the helical contents of the peptides were calculated using equation 5.1 where F_H is the fractional helicity and θ_{222nm} is the molar residue ellipticity at 222nm (Morriset *et al.,* 1973; Correa and Ramos, 2009). The values obtained only provide an estimation of the helical content present and cannot be expected to be very accurate since general parameters were used.

$$\%F_H = \frac{[\theta]_{222nm} - [\theta]^o_{222nm}}{[\theta]^{100}_{222nm} - [\theta]^o_{222nm}} \text{ x100} \quad \text{..... Equation 5.1}$$

Where $[\theta]^{o}_{222nm}$ is the value of a completely coil structure (3000 deg cm^2 dmol^{-1}) and $[\theta]^{o}_{222nm}$ is the molar ellipticity for a completely helical structure (36000 deg cm^2 dmol^{-1}).

Table 5.3: Alpha helical content of melittin and PLP peptide in different model membranes

The molar ellipticity at 222 nm (θ_{222nm}) of 10 μM melittin and 40 μM PLP combined with equation 5.1 were used to calculate the fraction of alpha helix present in melittin and the PLP peptide. These values only provide an estimate of the total helix content and might not be 100% accurate.

Lipid system	% Helical content	
	Melittin	PLP peptide
POPC	48	50
Raft	24	9
Plasma membrane	73	22
Cytosolic myelin model	48	18
Healthy myelin model	52	23
Diseased myelin model	54	23

Melittin appeared to have a higher propensity for forming alpha helices in membrane environments compared to the PLP peptide as shown in Table 5.3. It is well established that monomeric melittin in aqueous solution shows an essentially random coil conformation whereas membrane-bound melittin usually shows a signal characteristic of an α-helical structure (Klocek *et al.,* 2009; Hartings *et al.,* 2008). The results obtained in this study, showed that even though cholesterol can affect the secondary structure of membrane-bound melittin, it is not the only factor that controls it. This can be observed in the myelin-mimicking lipid systems used, all of which contained high amounts of cholesterol (31%-44%),

melittin still showed the formation of a relatively high level of helix formation. Furthermore, the plasma membrane model system which exhibited the highest levels of helical content, contained a lower cholesterol level (20 %mol) than the myelin systems as well as a 10 %mol negatively charged POPS, factors that would both seem to promote the binding of melittin. Previous studies (Hall *et al.,* 2010) have also described such high helicities of melittin in negatively charged and cholesterol containing lipid vesicles. The raft system on the other hand showed the least amount of helix formation which could be due to its very rigid structure as well as its lack of negative charge, whereas the zwiterrionic POPC bilayer showed a helix content of around 48%. In a recent study, the percent alpha helical content of melittin in SUVs composed of DMPC/DMPG/Chol (16:4:5), was also estimated to be around 51% (Hall *et al.,* 2010). Since DMPG is a negatively charged lipid, these results would indicate that electrostatics play a major role in determining the final secondary structure of melittin in these systems. When comparing the healthy myelin system to the diseased myelin system, it would appear that melittin had a more helical structure in the diseased system. In this case it could be possible that the higher level of cholesterol in this system could actually promote the start of an oligomerization process where melittin self associates into its tetrameric structure consisting of four alpha helices. This is further confirmed by the upward shift of the spectrum in the diseased myelin system shown in Figure 5.18 as well as the θ_{222nm} graph in Figure 5.16 which shows a decrease in the molar ellipticity of the peptide. All in all, it would be reasonable to affirm that the binding of melittin to membrane bilayers is strongly dependent on electrostatic interactions while the presence of cholesterol could promote oligomerization of the peptide on the surface of the bilayer. In cases where cholesterol is

absent, melittin could easily lyse these vesicles by forming a torroidal pore structure in the bilayer. Variables such as concentration of the peptide, the ionic strength and pH of solution and the composition of the lipid bilayers have all been shown to influence the way melittin interacts with membranes (Hall *et al.,* 2010).

The helicity content of PLP calculated in each of the lipid systems was much lower than melittin while CD measurements taken for the PLP peptide indicated that the peptide had a stronger affinity for bilayers that contained cholesterol at higher concentrations. According to Table 5.3, it would appear that the PLP peptide had the greatest helical content in the POPC system (50%) and the lowest helicity in the raft system (9%). This information would suggest that while the PLP peptide did not seem to favour interaction with cholesterol containing membranes. The rigidity of the bilayer as well as the lipid composition appeared to play key roles in the binding and the overall structure of the PLP peptide. PLP in the plasma model membrane and the healthy and diseased myelin models, showed a helical content that were very close to each other at around 23% whereas the cytosolic membrane contained the second lowest helical content after the raft system (18%). Our results also indicated that the increase in the cholesterol level during demyelination did not seem to affect the overall structure of the peptide since both the diseased and healthy myelin systems showed a helical content of around 23%. This would imply that the PLP peptide is not greatly affected by the levels of cholesterol in lipid bilayers but the presence of negative charges on the bilayer could instead promote easy aggregation of the peptide on the surface of lipid bilayers which would cause the peptide to lose part of it helical content. Previous studies focusing on the detergent extraction of proteins from the myelin membrane have

shown that PLP usually binds to cholesterol enriched domains thus preferring association with lipid rafts (Simons *et al.,* 2000). This would suggest that the protein has an important role in sorting and trafficking in compact myelin, processes that usually involve lipid rafts. The cytoplasmic loops of the PLP protein are thought to mediate interactions between the surface of the myelin membrane and other myelin proteins. Furthermore, the C-terminus has been suggested to be of considerable importance in immunological cross-reactivity in most vertebrate species, given that its phenylalanine residues define a highly conserved epitope (Linington and Waehneldt, 1990). As such, any changes in the structure of these loops could cause interruptions in the interaction of PLP with the myelin membrane. Fortunately, unlike melittin which has closer properties to the basic proteins usually found in the CNS, the structure of the PLP peptide does not seem to be greatly affected by the lipid fluctuations taking place during the demyelination process. Although our study did not detect any structural changes in the PLP peptide when it interacts with diseased myelin, the tendency of the peptide to self-associate does seem to be higher in the presence of higher cholesterol levels. PLP has been suggested to exist on the "edge of aggregation" (Ng and Deber, 2010), and this property could be greatly amplify if the lipid composition is significantly affected during MS.

5.6 Quantitation of the binding affinity of the PLP peptide using ITC

ITC can be used to quantitate the binding affinity of peptides to membrane bilayers. Peptide binding is usually initiated by electrostatic interactions between a cationic peptide to a more anionic membrane bilayer. Depending on the peptide's net positive charge and the

membrane potential, electrostatic attractions would dictate the concentration of the peptide near the membrane bilayer. Under the right conditions such as ionic strength and peptide and lipid concentrations, ITC can be used to determine the enthalpy of such adsorption reactions as well as the partitioning coefficients. ITC measurements with melittin have been widely studied in POPC/POPG systems where the binding enthaply of the peptide was found to be mostly endothermic. The folding of melittin into an alpha helix is very enthalpically favorable which enhances the binding process (Klocek *et al.,* 2009). When the concentration of the peptide increases, melittin has been shown to self-associate and induce pore formation, a process which has been found to be mostly endothermic (Klocek *et al.,* 2009).

The PLP peptide used in this study however, has never been studied in much depth and in order to better characterize its binding process, ITC was used to measure its being affinity to POPC and POPC/POPS (8:1) vesicles. POPC is a simple neutral bilayer while the POPC/POPS system has net negative charge due to the presence of 8%mol POPS. All ITC measurements were carried out at room temperature (25^{o}C) and the lipid suspension was titrated into the titration cell containing the peptide solution (20µM). Initial results obtained showed that the binding to POPC vesicles (5mM) had an extremely low heat of reaction indicating a very low binding affinity of the peptide to POPC bilayers as shown in Figure 5.18. Increases in the peptide concentration only resulted in the precipitation of the peptide and lipid vesicles from solution. Measurements carried out in the negatively charged POPC/POPS system (5mM), at varying concentration of the peptide (5µM to 40µM) also resulted in precipitation of the lipid vesicles and peptide. These results indicated that the PLP peptide was very prone to aggregation and that binding to lipid bilayers was very sensitive to the

peptide concentration. Results obtained with POPC vesicles however seem to indicate that the binding of the peptide is mainly driven by entropy.

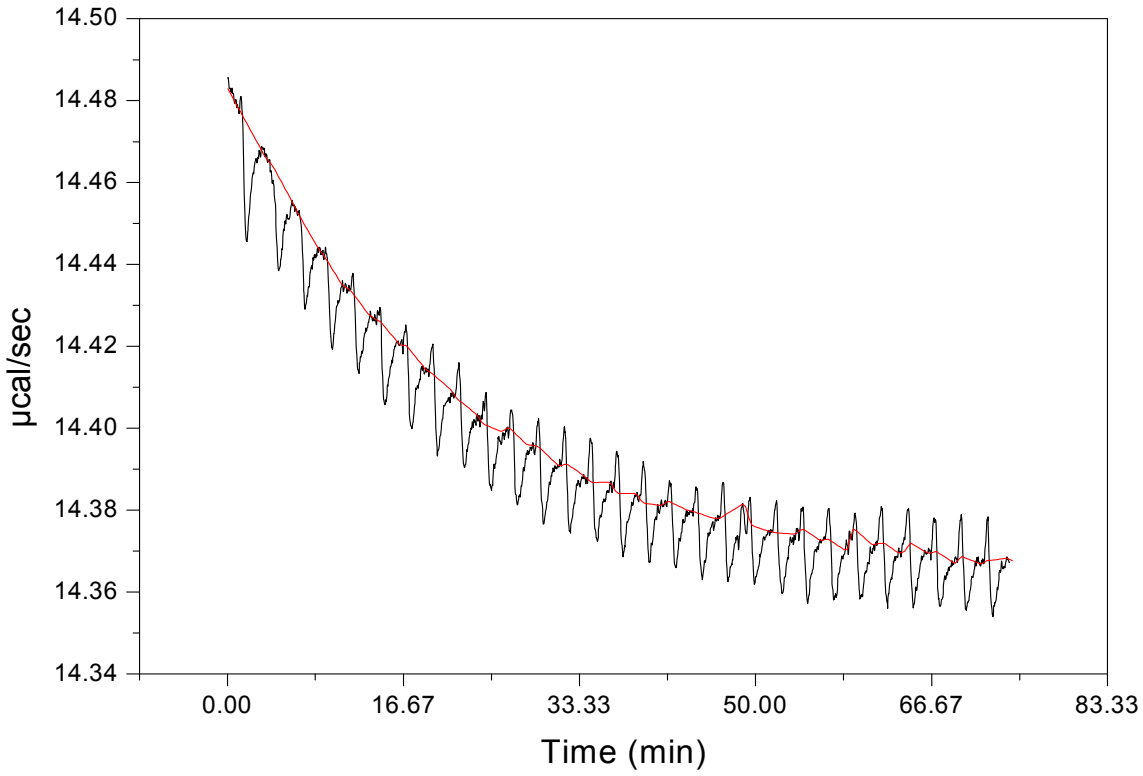

Figure 5.18: ITC graph for the titration of POPC LUVs into a solution of the PLP peptide

The lipid suspension (300µl) consisting of 5mM POPC LUVs, was titrated by small injections of 10µl into the Microcal Cell containing 1.5ml of 20µM PLP peptide dissolved in 5mM HEPES, 150mM NaCl buffer, pH 7.4.

Chapter 6

Conclusions and Future Studies

6.1 The effects of lipid composition on myelin's microdomains

A general study on the effects of the changes in lipid composition during MS in the myelin sheath was conducted and the consequences on protein-lipid interactions were characterized. This work has provided valuable insights into the properties of lipid rafts found in the myelin membrane and the consequences of disease on their structure and function. Our research work has shown that changes in terms of the lipid composition in the myelin membrane plagued by demyelination, especially the significant increase of the cholesterol level, greatly affected lipid microdomains present, particularly in terms of their size. FRET analysis indicated that the myelin mimicking systems used in this study contained L_o that were smaller than those found in the raft model membrane (PC/SM/Chol 1:1:1). Furthermore, the FRET studies carried out indicated that the decrease in sphingomyelin and an increase in cholesterol content during demyelination, promoted the formation of very small microdomains compared to healthy myelin. The presence of an increased amount of cholesterol reduced the binding of melittin but our results clearly showed that interaction with the peptide resulted in some membrane perturbation effects. The addition of melittin to the myelin model membranes was shown to promote an increase in the size of the membrane domains in both the healthy and diseased systems whereas the raft system which was predominantly in a L_o phase, underwent a decrease in the size of its microdomains. These results would suggest that melittin could potentially cause a rearrangement of the lipids in the bilayer to favour the formation of lipid domains within a specific size range. Results obtained seemed to indicate that the diseased myelin model, both in the presence

and absence of the melittin peptide, generally seemed to exhibit smaller domain formation compared to the healthy myelin model. The decrease in size of these domains during MS would cause problems when it comes to the partitioning of raft proteins in the membrane and their subsequent interactions in cellular processes. Rafts are known to come together during cellular processes, bringing their different sets of proteins together in a larger platform to promote interaction. If these rafts are already smaller to begin with, there could be issues when it comes to the protein sets that would usually associate with them and consequently leading to corrupted raft functions. If the cell cannot properly function, this will definitely lead to a multitude of symptoms and health issues, some of which are experienced during MS.

6.2 Differences in membrane interactions of melittin and C-terminus PLP peptide

The two peptides used in this study, showed different binding affinities to the various model membranes studied. Despite both their propensities to form alpha helices, melittin had a hydrophobic moment (5.18) which is almost double that of the PLP peptide (2.49). This would imply that melittin's interaction with lipid bilayers would be more favourable given that it can more easily fold into an amphipathic α-helix which can more easily interact with and penetrate into the lipid bilayer. Melittin appeared to interact differently with the different lipid systems and depending on the concentration of the peptide, it appeared that a number of conformations could exist. CD measurements combined with Trp fluorescence studies, seem to indicate that melittin could potentially exist as a monomer at low concentrations, but as the concentration increased, the peptide could undergo structural

changes which would allow it to self-associate and form either dimeric or tetrameric structures consisting of two and four α-helices respectively. However, while melittin showed signs of oligomerization at high concentrations as well as in the presence of membrane bilayers containing high levels of cholesterol, particularly the diseased myelin model and the cytosolic myelin model, the PLP peptide on the other hand showed a no real preference for either the cholesterol containing systems or the presence of negative charges on the surface of the bilayer. While the presence of cholesterol only resulted in reduced peptide-lipid interactions for the PLP peptide in most of the lipid systems, the presence of negative charge on the surface of the bilayers caused the peptide to self-associate. While the interactions of melittin were thought to be directed mainly by electrostatic interactions, the PLP peptide seemed to favour more hydrophobic interactions. Preliminary ITC measurements carried out confirm these results, as the peptide aggregated very easily in neutral and negatively charged system alike, whereas interactions with neutral cholesterol containing systems gave no heat of reactions, which would indicate that the binding of the peptide is most likely dictated by hydrophobic forces. CD spectroscopy results confirmed this theory, and showed that this peptide is mostly a combination of an alpha helix and random coil in most of the systems, with a change to a predominantly helical shape at high concentrations where self-association is most likely taking place. When comparing the lipid interactions with the healthy and the diseased systems which contained cholesterol, the PLP peptide showed no real difference in structure. Since the peptide showed very weak interactions with the myelin-mimicking myelin membrane, models, it could be possible that the PLP C-terminus may not act as a membrane anchor as was previously thought but instead could act as a mobile loop that

could potentially interact with cytosolic myelin proteins. Melittin on the other hand suffered a loss in lipid interactions and seemed more prone to self-associate. These results would suggest that the demyelination process would cause a decrease in the interaction of most of myelin's basic integral proteins with the myelin membrane. This could have dire consequences when it comes to protein folding which strongly depends on interactions with membrane lipids. Not only would this cause a loss in structure, but would also corrupt protein function thus leading to an interruption of normal cellular processes which would lead to health complications.

6.3 Future studies

In the next phase of this study, we are planning on studying the effects of the PLP peptide on the microdomains in the different lipid systems using FRET. Unlike melittin, this peptide seemed to prefer entropic reactions, and could hence affect the lipid organisation differently. Using FRET to study the interaction of the PLP peptide with the different lipid vesicles, should give an indication of how the peptide affects the lipid domain profiles. Furthermore, the interaction of melittin with the model myelin membranes will be further characterized using ITC to determine differences in the enthalpies of reaction in the healthy and diseased systems. This will allow us to better understand the effects of the change in lipid composition on the interactions of melittin with the bilayer, in terms of structure and function. Temperature dependent studies will also be carried out at physiological temperature of 37^{o}C, to determine if there are any changes in terms of peptide-lipid interactions, structure and consequent effects on the lipid domains.

References

Alonso, A. and Hernan, M. A. (2008) Temporal trends in the incidence of multiple sclerosis: a systematic review. *Neurology* **71**, 129–135

Anderson, D., Terwilliger, T.C., Wickner, W. and Eisenberg, D. (1980) Melittin forms crystals which are suitable for high resolution X-ray structural analysis and which reveal a molecular 2-fold axis of symmetry. *J Biol Chem* **255**, 2578-2582

Balashov, K.E., Rottman, J.B., Weiner, H.L. and Hancock, W.W. (1999) CCR5+ and CXCR3+ T cells are increased in multiple sclerosis and their ligands MIP1-alpha and IP-10 are expressed in demyelinating brain lesions. *Proc Natl Acad Sci* **96,** 6873–8.

Baumann, N. and Pham-Dinh, D. (2001).Biology of oligodendrocyte and myelin in the mammalian central nervous system. *Physiol Rev* **81,** 871–927.

Brown, D.A. and London, E. (1998) Functions of lipid rafts in biological membranes. *Annu Rev cell Dev* **14**, 111-136.

Chattopadhyay, A. (1990) Chemistry and biology of N-(7-nitrobenz-2- oxa-1, 3-diazol-4-yl)-labeled lipids: fluorescent probes of biological and model membranes. *Chem Phys Lipids* **53**, 1–15.

Chattopadhyay, A. and Rukmini, R. (1993) Restricted mobility of the sole tryptophan in membrane bound melittin. *FEBS* **335**, 341-344.

Chen, Y.H., Yang, J.T. and Martinez, H.M. (1972) Determination of the secondary structures of proteins by circular dichroism and optical rotator dispersion. *Biochem (Mosc)* **11,** 4120-4131.

Cherukuri, A., Dykstra, M., and Pierce, S.K. (2001) Floating the raft hypothesis: lipid rafts play a role in immune cell activation. *Immunity* **14**, 657–660.

Dabrowska-Bouta, B., Struzynska,L., Walski, M. and Rafałowska, U. (2008) Myelin glycoproteins targeted by lead in the rodent model of prolonged exposure. *Food Chem Toxicol* **46**, 961–966.

Deber, C., M. and Reynolds, S. J. (1991) Central nervous system myelin: structure, function, and pathology. *Clin Biochem* **24**, 113–134.

DeBruin, L.S and Harauz, G. (2007) White Matter Rafting—Membrane Microdomains in Myelin. *Neurochem Res* **32**, 213–228.

De Kroon, A.I.P.M., Soekarjo, M.W., De Gier, H. and De Krujffzv, B. (1990) The Role of Charge and Hydrophobicity in Peptide-Lipid Interaction: A Comparative Study Based on Tryptophan Fluorescence Measurements Combined with the Use of Aqueous and Hydrophobic Quenchers. *Biochem* **29,** 8229-8240.

DeBruin, L.S., Haines, J.D, Wellhauser, L.A., Radeva,G., Schonmann, V., Bienzle, D. and Harauz, G. J. (2005) Developmental partitioning of Myelin Basic Protein into membrane microdomains. *Neurosci Res* **80,** 211–225.

Dewey, T. G., and Hammes, G. G. (1980). Calculation of fluorescence resonance energy transfer on surfaces. *Biophys J* **32,** 1023–1036

Dupree, J.L. and Pomicter, A.D. (2010) Myelin, DIGs, and membrane rafts in the central nervous system. *Prostaglandins Other Lipid Mediat* **91**, 118–129.

Fancy, S.P.J, Chan, J.R., Baranzini, S.E., Franklin, R.J.M. and Rowitch, D.H. (2011) Myelin Regeneration: A recapitulation of development? *Annu Rev Neurosci* **34,** 21–43.

Friede, R.L. and Bischhausen R. (1982) How are sheath dimensions affected by axon caliber and internode length? *Brain Res* **235**, 335–350.

Goni, F.M., Alonso, A., Bagatolli,L.A., Brown,R.E., Marsh,D., Prieto,M. and Thewalt,J.L. (2008) Phase diagrams of lipid mixtures relevant to the study of membrane rafts. *Biochim Biophys Acta* **1781**, 665–684.

Greer, J.M. and Lees, M.B. (2002) Myelin Proteolipid protein- the first 50 years. *Int J Biochem Cell Biol* **34,** 211–215.

Haldar,S., Chaudhuri,A. and Chattopadhyay, A. (2011) Organization and dynamics of membrane probes and proteins utilizing the red edge excitation shift. *J Phys Chem* **115**, 5693-5706.

Hall, K., Lee, T.H. and Aguilar, M.I. (2011) The role of electrostatic interactions in the membrane binding of melittin. *J Mol Recognit* **24**, 108-118.

Hartings, M.R., Gray, H.B. and Winkler, J.R. (2008) Probing Melittin Helix-Coil Equilibria in Solutions and Vesicles. *J Phys Chem* **112,** 3202-3207 .

Hass, H., Torielli, M., Steitz, R., Cavatorta, P., Sorbi, R., Fasan, A., Riccio, P. and Gliozzi, A. (1998) Myelin model membranes on solid substrates. *Thin Solid Films* **329,** 627–631.

Huang, C.H. (1969) Phosphatidylcholine vesicles. Formation and physical characteristics. *Biochem **8*****:** 344–352.

Hudson,L.D., Friedrich,V.L., Behar,T., Dubois-Dalcq, M. and Lazzarini, R.A. (1989) The initial events in Myelin synthesis: Orientation of Proteolipid Protein in the plasma membrane of oligodendrocytes. *J Cell Biol* **109**, 717-727.

Inouye, H., & Kirshner, D. A. (1988) Membrane interactions in nerve myelin: II. Determination of surface charge from biochemical data. *Biophys J* **53**, 247-260.

Jahn, O., Tenzer, S., and Werner, H.B. (2009). Myelin proteomics: Molecular Anatomy of an insulating sheath. *Mol Neurobiol* **40**,55–72.

Jares-Erijman, E.A. and Jovin, T.M. (2003). FRET imaging. *Nature Biotech* **21,** 1387- 1395.

Kaier, H.J., Ortowski, A., Rog, T., Nyholm, T.K.M., Feizi, T., Lingwood, D., Vattulainen, I. and Simons, K. (2011) Lateral sorting in model membranes by cholesterol mediated hydrophobic matching. *Proc Natl Acad Sci* **108**, 16628-16633.

Kelly, S.M., Jess, T.J., and Price, N.C. (2005) How to study proteins by circular dichroism. *Biochim Biophys Act* **1751**,119 – 139

Klocek, G.,Schulthess,T.Shai, Y. and Seelig, J.(2009) Thermodynamics of Melittin Binding to Lipid Bilayers. Aggregation and Pore formation. *Biochem* **48**, 2586-2596.

Korade, Z. and Kenworthy, A.K. (2008) Lipid rafts, cholesterol, and the brain. *Neuropharmacol* **55,** 1265–1273.

Ladbury, J.E. and Chowdhry, B.Z. (1996) Sensing the heat: the application of isothermal titration calorimetry to thermodynamic studies of biomolecular interactions. *Chem & Biol* **3**: 791-801

Lakowicz, J.R. (2006) Principles of Fluorescence spectroscopy. Springer, New York, NY.

Lamarche, F., Mevel, M., Montier, T., Burel-Deschamps, L., Giamarchi, P., Tripier, P., Delepine, P., Le Gall, T., Cartier, D., Lehn, P., Jaffre, P.A., and Clement, J.C. (2007) Lipophosphoramidates as lipidic part of the lipospermines for gene delivery. *Bioconjugate Chem **18*:** 1575–1582

Lasic, D.D. (1998). The mechanism of vesicle formation. *Biochem J* **256:** 1-11

Leavitt, S. and Freire, E. (2001). Direct measurement of protein binding energetics by isothermal titration calorimetry. *Curr Opin Struc Biol* **11,** 560–566.

Lee, D.W., Min, Y., Dhar, P., Ramachandran, A., Israelachvilli, J.N. and Zasadzinski, J.A. (2011) Relating domain size distribution to line tension and molecular dipole density in model cytoplasmic myelin lipid monolayers. *Proc Natl Acad Sci* **108**, 9424-9430.

Lin, S., and W. S. Struve. (1991) Time-resolved fluorescence of nitrobenzoxadiazole-aminohexanoic acid: effect of intermolecular hydrogenbonding on non-radiative decay. *Photochem Photobiol* **54**,361–365.

Lingwood, D. and Simons, K. (2010) Lipid rafts as a membrane-organizing principle. *Science* **327**, 46-50

Linington, C. and Waehneldt, T.V. (1990) Conservation of the carboxyl terminal epitope of myelin proteolipid protein in the tetrapods and lobe-finned fish. . *Neurochem* **54**, 1354-1359.

London E. (2002) Insights into lipid raft structure and formation from experiments in model membranes. *Curr Opin Struct Biol* **12,** 480–86

Loura, L.M.S., De Almeida, R.F.M., Silva, L.C., Prieto, M. (2009) FRET analysis of domain formation and properties in complex membrane systems. *Biochim Biophys Act* **1788**, 209–224.

Loura, L.M. S., Fedorov, A. and Prieto,M. (2001) Fluid–Fluid Membrane Microheterogeneity: A Fluorescence Resonance Energy Transfer Study. Biophys J. **80**, 776–788.

Loura, L.M. S., Fernandes, F. and Prieto,M. (2009) Membrane microheterogeneity: Forster resonance energy transfer characterization of lateral membrane domains *Eur Biophys J.* **39**, 4, 589-607.

Michel, V. and Bakovic, M. (2007) Lipid rafts in health and disease. *Biol Cell* **99**, 129–140.

Morrisett, J.D., David, J.S., Pownall, H.J., Gotto, A.M. Jr. (1973) Interaction of an apolipoprotein (apoLP-alanine) with phosphatidylcholine. *Biochem* **12,** 1290-1299.

Moscho, A., Orwar, O. Chiu, D.T., Modi, B.P. and Zare, R.N.(1996) Rapid preparation of giant unilamellar vesicles. *Proc Natl Acad Sci* **93**, 11443-11447.

Mukherjee, S., and Chattopadhyay, A. (1996) Membrane organization at low cholesterol concentrations: a study using 7-nitrobenz-2-oxa-1,3-diazol-4-yl-labeled cholesterol. *Biochem* **35**, 1311–1322.

Mukherjee, S., and Maxfield, F.R. (2000). Role of membrane organization and membrane domains in endocytic lipid trafficking. *Traffic* **1**, 203–211.

Nelson, D.L. and Cox, M.M (2008) Lehninger Principles of Biochemistry. Freeman, New York, NY.

Ng, D.P. and Deber, C.M. (2010) Modulation of the Oligomerization of Myelin Proteolipid Protein by Transmembrane Helix Interaction Motifs. *Biochem* **49**, 6896–6902.

Niemz, A. and Tirell, D.A. (2001) Self-Association and Membrane-Binding Behavior of Melittins Containing Trifluoroleucine. *J Am Chem Soc*, ***123***, 7407–7413.

Pender, M.P. and Greer, J.M. (2007). Immunology of multiple sclerosis. Curr *Allergy Asthma Rep* 7, 285–292.

Pike, L. (2006). Rafts defined: a report on the Keystone symposium on lipid rafts and cell function. *J Lipid Res*, **47**:1597-1598.

Podbielska, M. and Hogan, E.L. (2009) Molecular and immunogenic features of myelin lipids: incitants or modulators of multiple sclerosis? *Mult Scler* **15**, 1011–1029

Raghuraman, H. and Chattopadhyay, A. (2004) Interaction of Melittin with Membrane Cholesterol: A Fluorescence Approach. *Biophys J* **87**, 2419–2432.

Reipert, B. (2004).Multiple sclerosis: a short review of the disease and its differences between men and women. *JMHG* **4,** 334–340.

Rajan, R. and Balaram, P. (1996) A model for the interaction of trifluorethanol with peptides and proteins. *Int J Peptide Protein Res* **48**: 328-336.

Rukmini,R., Rawat, S.S., Biswas, S. C. and Chattopadhyay, A. (2001) Cholesterol Organization in Membranes at Low Concentrations: Effects of Curvature Stress and Membrane Thickness *Biophys J* **81**, 2122–2134.

Samsonov, A.V., Mihalyov, I, Cohen, F.S. (2001) Characterization of cholesterol/sphingomyelin domains and their dynamics in bilayer membranes. *Biophys J* **81**,1486–500.

Schubert, D., Pappert, G. and Boss, K. (1985) Does dimeric melittin occur in aqueous solution. *Biophys J*. **48**, 327-329.

Simons, K. and Ehehalt, R. (2002) Cholesterol, lipid rafts, and disease. *J Clin Invest* **110,** 597–603

Simons, M., E.-M. Krämer, C. Thiele, W. Stoffel, and J. Trotter. (2000) Assembly of myelin by association of proteolipid protein with cholesterol- and galactosylceramide- rich membrane domains. *J Cell Biol* **151**,143–153.

Sengupta, P., D. Holowka and B. Baird. (2007) Fluorescence resonance energy transfer between lipid probes detects nanoscopic heterogeneity in the plasma membrane of live cells. Biophys J **92**, 3564-3574.

Silvius, J.R. (2003) Role of cholesterol in lipid raft formation: lessons from lipid model systems. *Biochim Biophys Act* **1610**, 174– 183

Simons, M., Kramer, E.M., Thiele, C. Stoffel. W. and Trotter, J. (2000) Assembly of myelin by association of proteolipid protein with cholesterol and galactosylceramide-rich membrane domains. *J Cell Biol* ***151***,143-153.

Sospedra, M. and Martin, R. (2005). Immunology of multiple sclerosis. *Annu Rev Immunol* **23**, 683–747

Taylor, C.M., Coetzee, T. and Pfeiffer, S.E. (2002) Detergent-insoluble glycosphingolipid/cholesterol microdomains of the myelin membrane. *J Neurochem* **81**, 993-1004.

Taylor, M.S., Marta, C.B., Claycomb, R.J., Han, D.K., Rasband, M.N., Coetzee, T. and Pfeiffer, S.E.(2004) Proteomic Mapping provides insights into functional myelin biology. *Proc Natl Acad Sci* **13**, 4643-4648

Terwilligert, T.C and Eisenberg, D. (1982) The structure of melittin: Interpretation of the structure. *J Bio Chem* **257**, 6016-6022.

Terra, R.M.S., Guimaraes, J.A. and Verli, H. (2007) Structural and functional behavior of biologically active monomeric melittin. *J Mol Graph Model* **25**, 767–772.

Thomas, D.D., Carlsen, W.F. and Stryer, L. (1978) Fluorescence energy transfer in the rapid-diffusion limit. *Proc Natl Acad Sci* **75**, 15746-5750.

Tillman, T.S., Cascio, M. (2003) Effects of membrane lipids on ion channel structure and function. *Cell Biochem Biophys* **38**, 161–190.

Van Meer, G. (1989). Lipid traffic in animal cells. *Annu Rev Cell Biol* **5**, 247–275

Veatch, S.L. and Keller,S.L. (2003). A Closer Look at the Canonical 'Raft Mixture' in Model Membrane Studies. *Biophys J* **84**, 725–726.

Verb, G., Szollosi, J., Matko, J., Nagy,P., Frakas,T., Vigh, L., Matyus, L., Waldmann, T.A. and Damjanovich, S. (2003) Dynamic, yet structured: The cell membrane three decades after the Singer–Nicolson model. *Proc Natl Acad Sci* **14**, 8053-8058.

Vivian, J.T and Callis, P.R. (2001) Mechanisms of tryptophan fluorescence shifts in proteins *Biophys J* **80**, 2093–2109.

Vogel, H. (1987) Comparison of the conformation and orientation of alamethicin and melittin in lipid membranes. *Biochem* ***26***, 4572-4583.

Werner, H.B., Kuhlmann, K., Shen, S., Uecker, M., Schardt, A., Dimova, K., Ofaniotou, F., Dhaunchak, A., Brinkmann, B.G., Mobius, W., Gurante, L., Casaccia-Bonnefil, P., Jhan, O. and Nave, K.A. (2007) Proteolipid protein is required for transport of sirtuin 2 into CNS Myelin. *J Neurosci* **27**, 7717-7730.

Wessman, P., Stromstedt, A. A., Malmsten, M. and Edwards, K. (2008). Melittin-lipid bilayer interactions and the role of cholesterol. *Biophys J* **95**, 4324-4336.

Winograd, E., Hume, D. and Branton, D. (1991) Phasing the conformational unit of spectrin. *Proc Natl Acad Sci* **88**, 10788-10791.

Wu, P. and Brand, L. (1994) Resonnance Energy Transfer: Methods and applications. *Analyt Biochem* **218,** 1-13.

Ybe, J.A., Clegg, M.E., Illingworth,M., Gonzalez, C. and Niu, Q. (2009) Two Distantly Spaced Basic Patches in the Flexible Domain of Huntingtin-Interacting Protein 1 (HIP1) Are Essential for the Binding of Clathrin Light Chain. *Research Letters in Biochemistry*, 5 pages. Article ID 256124, doi:10.1155/2009/256124

Zimet, D. B., B. J.-M. Thevenin, A. S. Verkman, S. B. Shohet, and J. R. Abney. 1995. Calculation of resonance energy transfer in crowded biological membranes. *Biophys J* **68**, 1592–1603.

APPENDIX A- FRET graphs in different lipid systems in the presence and absence of melittin

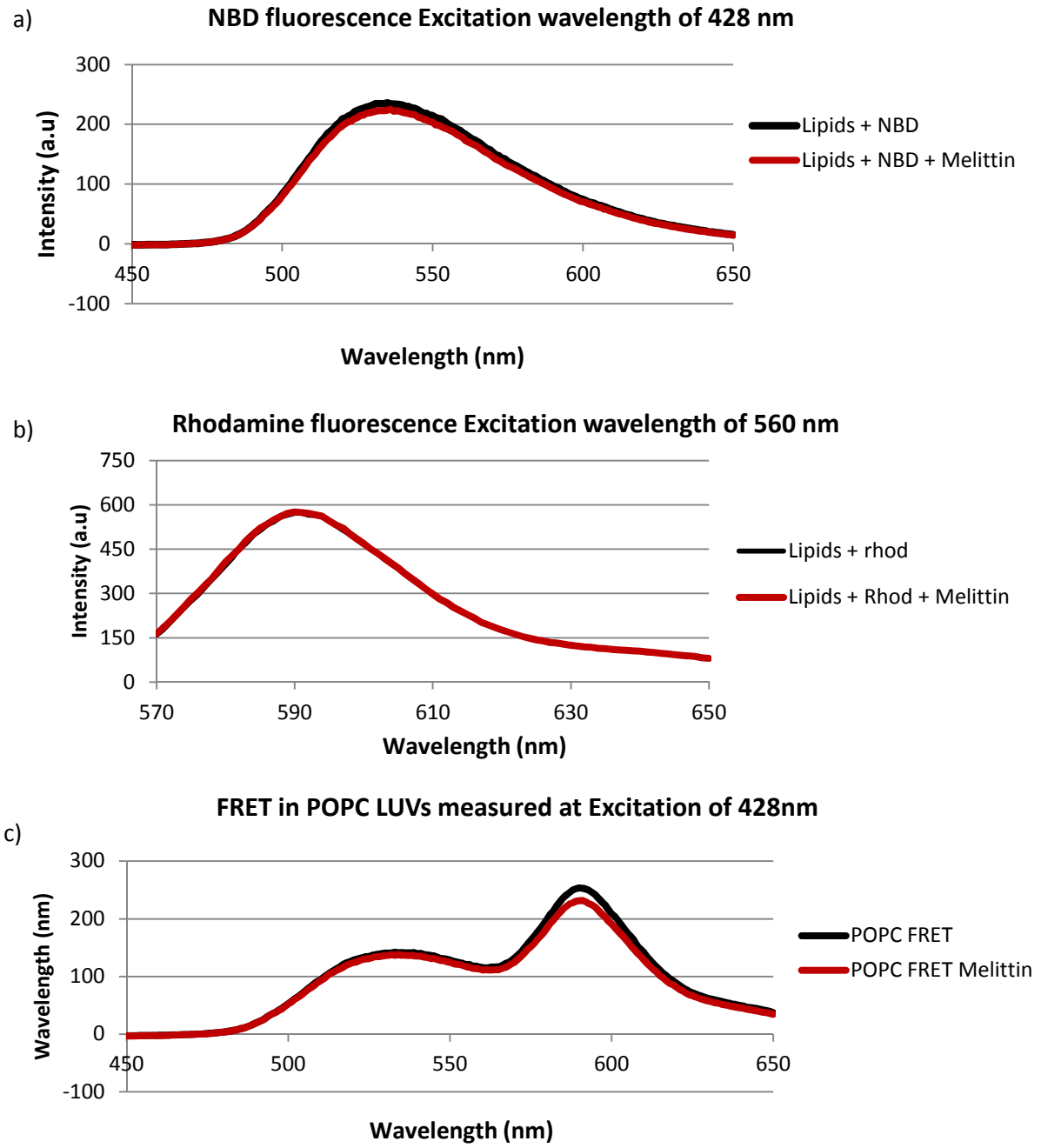

Figure A.1: FRET was used to study the lipid microdomains in POPC LUVs (100nm in size) and this was done by preparing 1mM lipid suspensions in 5mM HEPES, 150mM NaF, pH 7.4 buffer, containing either of the two probes NBD-PE and Rhodamine-PE for control purposes and both probes for FRET measurements. The fluorescence was measured both in the presence and absence of melittin to determine how the presence of the peptides affects the microdomains. Graphs **a)** show the fluorescence of NBD measured at 428nm **b)** Fluorescence of Rhodamine measured at 560 nm and **c)** shows the profile of the energy transfer taking place in the system that contains both probes.

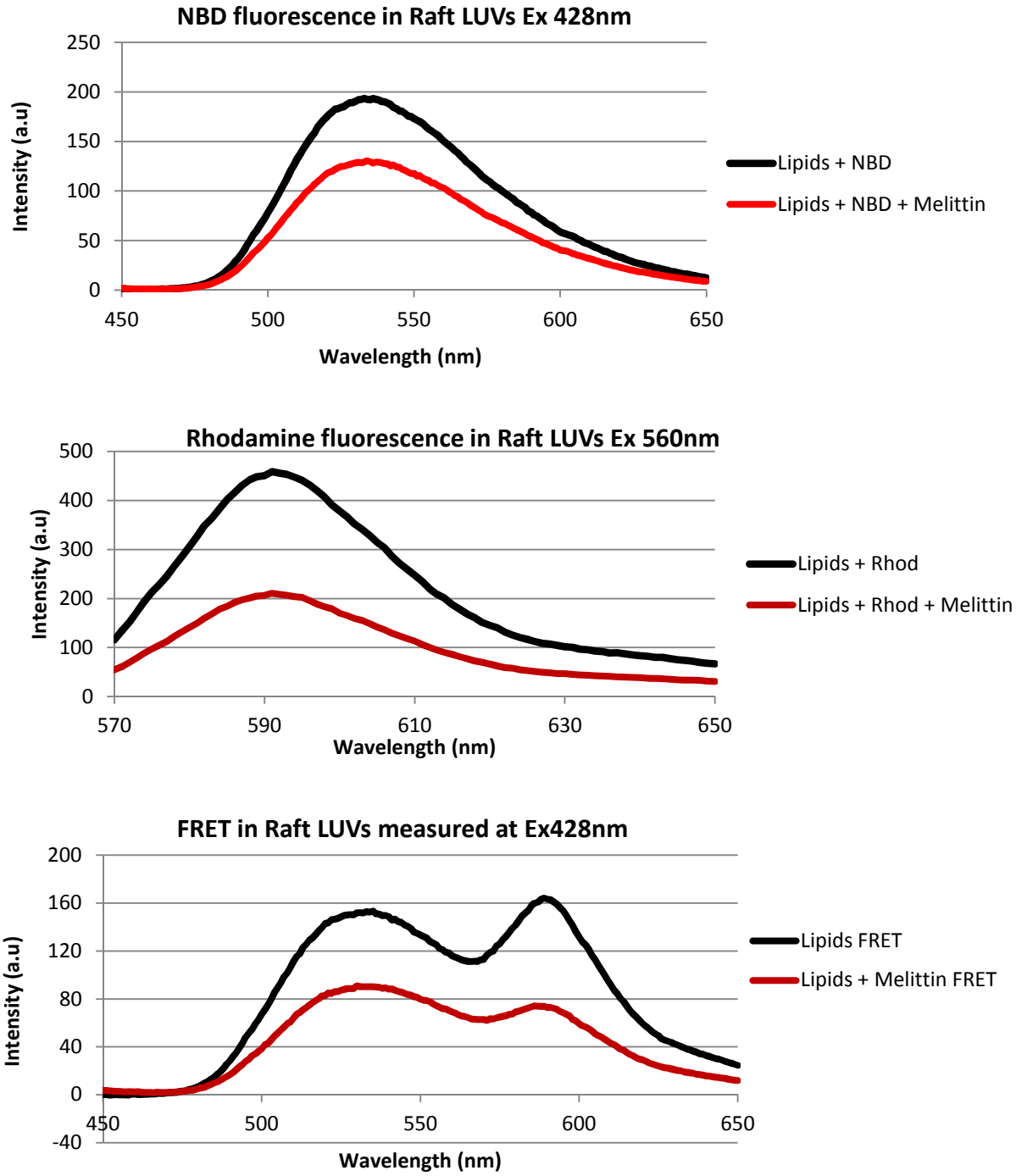

Figure A.2: FRET was used to study the lipid microdomains in Raft LUVs (100nm in size) and this was done by preparing 1mM lipid suspensions in 5mM HEPES, 150mM NaF, pH 7.4 buffer, containing either of the two probes NBD-PE and Rhodamine-PE for control purposes and both probes for FRET measurements. The fluorescence was measured both in the presence and absence of melittin to determine how the presence of the peptides affects the microdomains. Graphs **a)** show the fluorescence of NBD measured at 428nm **b)** Fluorescence of Rhodamine measured at 560 nm and **c)** shows the profile of the energy transfer taking place in the system that contains both probes.

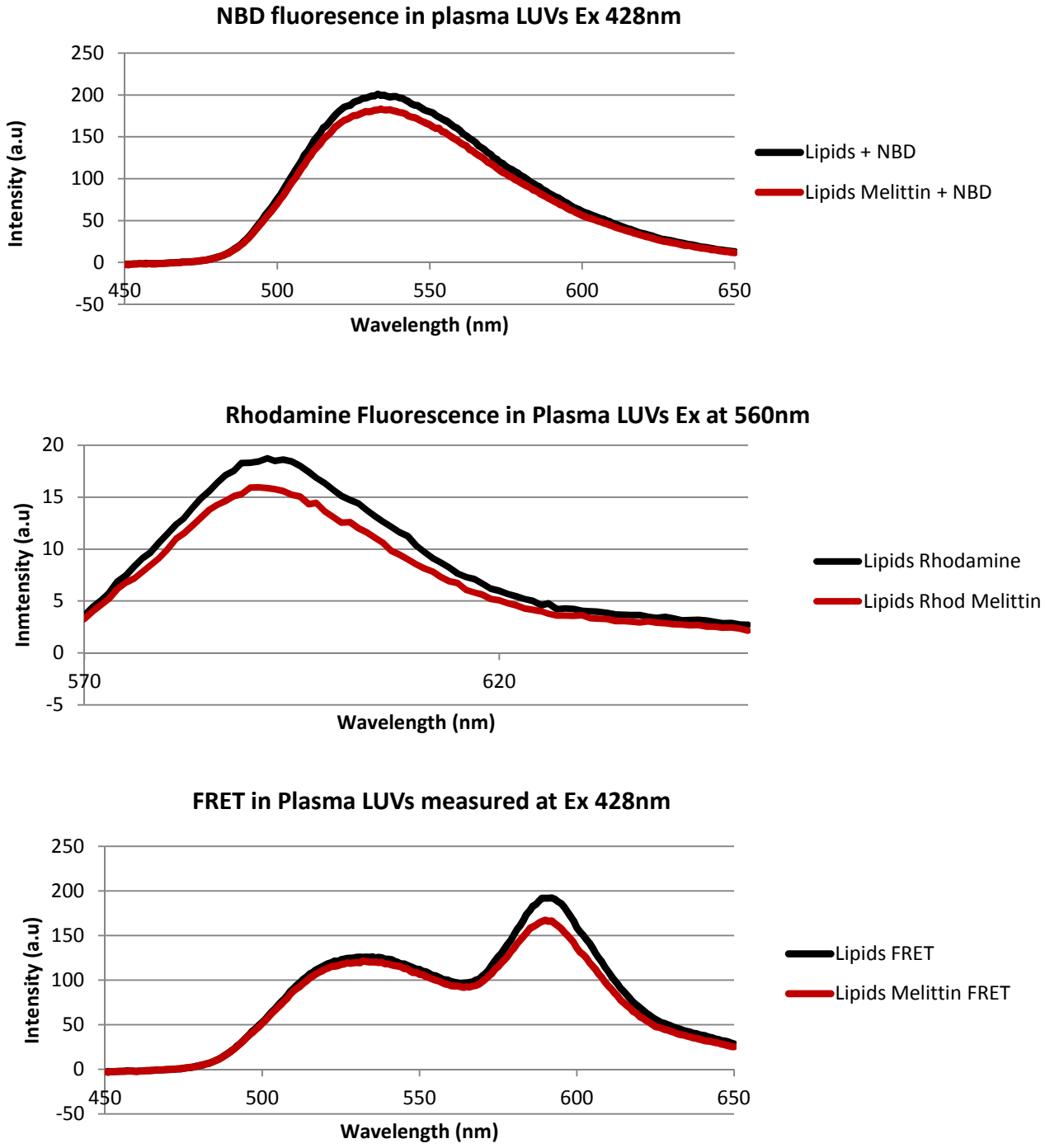

Figure A.3: FRET was used to study the lipid microdomains in Plasma LUVs (100nm in size) and this was done by preparing 1mM lipid suspensions in 5mM HEPES, 150mM NaF, pH 7.4 buffer, containing either of the two probes NBD-PE and Rhodamine-PE for control purposes and both probes for FRET measurements. The fluorescence was measured both in the presence and absence of melittin to determine how the presence of the peptides affects the microdomains. Graphs **a)** show the fluorescence of NBD measured at 428nm **b)** Fluorescence of Rhodamine measured at 560 nm and **c)** shows the profile of the energy transfer taking place in the system that contains both probes.

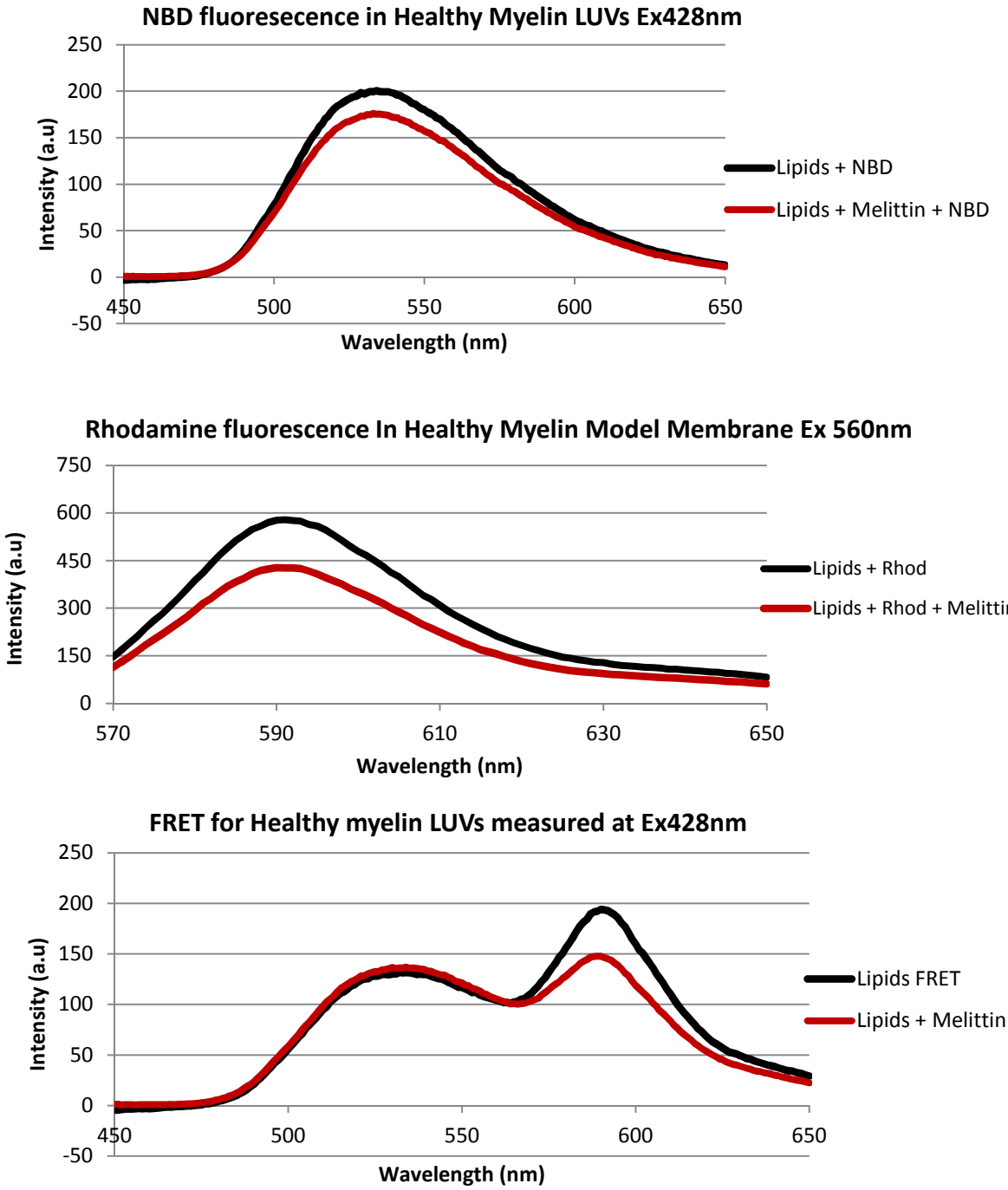

Figure A.4: FRET was used to study the lipid microdomains in Healthy LUVs (100nm in size) and this was done by preparing 1mM lipid suspensions in 5mM HEPES, 150mM NaF, pH 7.4 buffer, containing either of the two probes NBD-PE and Rhodamine-PE for control purposes and both probes for FRET measurements. The fluorescence was measured both in the presence and absence of melittin to determine how the presence of the peptides affects the microdomains. Graphs **a)** show the fluorescence of NBD measured at 428nm **b)** Fluorescence of Rhodamine measured at 560 nm and **c)** shows the profile of the energy transfer taking place in the system that contains both probes.

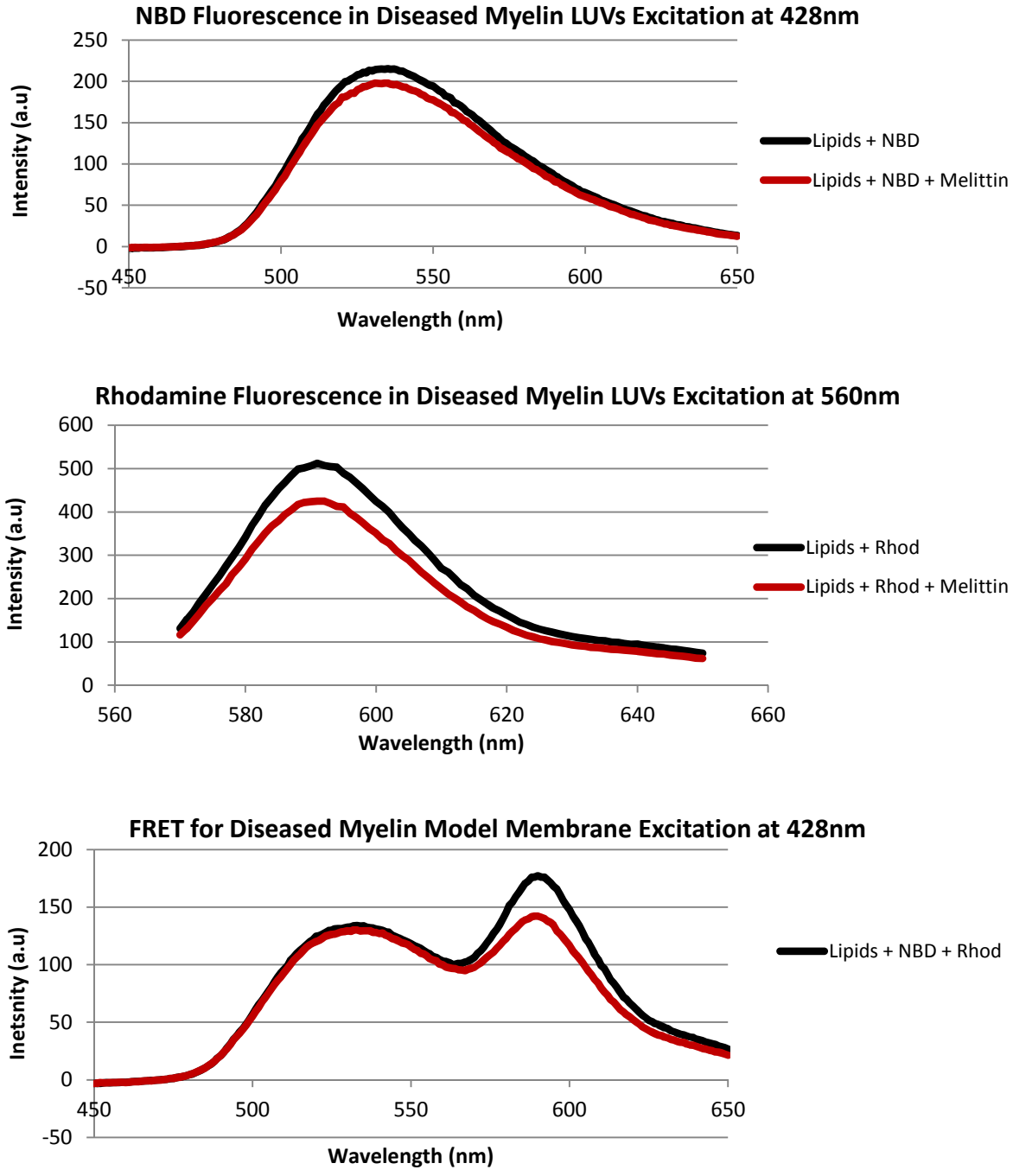

Figure A.5: FRET was used to study the lipid microdomains in Diseased LUVs (100nm in size) and this was done by preparing 1mM lipid suspensions in 5mM HEPES, 150mM NaF, pH 7.4 buffer, containing either of the two probes NBD-PE and Rhodamine-PE for control purposes and both probes for FRET measurements. The fluorescence was measured both in the presence and absence of melittin to determine how the presence of the peptides affects the microdomains. Graphs **a)** show the fluorescence of NBD measured at 428nm **b)** Fluorescence of Rhodamine measured at 560 nm and **c)** shows the profile of the energy transfer taking place in the system that contains both probes.

Appendix B- CD spectra of the C-terminus PLP peptide in TFE

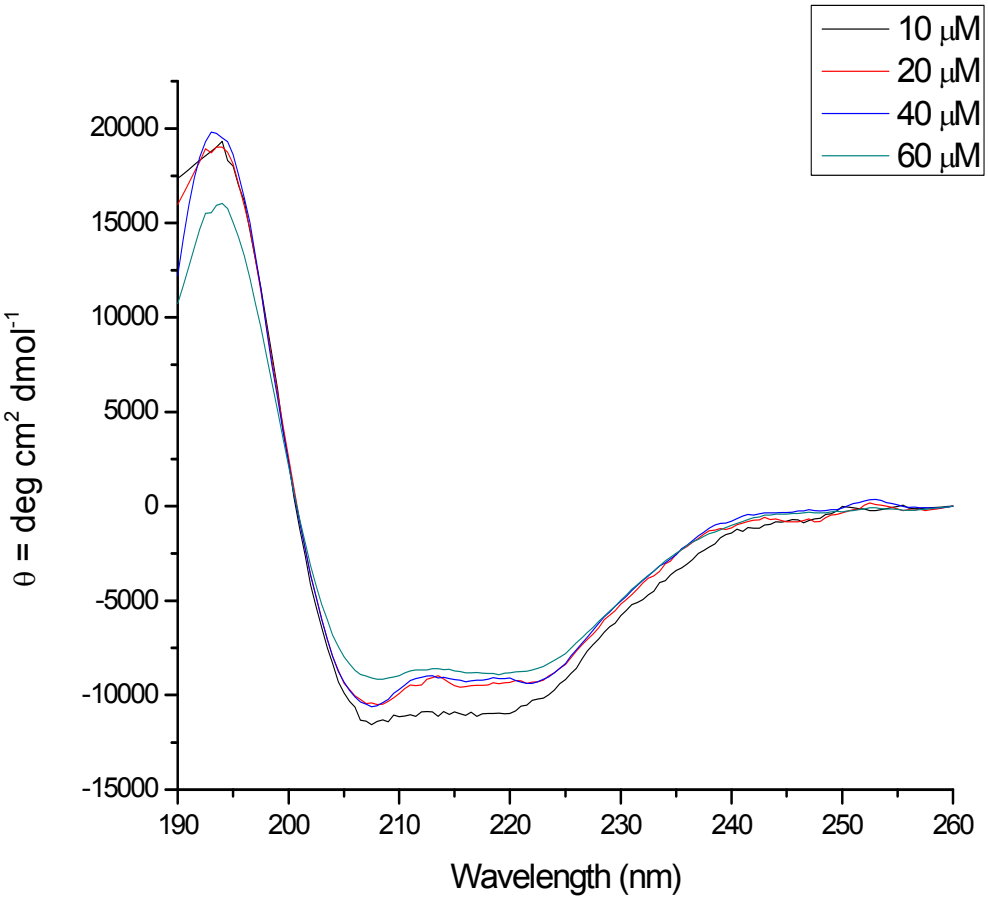

Figure B.1: Concentration-dependent far UV CD spectra of PLP in 20% TFE solution

The PLP peptide was added to the 20% TFE solution, approximately 3 minutes before the scan was started, vortexed and then briefly centrifuged before scanning. Four scans were taken for each sample and all measurements were carried out at 25^{o}C in a 1mm pathlength cuvette. The final averaged spectra were converted to molar ellipticities and further smoothed using the AVIV CD software.

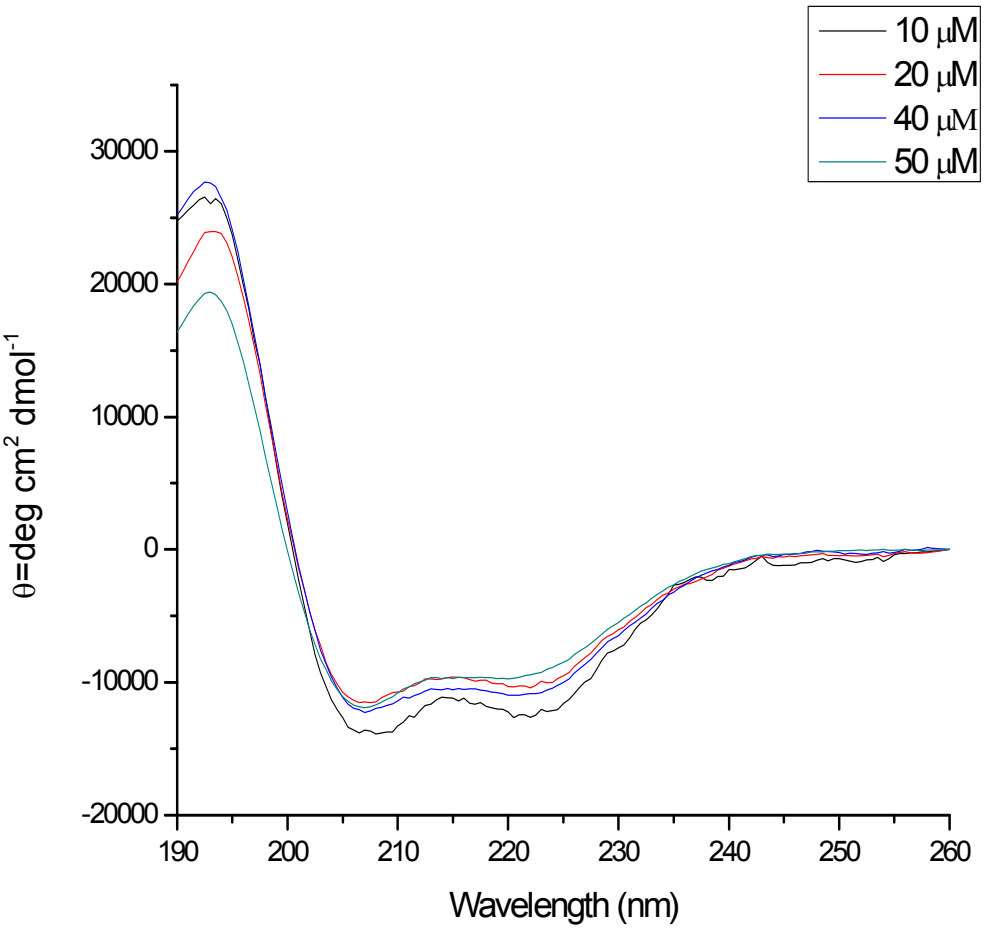

Figure B.2: Concentration-dependent far UV CD spectra of PLP in 50% TFE solution

The PLP peptide was added to the 50% TFE solution, approximately 3 minutes before the scan was started, vortexed and then briefly centrifuged before scanning. Four scans were taken for each sample and all measurements were carried out at 25^{o}C in a 1mm pathlength cuvette. The final averaged spectra were converted to molar ellipticities and further smoothed using the AVIV CD software.